Faculty of Civil Engineering

Resistance and Behaviour of Composite Beams with Web Openings

Dissertation Thesis

28250020243001

Ing. JAKUB BARTUŠ

Study program:	Theory of Structures and Engineering Constructions
Study field:	Civil Engineering
University:	University of Žilina
Supervisor:	doc. Ing. Jaroslav Odrobiňák, PhD.

Žilina, 2024

Declaration

The candidate confirms, the dissertation thesis submitted is of his own. An appropriate credit has been given to references mentioned.

Žilina, 2024

Signature

Acknowledgements

I would like to express my deepest gratitude to my supervisor and other colleagues for their invaluable patience and feedback. Without their generously provided knowledge and expertise, my research would never been accomplished. It would be remiss not mentioning my family. Their belief in me, has kept my effort endless during the entire process.

Abstrakt

BARTUŠ, Jakub: Odolnosť a pôsobenie spriahnutých oceľobetónových nosníkov s otvormi v stenách. [Dizertačná práca] – Žilinská univerzita v Žiline, Stavebná fakulta, Katedra stavebných konštrukcií a mostov – Vedúci dizertačnej práce: doc. Ing. Jaroslav Odrobiňák, PhD. – Žilina: SvF UNIZA, 2024

V rámci obsahu tejto dizertačnej práce bol vykonaný komplexný výskum v oblasti spriahnutých oceľobetónových nosníkov s otvormi v stenách. Táto práca spresňuje súčasné poznatky týkajúce sa daných nosných prvkov, v ktorých dochádza ku komplexnému napäťovému stavu vyvolanému prítomnosťou otvorov v oceľovej stene nosníka.

Spriahnuté konštrukcie sa vo všeobecnosti považujú za jeden z najefektívnejších konštrukčných systémov používaných nielen pre pozemné stavby, ale aj v oblasti mostných stavieb. Hlavný dôvod používania tohto nosného systému spočíva v minimalizácií negatívnych vlastností oboch spájaných materiálov. Okrem tejto skutočnosti, je možné dosiahnuť zníženie času výstavby, celkovej hmotnosti konštrukcie, rozmerov základov a tým aj celkových nákladov.

Jednými z najbežnejších nosných prvkov reprezentujúcich tento druh konštrukčného systému sú spriahnuté oceľobetónové nosníky. Napriek ich neodmysliteľným výhodám, vzniká zavedením otvorov do oblasti steny mnoho nejasností týkajúcich sa posúdenia ich odolnosti. Pre takýto druh nosníkov je charakteristické použitie oceľového symetrického prierezu v tvare I s rovnomerným rozmiestnením šmykových tŕňov.

Avšak, vo viacerých teoreticky orientovaných štúdiách bola upriamená pozornosť práve na rozmiestnenie šmykových prostriedkov a ich vplyv na odolnosť voči Vierendeelovmu namáhaniu a teda aj na celkovú odolnosť. A práve toto tvrdenie podnietilo náš výskum s cieľom detailnejšieho popisu danej problematiky.

S postupným napredovaním výskumu sa objavili ďalšie zaujímavé témy, ktoré bolo možné zahrnúť nielen do plánovaných experimentálnych meraní, ale aj numerických výpočtov. Z toho dôvodu bola tematika tejto dizertačnej práce obohatená o širšiu diskusiu týkajúcu sa konštitučných modelov pre betón v programovom prostredí ANSYS, a azda najvýznamnejšou časťou zameranou na prerozdelenie šmykového namáhania medzi horným a dolným T prierezom v spriahnutých nosníkoch s otvormi v stenách.

Nadobudnuté poznatky majú významné praktické použitie. Z numerického hľadiska, bol navrhnutý algoritmus zabezpečujúci automatické nastavenie vstupných parametrov pre Microplane model pri simulácií odozvy betónu na zaťaženie v zhode s viacerými

analytickými modelmi. Z hľadiska návrhu spriahnutých nosníkov s otvormi, je prezentovaný postup zjednodušujúci momentálny analytický výpočet. Konkrétne, bola jednoznačne stanovená miera šmykového namáhania pre jednotlivé T prierezy výsledkom čoho sa návrh odolnosti voči Vierendeelovmu namáhaniu zy prítomnosti vysokých šmykových síl výrazne sprehľadnil.

Na základe získaných vedomostí si autor dovoľuje navrhnúť vhodné pokračovanie budúceho výskumu.

Kľúčové slová: spriahnutie, oceľ, betón, otvory v stene, namáhanie

Abstract

BARTUŠ, Jakub: Resistance and Behaviour of Composite Concrete and Steel Beams with Openings. [Dissertation thesis] – University of Žilina, Faculty of Civil Engineering, Department of Structures and Bridges – Supervisor: Jaroslav Odrobiňák –Žilina: SvF UNIZA, 2024

Within the content of this research work, a comprehensive investigation has been carried out in the field of composite steel-concrete beams with web openings. This thesis refines the current knowledge and provides enhancements for composite beams experiencing very complex stress state induced by introduction of openings.

In general, composite structures are considered one of the most efficient structural systems used not only for civil engineering but for bridge structures as well. By the usage of this load bearing system, one attempts to minimize the negative properties of the two materials being coupled. In addition, it is possible to achieve a reduction in construction time, total weight of a structure, dimensions of foundations and thus the overall cost.

One of the most common load-bearing elements representing this type of structural system constitutes a composite steel-concrete beam. Despite its inherent advantages, introduction of openings in the web region provides a fertile ground for numerous uncertainties regarding its resistance assessment. For this type of beams, the configuration having symmetrical I-shaped steel section with evenly spaced shear connector is usually employed.

However, in several theoretically oriented studies was declared, the layout of shear connectors tends to have a significant effect not only on the Vierendeel bending resistance but also on the overall response of this type of load-bearing elements. It was exactly this assertion that stimulated our research aiming to bring to light explicit evidence.

As the research was progressing, additional topics emerged that were worth to include in the framework of this dissertation. Hence, it was enriched with a broader discussion regarding constitutive models for concrete within the ANSYS software environment and, perhaps the most significant, a section focusing on the redistribution of shear forces between the top and bottom T-sections in composite beams with web openings.

The acquired findings have significant practical potential. From numerical standpoint, it was proposed an algorithm providing an automated definition of the input parameters for the Microplane model covering concrete load response in agreement with established analytical models. Moreover, considering design procedure of composite beams, a

concept simplifying the current analytical estimation is presented. Especially, a novel concept defining the shear force proportion for the top and bottom Tee was proposed which significantly clarifies the resistance evaluation Vierendeel bending by presence of high shear forces.

To the end, the author summarizes outcomes and suggests an appropriate continuation of the future research.

Anotácia

Žilinská univerzita v Žiline, Stavebná fakulta,

Katedra stavebnych konštrukcií a mostov

Dizertačná práca: Odolnosť a pôsobenie spriahnutých nosníkov s otvormi v stenách

Titul, meno autora: Ing. Jakub Bartuš

Akademicky rok: 2023/2024

Počet strán:	190	Počet obrázkov:	124	Počet tabuliek:	14
Počet rovníc:	27	Počet príloh:	3	Použitá literatúra:	38

Cieľom tohto výskumu bolo poskytnúť detailnejší pohľad na namáhanie spriahnutých oceľovobetónových nosníkov s otvormi v oceľovej stene. Z toho dôvodu práca zahŕňa poznatky z teoretického, experimentálneho a numerického výskumu. Výsledkom je inovatívna koncepcia definujúca prerozdelenie šmykovej sily medzi horným a dolným T-prierezom s ohľadom na posúdenie Vierendeelovho ohybového namáhania.

Kľučove slova: spriahnutie, oceľ, betón, nosník, namáhanie

Annotation

University of Žilina, Faculty of Civil Engineering,

Department of Structures and Bridges

Dissertation thesis: Resistance and behaviour of composite beams with web openings

Title, name of the author: MSc. Jakub Bartuš

Academic year: 2023/2024

Number of pages:	190	Number of figures:	124	Number of tables:	14
Number of equations:	27	Number of appendixes:	3	Reference:	38

This research work aims to provide deeper insight into the field of composite steel and concrete beams with web openings. Hence, it encompasses evidence from theoretical, experimental, and numerical investigation. As a result, a novel concept defining the shear force redistribution between the top and bottom Tee section with respect to justification of the Vierendeel bending effects is presented.

Key words: composite, steel, concrete, beam, stress

Declaration

Acknowledgements

Abstrakt

Abstract

Anotácia

Annotation

Table of Contents

List of Figures

List of Tables

INTRODUCTION

As is known, composite structures are in general considered as a highly efficient construction solution. They provide economic benefits owing to rapid construction process, overall low self-weight, and versatile internal layout. Furthermore, they meet sustainability requirements, thus they often represent effective load-bearing systems for modern commercial buildings.

One of the most widely used structural elements of such structures are composite beams. These normally consist of a concrete slab, steel section and coupling elements. Each of the above-mentioned components of composite beam has inherent characteristics which make this structural solution unique. For this type of load-bearing members, the current design standards provide a sufficiently concise approach with respect to assessment of their overall resistance.

However, when one or more web openings are introduced, the resistance calculation becomes notably complicated. The openings are most often created due to passage of service ducts. On the contrary, the opening existence can be used to maintain or reduce the overall structural weight of the building, thus cut a certain part of cost. In addition, if the openings are appropriately integrated into the building environment, their function can also fulfil an architectural aspect.

For wider implementation of these structural elements, many studies have been carried out. Some of them, especially those focusing on an optimized layout of shear connectors, have broadcasted its great potential in enhancement of the overall load response emerging solely from theoretical fundamentals. As this subject has not been currently adequately underpinned by relevant experimental evidence, it has formed the first of two main objectives.

In order to deeper general insight into this field, a number of analytically-numerically oriented studies investigating an impact of individual parameters were executed. Since the design approach is still missing in the standards, the vast majority of the analytical calculations were carried out according to the up-to-date research. Despite its large domain, an alarming paucity of awareness in reference to the shear force redistribution within individual T-sections of composite beams with web openings was witnessed. As this aspect has a great importance regarding the resistance justification against the Vierendeel bending by coexistence of high shear forces, an effective remedy of this improper state constituted the second main objective of our research.

AIMS OF THE THESIS

As this research aspired to contribute to the current knowledge in the field of composite steel-concrete beams with web openings, the following subjects were of a prime interest:

1. Proposal and realisation of the experiment focused on the resistance and behaviour of composite beams with web openings.
2. Creation and calibration of a numerical model based on the FE method.
3. Conduction of the following parametric studies focusing on:
    a. shear flow in composite beams with web openings using uneven distribution of shear studs,
    b. effect of the openings' presence on the lateral-torsional stability of composite beams with web openings in the assembly and operational stages,
4. Recommendations refining the current design procedure of non-symmetrical composite beams with web openings.

Trying to meet these ambitions, an overview of the up-to-date research and appropriate literature regarding fundamental design concepts was compiled in the first place. Secondly, an analytical procedure covering the key aspects was adopted and followed by design of the experimental samples. During the preparation stage of experimental testing, several analytical-numerical studies were performed. These were analysing broader domain aiming to identify the weight of various factors. By doing so, collected evidence from these studies provided an essential basement for the proper navigation of further research. By subsequent creation of the reference FE model for the experimental samples, several numerical challenges have arisen. These circumstances drove the expansion of the research framework by discussion on modelling of concrete in ANSYS. A s side effect, a calibration procedure for definition of input parameters for the Microplane model in ANSYS was developed. Surmounting the aforementioned challenges, validation process between experimental and numerical evidence was provided. As the correlation between the data displayed acceptable agreement, comprehensive parametric FE analysis was performed. By doing so, the outcomes of rigorous data treatment vigorously signalised their significant practical potential. In particular, a novel concept defining the shear force redistribution between the top and bottom T-sections in composite beams with web openings was proposed.

Towards the end of this research work, the acquired evidence is being summarized, practical resolutions to the main objectives are presented, and proposal for the future research is submitted.

The main points briefly summarizing the course of the entire investigation are as follows:

- State-of-the-art analysis.
- Theoretical background for design of experimentally tested samples.
- Conduction of analytical-numerical oriented studies focusing on:
    - Lateral-torsional buckling of non-symmetrical plate beams with web openings.
    - Distribution of longitudinal shear forces in composite beams with web openings.
    - Influence of web openings presence on structural performance of composite steel-concrete beams.
    - Composite beams with web openings employing alternative layout of shear connectors.
    - FE modelling techniques of concrete in steel-concrete composite beams.
- Execution of the experimental programme.
- Creation of the reference FE model and discussion on modelling of concrete in ANSYS.
- Conduction of the parametric FE analysis investigating:
    - Effects of non-uniform layout of shear connectors on behaviour of composite beams with web openings.
    - Redistribution of shear force between the Tees of composite beams with web openings.
- Proposal of a novel concept defining shear force proportion for the top and bottom T-sections of composite beams with web openings.
- Summarization of the results and related recommendations.
- Discussion of deficiencies emerged by conduction of this research and consequent proposal of the future research course.

1 METHODOLOGY

Adopting the following approach, the author attempts to accomplish the aims of the thesis and produce outcomes being generally accepted by the scientific community.

1.1 State-of-the-art Analysis

As an inevitable part of a successive investigation, current research findings with respect to the investigated objectives have to collected and analysed. Thus, an appropriate endeavour within this research was devoted to the state-of-the-art analysis. In our case, this analysis paved the way for identification of the most relevant design approach subsequently used for the experimental samples. In addition, it revealed paucity on two main objectives of this thesis:

- Actual effects of non-uniform layout of shear connectors on behaviour of composite beams with web openings.
- Redistribution of shear force between the Tees of composite beams with web openings.

1.2 Analytical-numerical Studies

On the basis of the state-of-the-art analysis, a series of FE-based parametric studies verified against established analytical models were conducted aiming to analyse the complex structural response of composite beams having web openings. These studies are representatives of three primary ideas:

- gaining of a deeper insight into the structural response,
- identifying an impact of various parameters,
- building foundation for subsequent parametric FE investigation.

Unfortunately, performance of these studies was limited by the following conditions:

- for FE discretization of composite beams solely 1-D and 2-D elements were used,
- derived results were verified only against analytical relations for the global actions.

These studies could express only fundamental ideas but laid a basement for further, more detailed research.

1.3 Experimental Programme

The experimental programme conducted within this work is represented by measurements of deflection, slip and deformation under particular load conditions. The force is applied in the form of a gradual increasing static load induced by a hydraulic jack using configuration of the 4-point bending test. As the one of main objectives is to inspect the impact of shear connectors' layout on the overall load response of composite beams with web openings, only this aspect represented a dynamic parameter for the experimental samples.

Ensuring the relevance of obtained data, the positioning of individual measurement gauges was carefully determined on the basis of record & control principle. That means, a certain number of devices had the only role to record and store the load response for validation process of the reference FE model. Contrarywise, gauges using the control principle explicitly controlled the entire process of loading, because they were applied in areas which were identified to undergo the desired failure mode.

A detailed description of the experimental programme conduction can be found in Chapter 4.

1.4 Finite Element Model

Within this part, a detailed description of the reference FE model is addressed. The following topics conveys its core body:

- Discussion on modelling of concrete in ANSYS
- Definition of parameters for concrete, steel and FE contact.
- Structure of the FE model.
- Validation of the FE model.

Meeting the strict requirements for the correlation process between experimental and numerical data, no impediments to a detailed inspection using parameterization principles were present.

1.5 Parametric FE analysis

Results methodology

Aiming to provide detailed inspection of the main objectives of this research work, the following domains were prime of interest:

- Shear connectors.
- Concrete component.

- Steel component.
- Opening size.

Under these domains, an impact of modification of layout of shear connectors, concrete strength, steel strength, cross-section configuration and web opening size were examined.

After identification of the key parameter (the opening depth) influencing the shear force redistribution between the Tees at most, additional FE calculations are performed. On their basis, novel concept for redistribution of shear forces between the Tees in composite beams with web openings is proposed. In this way, compared to the current approach, simplicity and accurateness is ensured.

1.6 Conclusions

Using acquired evidence from the entire course of this research, conclusion is formed. Within this part, overview of conducted research is provided, practical recommendations are proposed, and completion of the thesis aims is assessed.

1.7 Future Research

Completing this research endeavour, the future trends of investigation, mainly based on emerged deficiencies by conduction of this research, are submitted.

2 STATE OF THE ART

As this part of research conveys the corner stone for enhancement of already or establishment of newly derived concepts, its content follows:

- Overview of up-to-date research.
- Description of mechanical behaviour of individual components of the composite beams with web openings.
- Analysis of the current design procedure.

2.1 Up-to-date state of research

In recent years, a gradual increase of global market share in respect of composite steel-concrete structural systems is visible. In general, they benefit from a vital combination of materials resulting in a reduction of their negative natures. Speaking of particular, plain concrete has a negligible tensile strength compared to the compressive one. On the other side, steel elements can achieve a great magnitude of stresses, but are prone to instability. However, by coupling, a significant increase in the flexural strength might be achieved. This strength enhancement normally spans from 50% to 100% compared to the resistance of a beam with plain steel cross-section.

A typical composite beam consists of a steel and concrete component which are mostly coupled by usage of mechanical connectors (Fig. 2.1). Consequently, the composite action arises, and notable leap of the load-bearing capacity is attained. It is exactly the composite action that gives this type of structural members their superiority. Therefore, when designing, it is crucial to understand not only the global structural response of a composite beam, but also the connection. So far, as the individual components are not coupled, each element is stressed separately. By limiting slippage between the two elements, longitudinal shear stresses at the level of connection are generated. Thus, if the slip is prevented completely, the full degree of interaction is assumed. On the contrary, when a certain portion of slippage is permitted, partial interaction is assumed.

Fig. 2.1 - Typical composite steel-concrete beam with web openings.

The connection between concrete and steel can be provided in various ways. Each method of connection has specific properties and thus influences overall behaviour of a composite member. Common types of mechanical connection constitute shear studs, bolts, rib shear connectors and cold-formed sections. In general, there are many variations, but they all have the same primary task - transfer internal forces between individual components and prevent their separation.

With increasing demand for both the structural and economic efficiency, passage of building service ducts was moved to the level of floor system. In this way, introduction of an opening in a web region of a composite beam was imminent. The openings can be of different size, number, position, and shape. Regardless their configuration, the removed part of a web affects not only the shear flow pattern but the overall structural behaviour of an element for both ultimate (ULS) and service limit state (SLS). From a design viewpoint, the resistance evaluation of composite steel-concrete beams constitutes a complex task because of local effects´ treatment.

Early research into this field was conducted by Granade [1] who pioneered the first analytical model for the resistance evaluation. Within this analysis, a prediction of stress redistribution based on the theory of Vierendeel mechanism was presented. Unfortunately, as later shown by experimentally obtained data, estimated stresses in accordance with this method proved to be not sufficiently accurate. Nonetheless, Granade´s work pave the way for succeeding concepts trying to establish proper design approach for so complex stress state (Fig. 2.2) occurring in this type of load-bearing members.

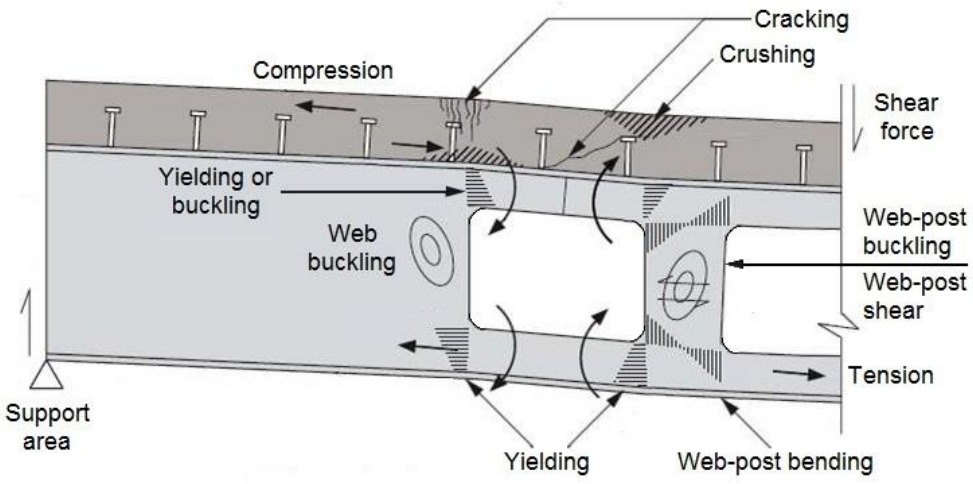

Fig. 2.2 - Complex stress state typical for composite beams with web openings.

His successors, Todd and Cooper [2] exactly followed Granade´s pivotal idea. They built a novel methodology on the existing body of his analytical model. By doing so, the

moment-shear interaction diagram for justification of the resistance has been presented for the first time. However, this design model was able to determine the carrying capacity only under following assumptions:

- full degree of interaction at the bond interface,
- single plastic neutral axis lying in a concrete component,
- concrete resistance only in compression,
- shear load carried only by a steel component,
- no instability problems.

Undoubtedly, deeper inspection was still needed, especially for proper shear carrying capacity description. In this context, Darwin D. [3] and Redwood R.G. [4], respectively, have carried out an investigation assessing contribution of a concrete slab to the shear resistance. This effort has resulted in more adequate methodology for overall resistance evaluation. Concretely, principles of both methods originated in determination of pure resistance in bending and in shear at the location of an opening. In conclusion, interaction between these actions was emerged by the moment-shear diagram - slightly adjusted to the previous one presented by Todd and Cooper (Fig. 2.3).

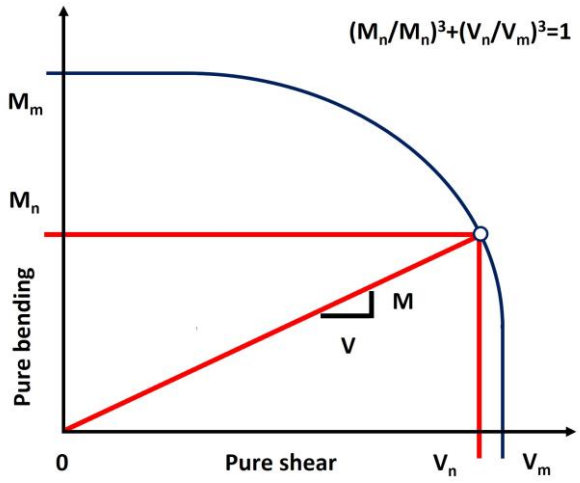

Fig. 2.3 - Moment-shear diagram.

Further remarkable development has been achieved by Donoghue, who in his work [5] laid fundamentals for strengthening techniques (Fig. 2.4) with respect to the Vierendeel action which causes a significant concentration of stresses in the vicinity of openings leading to premature failure of a steel web.

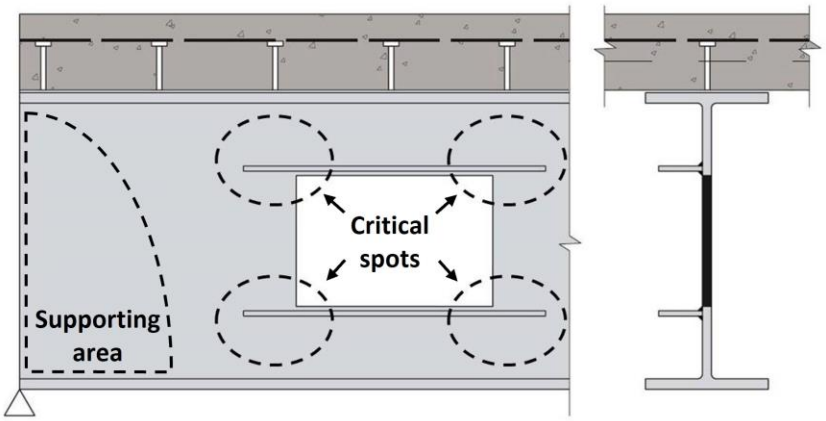

Fig. 2.4 - Example of strengthening techniques in the vicinity of an opening.

In the 1990´s, the current knowledge was summarized in the work of Oehlers D.J. and Bradford A.M. [6]. Their publication covered a great span of issues, starting with material description, going through general design, ending with fatigue assessment.

In 2003, comprehensive European research [7] investigating the structural performance of non-composite and composite beams with web openings was carried out. This technical report offers probably the most comprehensive extent of different analyses. In order to compile so extensive volume of adequate evidence, a large number of experiments was performed. Especially, the following subjects were primarily investigated:

- variety of failure modes,
- structural response of stub girders,
- employment of non-symmetric steel cross-sections,
- impact of size, shape and location of an opening,
- effect of large openings,
- behaviour of a shear connection,
- strengthening methods.

Numerous FE models, presented within this technical report, formed the basis for subsequent studies investigating significance of individual parameters. The following conclusions were drawn for composite beams with web openings:

- location of the opening must be wisely selected to minimise negative consequences,
- effect of asymmetry of steel cross-section is not that significant as expected,
- stiffness is strongly influenced by the presence of openings and has a large impact on the serviceability limit state.

Besides, novel or adjusted design methods were proposed for evaluation of:

- local stresses acting on principles of the Vierendeel mechanism,
- shear buckling resistance exploiting strut model principles,
- lateral torsional instability.

Important to underline, all of the design concepts defined on the basis of this technical report were validated against experimental and numerical data displaying satisfactory and conservative results.

In a reference to the above-mentioned research, a complex guidance for design of composite beams with web openings was published in 2011 by Lawson [8]. Owing to excellence of this publication, it was adopted as a verification basement for conducted simplified FE studies and for design of the experimental samples. The additional resources concerning design procedure of both composite and non-composite perforated beams can be found in [9, 10].

Due strong commitment of scientific community fully comprehends the complex stress state present in composite steel-concrete perforated beams, recent endeavour in this field was devoted to:

- use of asymmetric steel cross-sections [11],
- effect of different sizes and shapes of openings [12],
- impact of opening presence on deflection of a composite beam [13],
- pull-out forces acting at the material interface [14],
- development of mechanical model capturing the vast majority of likely-to-occur failure modes [15].
- alternative spacing of shear connectors [16],
- redistribution of internal forces within particular components of a composite beam [17],

Surprisingly, negligible attention has been paid to the two last subjects.

Especially, the first one of them was examined and discussed predominantly from the theoretical point of view, albeit the connectors´ layout plays a crucial role in transfer of internal forces between the steel and concrete component.

The second one, although its great importance for reliable justification of the Vierendeel resistance, relevant evidence supporting an accurate design concept is still lacking. So, while the shear redistribution is well understood for composite beams having solid steel web, by composite beams with web openings remains this aspect unclear. Despite

existence of some approaches to this issue, no general agreement on the exact shear force redistribution between the top and bottom Tee exists.

2.2 Mechanical Behaviour of Individual Components of the Composite Beams with Web Openings

From a design viewpoint, as the overall resistance evaluation of composite beams having web openings constitutes a complex task, behaviour of their individual components will be addressed.

2.2.1 Concrete Component

By a load transfer from steel to concrete component, the slab experiences a great concentration of load at the contact domain of concrete and shear studs. As these concentrated stresses are spread into the concrete slab, longitudinal shear and transverse tension occur. This stress state can lead into longitudinal cracking or transverse splitting of a slab (Fig. 2.5). In the case of longitudinal slab splitting, the resulting crack may interfere with a bearing zone of connectors, thereby affecting their stiffness and load-carrying capacity. Occurrence of this failure mode is commonly prevented by sufficient amount of transversal reinforcement. Methods evaluating the resistance against both mentioned failure modes can be found in [6].

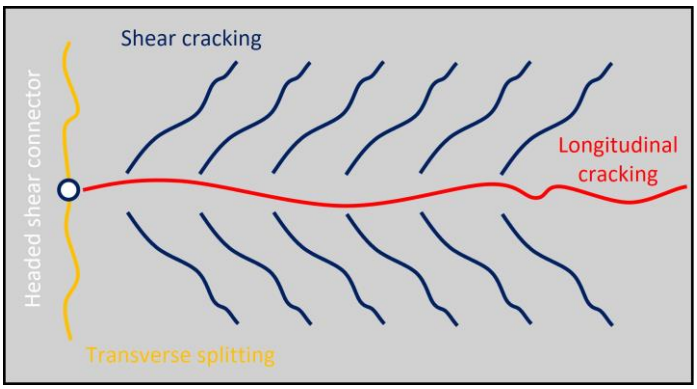

Fig. 2.5 - Top view of a concrete slab and possible failure modes.

Due to presence of a web opening, redistribution of global forces arises and is followed by local stresses occurrence (Fig. 2.6). While the shear failure of a slab is characterised by a diagonal crack above an opening, collapse in bending is manifested at its edges. Considering behaviour of bending diagram, two fundamental positions are distinguished - low (LME) and high moment end (HME). These terms relate to a value of global bending moment at position of a particular opening edge. At the HME, crushing at the top part and cracking at the bottom part of a slab can be initiated. On the other hand, at the LME

fibres of a slab are stressed in the opposite manner. Hence, a vertical shift of compressive force acting within a slab is present. This phenomenon induces normal forces at the bond interface, that can lead to a separation of connected components. If this occurs, these normal forces are resisted by shear studs, where they can trigger a failure of a shear stud embedment. Currently, by evaluation of load-carrying capacity of composite steel-concrete beams having openings, this type of collapse is neglected in terms of a design.

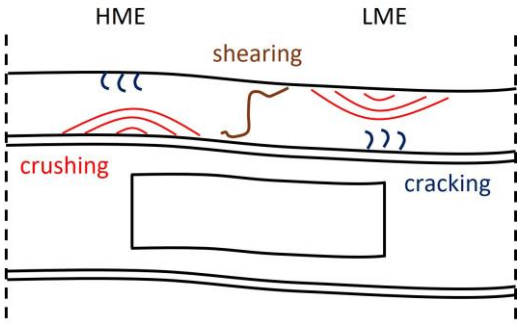

Fig. 2.6 - Local stresses within a concrete slab at an opening.

2.2.2 Steel Component

When designing a composite beam, an optimal position of the plastic neutral axis is generally assumed to be within a concrete slab. The reasoning is evident, both materials utilize fully their potential. That means, concrete component is loaded in compression and steel component in tension. This prevents composite beam from unfavourable response to load.

Considering an influence of opening presence on the global response, both the bending and shear resistances are affected. In fact, the bending resistance does not undergo so substantial reduction in bearing capacity compared to the shear resistance. Nevertheless, parts of a beam having solid web cross-section might be not so stressed, indeed redistribution of shear force between individual components is present, so this significant weakening by openings can be accepted.

Moving spotlight to the local effects, a given stress state is known as the Vierendeel action. It conveys the transfer of shear forces over certain length of a web opening. Consequently, both the vertical and horizontal shear act on a lever arm and cause concentration of stresses. This stress state in the vicinity of an opening can be imagined by simple mechanism, where the top and bottom Tee are represented as simply supported beams loaded by end moments (Fig. 2.7). If this applies, a rise of additional bending stresses is unconditional. Thus, a formation of local plastic hinges at certain locations is impending.

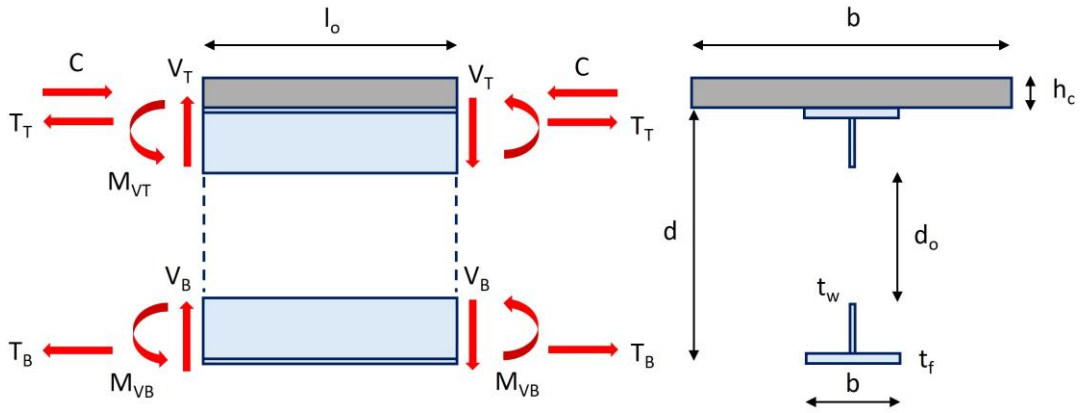

Fig. 2.7 - Mechanism of internal forces transfer at the opening region.

Regarding this failure mode, an opening shape represents one of the most influencing factors. A considerable amount of literature has been published on this topic [18]. The findings have unambiguously concluded, openings curved in a shape experience a lesser magnitude of local stresses.

Another important aspect highlights importance of both the opening size and their configuration. In fact, the web-post region (the area between openings) might experience excessive horizontal shearing or the local instability (Fig. 2.8). To prevent the former problem, a simple solution in a form of sufficient length between two subsequent openings is needed. Speaking of the latter issues, number of analytical models based on the strut and tie principles has been developed [19].

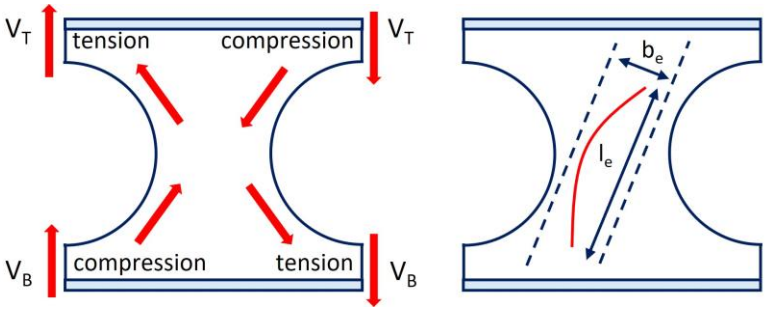

Fig. 2.8 - Strut-and-tie model for analysis of the local instability.

Surprisingly, the effect of local instability might arise also at the level of the top steel flange (Fig. 2.9). This phenomenon depends on both longitudinal distance of shear connectors and slenderness of the top Tee being under pressure. However, no large-scale research has been conducted regarding this issue yet.

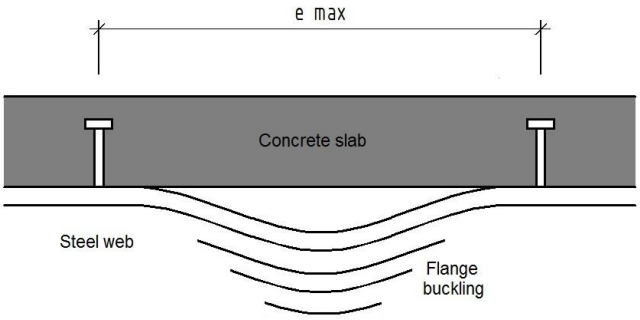

Fig. 2.9 - Local instability at the level of the top flange.

2.2.3 Shear Connection

Degree of interaction expresses mutual relation at the material interface. When the sum of individual shear studs' resistances over particular length is equal or greater than compressive strength of a concrete slab or tensile strength of a steel profile, the interaction is defined as the full shear connection. In the case of no interaction, the bending resistance of a beam is assigned only to a steel component. Between these two extreme cases, the interaction of individual components is classified as partial.

Based on that, the bending resistance gradually increases along the composite beam as the current number of shear studs increases. From the resistance standpoint, the full degree of shear connection has to be attained only at the point where the greatest bending moment acts (Fig. 2.10).

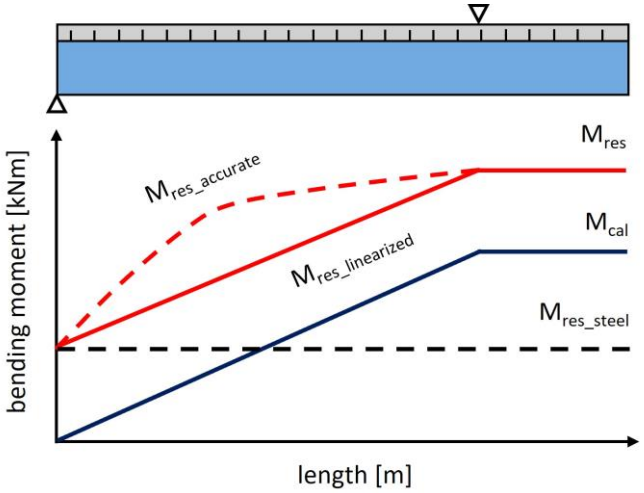

Fig. 2.10 - Behaviour of the flexural resistance in a composite beam.

Further, the nature of connection influences the deformation and stress state of a composite member to a great extent. The origin of so large importance lies in a type of employed connectors which are basically treated as rigid or flexible. Using headed shear studs representing the flexible type of a connection, the connector prior to achievement

of its maximum strength shares a particular load with adjacent connector leading to development of a plastic deformation by either. This flexibility of connection ensures almost full utilisation of both the concrete slab and the steel beam.

As known, shear studs are subjected to shear, bending and axial loading. These loads are resisted not only by shear stud shank but also by contribution of surrounding concrete. This results in an overall resistance enhancement owing to formation of the typical bearing cone (Fig. 2.11).

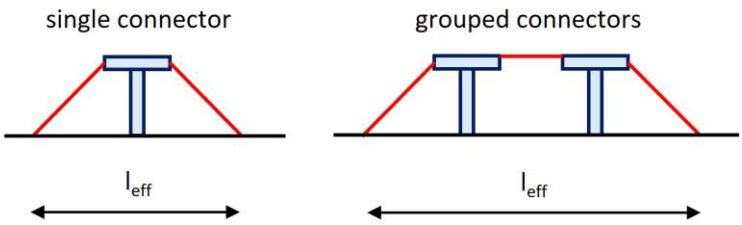

Fig. 2.11 - Bearing cone of headed shear studs.

By a sagging bending of a general beam, the upper fibres are under compression and exhibit longitudinal contraction, while the lower fibres are under tension and experience longitudinal elongation. This phenomenon is the main cause of slippage at the contact interface by composite beams. Concretely, as each material component undergoes a certain displacement, a difference of these two determines the slip value. In accordance with design standards, only limited amount of slip is permitted. When this limit is passed, the failure of connection is not urgent, but a demand for a safe service is imperilled.

In order to evaluate the shear resistance of headed shear studs, experimental-based formulas are needed. The reasoning for this treatment comes from a great variety of stresses acting within the bearing cone domain. To be specific, the resistance depends on the following parameters:

- Compressive strength and elastic modulus of concrete.
- Ultimate strength of steel used for connectors.
- Friction between concrete and steel component.
- Quality of a weld collar.

Noteworthy, the latter one plays a crucial role by fatigue assessment also.

2.3 Current Design of Composite Beams with Web Openings

Aiming to provide concise design approach for so complex stress state, a great effort was made regarding research of composite steel-concrete perforated beams in the last decade. Unfortunately, no standardised design approach has been established yet. So,

when analysing this type of bearing members, a combination of European Standards and knowledge based on up-to-date research should be used.

Attempting to provide a sufficiently concise overview, several ultimate limit states will be discussed considering global and local viewpoints. The focus will be paid to the most crucial parts of the resistance assessment concerning the scope of this research work.

2.3.1 Global and Local Analysis

As the stress state in composite beams having web openings signals great complexity, the possible failure modes were divided in two main domains - global and local. These terms are related to a type of corresponding load response. So, if the load response is induced by primary effects, for instance the global bending moment, the global action is thought. Conversely, if the load response originates in secondary effects, for instance caused by opening presence, the local action is assumed.

However, before execution of any resistance analysis of composite beam, following premises have to be accomplished:

- static scheme determination,
- material grade selection,
- size definition of a cross-section,
- calculation of the effective width,
- definition of a shear connection.

After these fundamental assumptions, it is possible to proceed to the main part of the design process.

2.3.2 Global Analysis

Considering the global actions, the resistance of a composite beam shell be checked at the position of critical cross-sections against:

- bending,
- vertical shear,
- interaction of the two already mentioned,
- and longitudinal shear.

Respecting the scope of this thesis, only the first three are addressed bellow.

2.3.2.1 Plastic Bending Resistance

Assuming the sagging bending for a simply supported beam, by a load transfer from steel to concrete component, a large compression force develops within the concrete slab. Conversely, the steel section experiences a high tensile force which is redistributed into both the steel top and bottom Tees.

It is standard to verify the global bending resistance at the centre of an opening, where the effect of the Vierendeel action is negligible. As the extensive tensile force, able to cause development of large plastic strains, is present predominantly at the level of the steel bottom Tee, contribution of the steel top Tee to the plastic bending resistance is disregarded. It is worth noting, in order to fully utilize the capacity of bending plastic resistance, the steel section with web opening shell be classified into 1 or 2 cross-section class.

As the literature states, only two cases of the plastic neutral axis location might occur in respect of the equilibrium of forces. Thus, the axis can lay in a concrete slab or the steel top Tee. However, by employment of non-symmetric steel section, having the bottom flange area compared to the top one larger 2 or 3 times, the axis might move to the bottom part as well. This can considerably influence the local stability at the level of the steel top Tee.

While the tensile resistance of the steel bottom Tee is defined by its cross-sectional area and yield strength, the compression resistance of the concrete slab is determined as the minimum of:

- sum of the shear resistances of connectors located from the support to the opening centre,
- area considering the effective width of a concrete slab having particular compression strength.

Typically, forces acting within individual parts of a cross-section at certain distances from the material interface ensure by the lever arm mechanism the resistance against the flexural forces.

2.3.2.2 Plastic Shear Resistance

Considering the general case, the shear resistance of a composite beam depends predominantly on the area of a steel web. A simplified portrayal of shear force redistribution between the Tee sections (TT – top Tee, BT – bottom Tee, TOT – total shear force) of a composite beam under 4-point bending test is pictured below (Fig.

2.12). It must be explained, the borderline between the top and bottom Tee is assumed to lay at the mid-depth of the steel web.

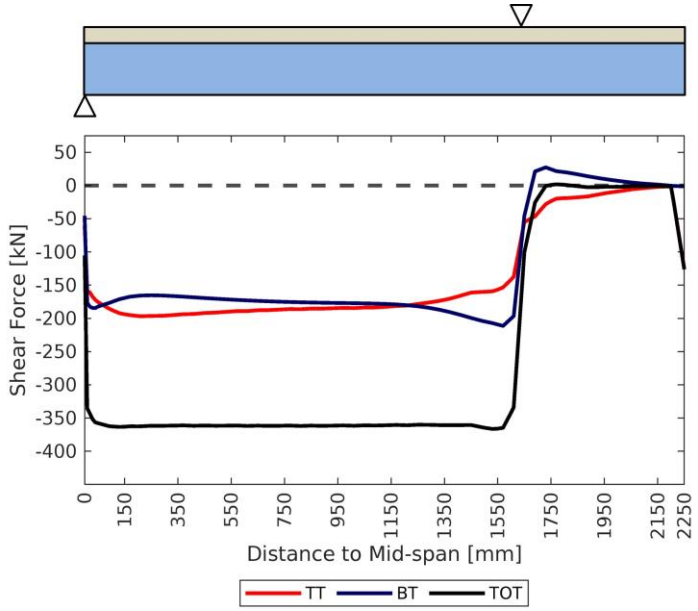

Fig. 2.12 - Shear force redistribution between the T-sections of a composite beam.

However, by an introduction of web openings, the shear resistance is significantly reduced and divided between the Tees. In this way, the major portion of shearing has tendency to shift to the top Tee. To illustrate this shear force redistribution, see Fig. 2.13.

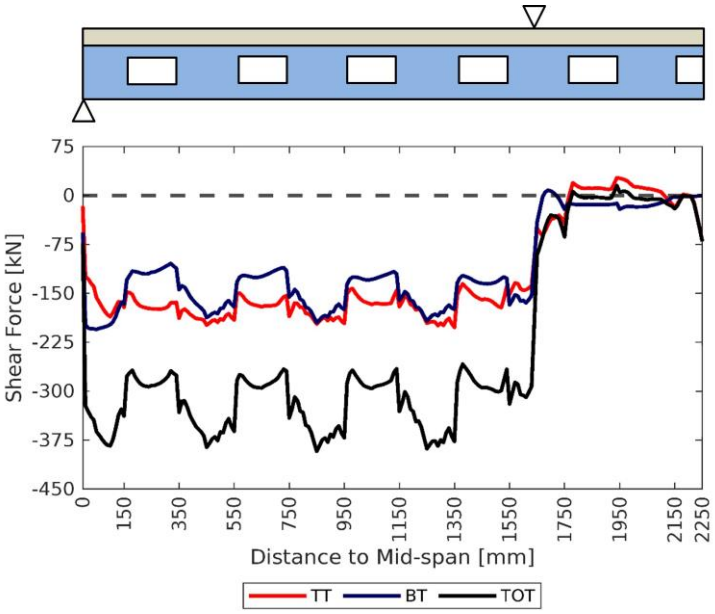

Fig. 2.13 - Shear force redistribution between the T-sections of a composite beam with web openings.

Concentrating on the shear resistance of a composite section with web opening, it is mostly expressed as an aggregate of the strength of a concrete slab over particular width

and the residual steel section. In addition, expressions presented in [8] demonstrate a strong association between the composite action and the shear resistance at the opening. On this basis, mutual dependence of the Vierendeel bending resistance and shear force redistribution arises. In more detail, the Vierendeel bending resistance is considerably affected by redistribution of shear and normal forces between individual components. Thus, if their proportions are not clearly determined, a proper estimation of the Vierendeel bending resistance is difficult to obtain. Moreover, if the layout of shear connectors changes, the composite action does the same leading to redistribution of shear forces and consequent variation of the Vierendeel bending resistance.

So, attempting to solve this laborious task, a design approach adopting an iterative procedure has been developed and published in [8]. Its brief outline is presented in section 2.3.3.4.

2.3.2.3 Plastic Bending Resistance Considering Shear

In the case of presence of high shear forces, the web resistance contributing to the overall bending resistance is typically reduced by a simple interaction formula given in EC3 [20].

2.3.3 Local Analysis

Due to opening presence, a composite beam experiences a complex stress state. This state is characterized by development of additional stresses caused by redistribution of shear force around an opening. In many cases, the consequent local effects tend to be the governing aspect of resistance verification. Therefore, composite beams having web openings shell be verified at least against the following actions:

- the Vierendeel bending of the T-sections,
- horizontal shear at web posts.

2.3.3.1 Bending Resistance of Tee Sections

As the main cause of the Vierendeel bending existence originates in a transfer of shear forces over a depth of an opening, large strains arise in the vicinity of opening corners. Furthermore, these strains are being developed in a specific manner which allows retaining of forces across an arbitrary opening in equilibrium, thus, a formation of additional bending moments and shear forces is of the utmost necessity.

2.3.3.2 Vierendeel Bending Resistances

To satisfy a demand for a safe structural design, the Vierendeel bending resistance has to be evaluated. It consists of three individual components:

- bending resistance of the top Tee ($M_{tT,NV,Rd}$),
- bending resistance of the bottom Tee ($M_{bT,NV,Rd}$),
- local composite Vierendeel bending resistance ($M_{vc,Rd}$).

Consequently, it has to be verified against the Vierendeel bending moment ($M_{vc,Ed}$). The equation covering this assessment may be expressed as:

$$2.M_{tT,NV,Rd} + 2.M_{bT,NV,Rd} + M_{vc,Rd} \geq M_{vc,Ed} \quad (1)$$

where

$M_{tT,NV,Rd}$ = *the bending resistance of the bottom Tee, reduced for coexisting axial tension and shear*

$M_{bT,NV,Rd}$ = *the bending resistance of the top Tee, reduced for coexisting axial compression and shear*

$M_{vc,Rd}$ = *the local composite Vierendeel bending resistance*

$M_{vc,Ed}$ = $V_{Ed}.l_o$ *(the Vierendeel bending moment)*

where

V_{Ed} = *the design value of the vertical shear force*

l_o = *the effective length of an opening*

As could be noticed, the co-existence of additional forces acting on the Tee sections has to be taken into consideration as well.

2.3.3.3 Bending Resistance Considering Axial Force

In the case of simultaneous existence of bending and axial force acting on the Tee, the reduction of plastic bending resistance may be expressed using standard formula:

$$M_{pl,N,Rd} = M_{pl,Rd}.(1-(N_{ed} / N_{pl,Rd})^2) \quad \textit{for Class 1 and 2 sections} \quad (2)$$

where

$M_{pl,N,Rd}$ = *the reduced plastic resistance of the Tee taking account of axial forces*

$N_{pl,Rd}$ = *the axial resistance of the Tee*

N_{Ed} = *the design value of the axial force in the Tee due to the global bending action*

2.3.3.4 Bending Resistance Considering Shear

In a general case, a composite beam is stressed by combination of flexural and shear forces. So, by its local resistance justification at an opening, it is vital to exactly know the proportion of shear forces for the Tees, because it may reduce their effective thickness for bending and axial resistances. In other words, if the top Tee is more utilized in shear as the bottom Tee, it can contribute less to the to the Vierendeel bending resistance what leads to development of much more extensive axial stresses in the bottom Tee and vice versa. Recently, the Vierendeel bending resistance considering axial and shear forces is defined using the following procedure:

- The shear resistance of the bottom Tee $V_{b,Rd}$ is firstly set to zero.
- The effective web thickness of the top Tee $t_{w,eff}$ is evaluated.
- The plastic bending resistance of the top Tee $M_{tT,NV,Rd}$ is determined.
- The plastic bending resistance for the bottom Tee $M_{bT,NV,Rd}$ is estimated.
- The associated shear force in the bottom Tee $V_{b,Ed}$ is evaluated as:
    - $V_{b,Ed} = 2.M_{bT,NV,Rd}/l_e$.
- The coexisting shear force in the top composite Tee $V_{t,Ed}$ is figured as:
    - $V_{t,Ed} = V_{Ed} - V_{b,Ed}$.
- The Vierendeel bending resistance is verified.
- If the verification does not meet the conditions, the utilization of the Tees may be determined from the calculated values of $V_{t,Ed}$ and $V_{b,Ed}$ and the Vierendeel bending resistance is re-evaluated. A single iteration is generally adequate.

Even though the presented approach seems to be straightforward and ease to apply, lack of conciseness might be witnessed.

For more convenient design process, it is typical to attribute the shear resistance only to the top part of a composite cross-section. This assumption is based on an extensive utilisation of the steel bottom Tee in bending, thus reducing residual carrying capacity for other actions. On the other side recent evidence from [11] has established, the steel bottom Tee is able to carry from 10% to 40% of the total shear force.

On the basis of presented, significant lack of conciseness can be witnessed.

2.3.3.5 Contribution of the Local Composite Action to the Vierendeel Resistance

From the global point of view, the bending resistance of a beam section owing to the composite action might be increased by 50% to 100% compared to a beam solely fabricated from steel. Furthermore, this phenomenon plays a crucial role in the Vierendeel bending as well. As was mentioned in [8], the composite action between the

steel top Tee and a concrete slab can significantly increase the local bending resistance of the top Tee compared to the only-steel beam with web openings. The factor by which is the resistance amplified spans from 2 to 3. Owing this capability, the openings of a larger size for composite beams can be designed. However, it is important to note, this vital resistance enhancement strongly depends on the layout of shear connectors over the opening length (Fig. 2.14).

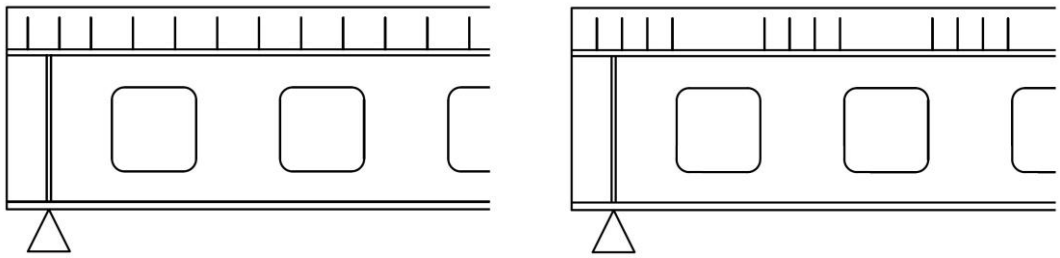

(a) (b)

Fig. 2.14 - Alternatives of shear studs´ redistribution a) uniform, b) non-uniform.

This can be clearly seen from a formula defining the Vierendeel bending resistance as:

$$M_{vc,Rd} = \Delta N_{c,Rd}.(h_s + z_t - \frac{5}{10}.h_c).k_o \qquad (3)$$

where

h_s = *the overall depth of the slab*

z_t = *the depth of the centroid of the top Tee from the outer edge of the flange*

h_c = *the depth of concrete above the decking profile*

k_o = *a reduction factor due to the flexibility of the opening*

$\Delta N_{c,Rd}$ = $n_{sc,o}.P_{Rd}$, *the compression force developed by the shear connectors placed over the opening*

where

$n_{sc,o}$ = *the number of shear connectors placed over the opening*

P_{Rd} = *the design resistance of the shear connectors*

As was documented, a change of shear connector layout might have a great importance for the Vierendeel bending resistance, thus leading to yet undefined force redistribution. For instance, considering Figure 5.4 this means, if the composite action is weakened over an opening, the stress state has to undergo a certain change. Especially, forces acting around an opening could be transferred, which might result in more extensive utilization of the web-post areas or the bottom Tee. This might work also in the opposite manner.

2.3.3.6 Horizontal Shear Resistance of the Web-post

The horizontal shear force acting on the web-post region is defined as a change of the tension force in the bottom Tee at the length of centre-to-centre opening. Likewise, as by the Vierendeel bending resistance, the composite action represents a significant aspect for the horizontal shear resistance evaluation. To be specific, its value varies depending on the number of shear connectors above the web-post. That means, if there is inadequate magnitude of the composite action, the web-post region stresses increase and vice versa. So, when designing, the design value of the longitudinal shear force ($V_{wp,Ed}$) acting on the web-post should be determined at first. This might be defined as follows:

$$V_{wp,Ed} = \frac{V_{Ed}.s - \Delta N_{cs,Rd}.(z_t + h_s.\frac{5}{10}.h_c)}{he_{ff}} \quad (4)$$

where

Ved = *the design value of the average of the shear forces at the centrelines of adjacent openings*

s = *the centre-to-centre spacing of the openings*

z_t = *the depth of the centroid of the top Tee from the outer edge of the flange*

h_s = *the overall depth of the slab from the outer edge of the flange*

h_c = *the depth of concrete above the decking profile*

$\Delta N_{c,Rd}$ = $n_{sc,s}.P_{Rd}$, *the compression force developed by the shear connectors placed over the opening*

where

$n_{sc,s}$ = *the number of shear connectors between the centrelines of adjacent openings*

P_{Rd} = *the design resistance of the shear connectors*

Regardless of the complex stress state at the web-post due to the local forces, its resistance in the horizontal shear might be expressed as:

$$V_{wp,Rd} = \frac{(s_o.t_w).f_y / \sqrt{3}}{\gamma_{M0}} \tag{5}$$

where

s_o = *the edge-to-edge spacing of the openings*

t_w = *thickness of the web*

So, with respect to demonstrated, it can be presented the same conclusion as in the previous chapter. That means, the composite action, so the shear connector layout, might have a great importance not only for the web-post resistance but for the Vierendeel bending resistance as well, because it affects into some extent redistribution of shear forces.

2.4 Summary

A was demonstrated, studies over the past few decades have provided important information on behaviour of composite beams. It might be concluded, fundamental principles describing the load response are understood well. In fact, several design concepts have been established.

Reflecting one of the most complex of these, an unacceptable paucity was witnessed for the following subjects:

- Actual effects of non-uniform layout of shear connectors on behaviour of composite beams with web openings.
- Redistribution of shear force between the Tees of composite beams with web openings.

Especially, the first one was examined primarily from the theoretical point of view. To remedy this adverse state, two alternatives of the shear connectors' layout (uniform (BRU) and non-uniform (BRN)) were applied for the experimental samples.

Regarding the second subject, there is still lacking an exact approach classifying the shear force proportion for the T-sections, albeit its great importance for the Vierendeel resistance evaluation. Aiming to provide more concise approach, comprehensive parametric FE analysis is caried out. In which, configuration of shear connection and composite cross-section are deeply examined.

Based on the presented in this chapter, strong fundamentals for partial completion of the first aim of the thesis:

1. Proposal and realisation of the experiment focused on the resistance and behaviour of composite beams with web openings.

were built.

3 ANALYTICAL-NUMERICAL PARAMETRIC STUDIES

Combining approach from design standards, up-to-date research and FE-based software, the following parametric studies have been conducted to enlarge understanding of behaviour of composite beams with web openings and pave the way for the following parts of this research - the experimental programme and the parametric FE investigation.

In general, these studies have followed a concept of a systematic continuous work. Respecting said, the core body of the following sections can be divided into three main parts investigating:

- behaviour of composite beams with web openings during the erection stage (section 3.2),
- effects of configuration of shear connectors and web openings (section 3.3, 3.4, 3.5),
- possibilities of concrete modelling in ANSYS (section 3.6).

It has to be noted, excepting the last topic, herein presented studies have very the same methodology. Therefore, its general description will be addressed. Later, outcomes from individual surveys will be discussed. At last, the general conclusions will be drawn.

3.1 General Methodology

Generally, these studies served as a starting point for an analytical design phase of the experimental programme.

To produce sufficient number of relevant evidence, analytical-numerical calculations were conducted. By doing so, the numerical data were verified against analytical ones – based on principles of the beam theory. However, the correlation between these data sets was based only on a comparison of the global effects. That means, no local effects were considered.

Further, these parametric studies have taken into account a particular amount of beam samples having different classes of spans, consequently different cross-sections. The location of the openings, their size and other parameters were designed according to the recommendations in [8]. Besides mentioned, the shape of web openings had rectangular form across all the samples.

Ensuring relevance of obtained results from individual classes of beams, certain constraints were placed on cross-section characteristics and utilization in certain type of loading.

Speaking of the former, for instance, the heights of steel and concrete parts, respectively, were fixed in proportion to individual beam spans (L/15 for steel and L/25 for concrete).

Considering the latter, the global resistance of beam samples was justified according to EC3 [20] and EC4 [21]. Moreover, the beams were designed in a manner allowing them to achieve only a certain magnitude of utilization in bending and shear at the critical sections. The evaluation of the overall resistance considers only the full degree of interaction. Further, boundary conditions were applied in the form of simply supported beam with uniformly distributed load of magnitude determined according to EC3 [20].

From the material perspective, strength of employed materials was across all of the studies of the same class as well. That means, a strength class considered for steel was S235, while for concrete it was C20/25.

Moving spotlight to the numerical part of these analyses, the composite beam samples has been examined in a simplified manner, although attempting to capture the load-response precisely. Hence, only beam and shell elements were used in these FE models. The basic form of the model can be seen in (Fig. 3.1).

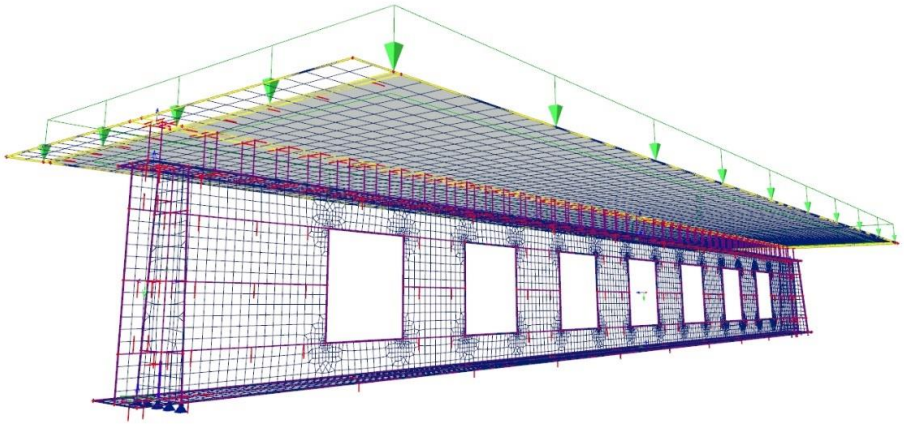

Fig. 3.1 - Representative of simplified FE models.

In the model, shell elements discretizing both steel and concrete components were associated with material nonlinearities. In detail, these elements are capable of plasticity, stress stiffening, large deflection, and large strain. In contrast, the one-dimensional beam elements presenting shear connectors were able to capture their behaviour only in the range of elastic stresses using composite cross-section with corresponding stiffness in bending and shear.

In this way, two fundamental principles with respect to mechanical behaviour of shear connectors could be expressed, namely:

- contribution of concrete surrounding the shear stud to the bending resistance of an individual connector, also known as the bearing cone,
- contribution of only the steel part of a stud to the shear resistance.

This provision was based on the general knowledge regarding behaviour of a shear connection and the research carried out in [6].

Further, individual components of FE model were meshed in a mapped manner, excepting regions near corners of openings, where the mesh was refined in order to obtain more reliable results. As the full degree of interaction was assumed, the connection between studs and top flange was modelled as rigid.

3.2 Lateral-torsional Buckling of Non-symmetrical Plate Girders with Web Openings

During the erection phase of composite steel-concrete structural systems, steel beams behave as an individual bearing components and need to be designed predominantly against bending, shear, and their mutual combination. However, behaviour of these bearing members depends not only on their material properties, but also on their properties with respect to a cross-section, the member slenderness, support conditions, and a configuration of the applied load. So, if such beams do not have sufficient lateral stiffness or lateral support, it might buckle out of the loading plane. The critical value of a load at which buckling occurs may be much less than the girders' in-plane bending resistance. The lateral-torsional resistance, usually given in the form of the maximum moment that can be safely carried M_{cr}, could be affected by many factors. One of the most important that has an eminent impact is the existence of web openings. Hence, the principal reason for this investigation laid in an influence assessment of web openings on the lateral-torsional buckling resistance. So, a set of composite beams having web openings were investigated under the construction phase conditions. It should be noted, this topic has caught our attention especially for very common employment of an asymmetric steel section, which even more highlight the importance of the instability mode justification. By usage of asymmetric steel section, an increase of the moment capacity is ensured, but in contrast, the position change of the gravity centre leads to a notable decrease in the buckling resistance. Thus, an analytical-numerical calculations within this study were performed.

Design of investigated samples considered two construction stages. In the erection stage, the beam samples behaved as individual steel bearing members, while in the service stage, they became composites (Fig. 3.2).

Fig. 3.2 - Investigated samples during the erection and service phase.

In general, for an elastic idealized perfectly straight beam, there are no out-of-plane deformations until the applied moment M reaches the elastic buckling moment M_{cr}. Subsequently, the beam buckles by twisting and lateral deflection. In general, the elastic critical moment M_{cr} depends on the minor axis flexural rigidity EI_z, torsional rigidity GI_t, and warping rigidity EI_ω of the girder.

$$M_{cr} = \sqrt{\left[\left(\frac{\pi^2.E.I_z}{L^2}\right).\left(G.I_t + \frac{\pi^2.E.I_\omega}{L^2}\right)\right]} \tag{6}$$

The critical load factor α_{cr} defines susceptibility to the lateral-torsional instability; it represents the value by which the applied moment should be multiplied to attain the point of instability.

$$M_{cr} = \alpha_{cr}.M\,, \;\rightarrow\; \alpha_{cr} = \frac{M_{cr}}{M} \tag{7}$$

The design rules are often based on a simple analysis assuming initial imperfection in the form of crookedness and twist. Hence, the reduction factor χ_{LT} for the lateral-torsional buckling is adopted. One of the most notable parameters is the critical slenderness. For the lateral-torsional buckling the reduction factor is calculated as:

$$\chi_{LT} = \frac{1}{\Phi_{LT} + \sqrt{\Phi_{LT}^2 - \overline{\lambda_{LT}^2}}} \tag{8}$$

Currently, as the standards use for the lateral-torsional resistance evaluation only the steel section omitting presence of the web-post regions, the resistance might be overly conservative. In order to properly define this abundant resistance, the analysis based on FE method was performed. So, as the elastic lateral-torsional buckling M_{cr} represented

the desired failure mode of the beam specimens, the material stress-strain diagram was defined only as linear. The stability analysis was executed to obtain the ratio α_{cr} of the buckling load F_{cr} to the applied load F. Trying to attain this ambition, Lanczos algorithm scheme was exploited using an iterative procedure to determine the critical load factor α_{cr}.

Speaking of the results, the analytical examination indicated, evaluation of the elastic critical moment M_{cr}, based on full and net cross-sectional properties, has produced considerable discrepancies (Fig. 3.3).

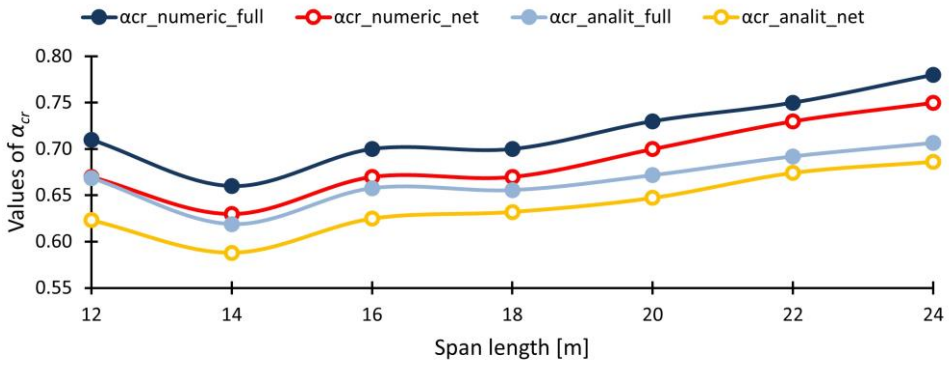

Fig. 3.3 - Values of critical load factor α_{cr} for beams with 4 meters load width.

Concentrating only on findings derived on the basis of the analytical approach, an apparent decrease in a magnitude of the critical load factor α_{cr} at the level of 0.05 can be seen between samples having full and net steel section. This can be associated primarily with reduction of the cross-sectional web area by openings´ introduction.

Further, the data obtained from both the analytical and the numerical analysis, show similar contours. By their comparison, the results from the FE models show an increase of almost 10% compared to the analytical outcomes. Moreover, this applies for both of cross-sectional types. Clearly, this enhancement can be directly linked to the configuration of the FE models allowing for contribution of the web-post regions to the buckling resistance M_{cr}. On this basis, it can be stated, the values derived from the analytical examination tend to be slightly more conservative in comparison to the numerical ones. In this sense, the resistance assessment under European standards [20] could be described as safe but neither sufficiently precise nor cost saving.

In the following, relation between reduction of a web area section and the critical load factor α_{cr} was studied. In order to evaluate this possible dependence transparently, ratio forms of:

- web section area with and without opening,

- critical load factor α_{cr} having net and full cross-section,

were considered. As shown in Fig. 3.4, the reduction in a value of the critical load factor α_{cr} had almost the same tendency as the reduction of the overall web area. That means, the change of a web section area has a direct impact on a value of the critical load factor α_{cr}.

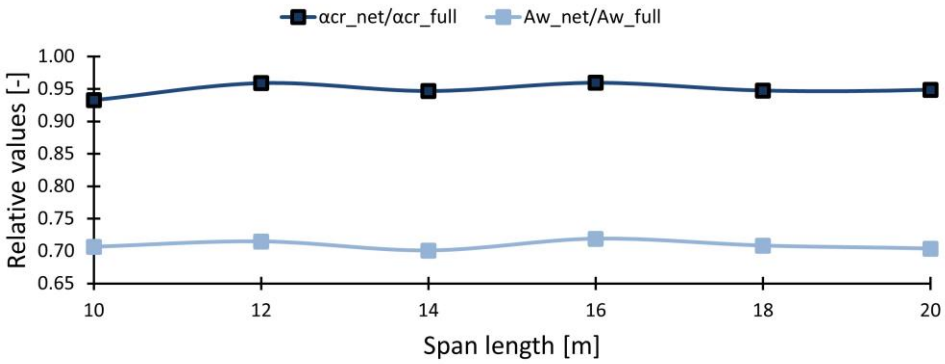

Fig. 3.4 - Dependence of the change of a web section area and the critical load factor in a ratio form.

The additional findings are related to the reduction factor for the lateral-torsional buckling χ_{LT}. Results are illustrated in Fig. 3.5. As is visible, values of the buckling reduction factor χ_{LT} have varied independently among the samples regardless of the limitations applied for resistance utilization, geometry, and other considered constraints.

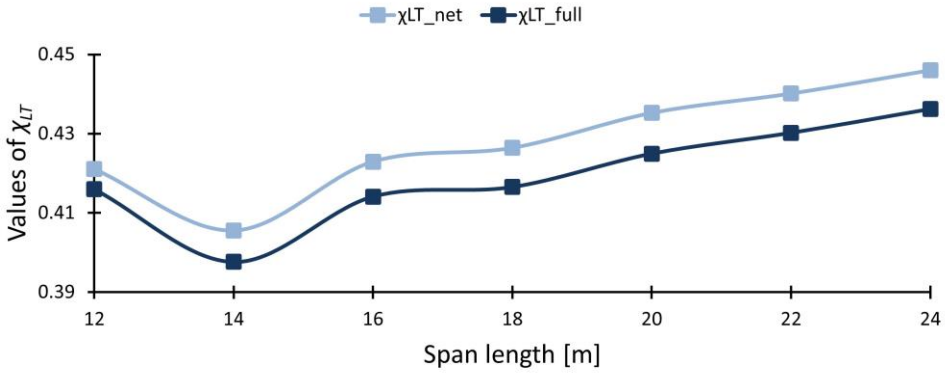

Fig. 3.5 - Variation of the buckling reduction factor χ_{LT}.

Among other findings, it was observed, the cut-down of the cross-sectional web area generated a serious decrease of torsional rigidity G_{It} compared to the horizontal flexural rigidity EI_z and the warping rigidity EI_ω (Fig. 3.6).

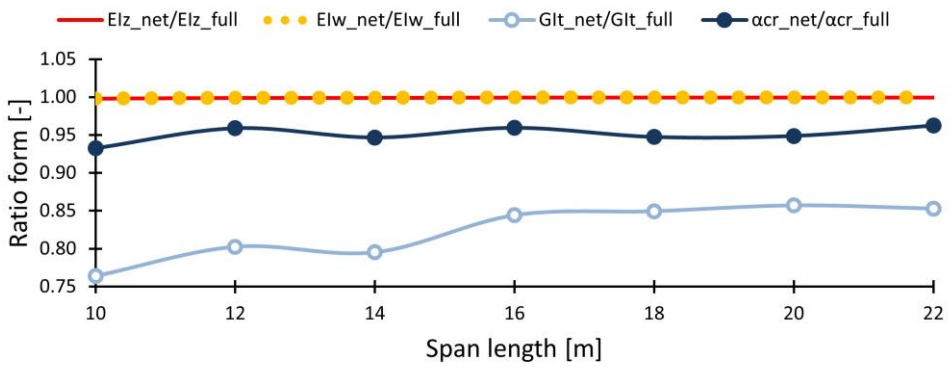

Fig. 3.6 - Change of rigidity and α_{cr} of net and full steel cross-section.

Focusing solely on contours of α_{cr} and G_{It}, it was confirmed, their relation could be defined a strongly interconnected. In other words, as the ratio values of α_{cr} varied, the values of G_{It} did almost the same. In contrast, the change of horizontal flexural rigidity EI_z and warping rigidity EI_ω is negligible, so their values are coincidental and equal to 1.0.

Summarizing the study, it was shown, the lateral-torsional stability of composite bearing members is doubtlessly affected by existence of web openings.

The data has also pointed out, the magnitude of critical load factor α_{cr} is sensitive not only to flanges' dimensions, but also to the web ones. That means, if the web area is reduced by an opening, the value of critical load factor α_{cr} experiences notable reduction as well. Especially, the torsional rigidity G_{It} has experienced a notable reduction varying from 8 to 33% depending on the particular cross-section dimensions.

Based on the presented results, more conservative assessment of the resistance against bending instability can be assigned to the analytical approach. That means, an enhancement in a form of a factor incorporating the overall web area, expressing the unused lateral-torsional resistance of a member, could be implemented into standards.

Notwithstanding the presented conclusions, a detailed investigation having experimental basis and accounting for imperfections will be necessary for definition of an enhanced approach.

3.3 Distribution of Longitudinal Shear Forces in Composite Beams with Web Openings

The main purpose of this parametric study was to investigate the shear flow behaviour at the material interface in the range of the elastic deformations. Three alternatives of shear studs´ layout using the same number of connectors were considered (Fig. 3.7).

The studs were spaced along the length of the investigated beams according to the following manner:

a) uniformly (Alternative 1),
b) concentrated above the edges of the openings (Alternative 2),
c) concentrated above the web-posts (Alternative 3).

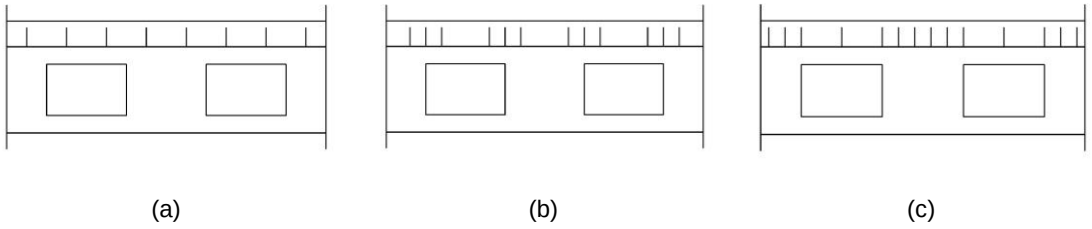

Fig. 3.7 - Three alternatives of shear studs´ layout.

Then, the findings from both the analytical and numerical parts were compared.

The following figure (Fig. 3.8) demonstrates behaviour of shear forces along the individual beam samples. significantly uneven distribution of horizontal shear forces can be observed. This phenomenon might be attributed to the impact of both, the presence of web openings and layout of shear connectors.

In Alternative 1, which considered a uniform distribution of shear studs, the values of the shear flow oscillate around the curve determined by the theoretical treatment. So, as no additional adjustments were performed excepting introduction of openings, the given longitudinal shear force contour is predominantly influenced by the presence of openings.

Considering Alternative 2, in which the concentration of shear studs at the edges of openings was adopted, a considerable difference in respect of individual utilization of connectors in shear can be observed. Therefore, this alternative does not seem to represent an optimal layout.

Moving to Alternative 3, which employed concentration of shear studs above the web-post regions, the survey has revealed, the obtained values are almost of the same nature as data having theoretical foundations which represents a smooth response.

That means, this alternative might have potential to reduce the additional stresses in individual connectors caused by the opening existence, thus allowing more uniform distribution of forces resulting in more effective utilization of connectors´ total load-bearing capacity.

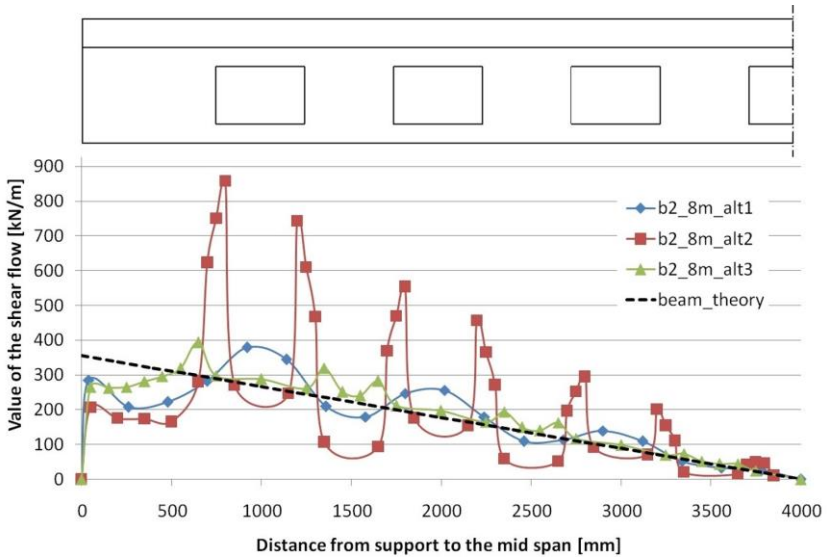

Fig. 3.8 - Shear flow behaviour of three alternatives of shear studs´ layout.

This potential might be more visible from the following figure (Fig. 3.9) exploiting relative values of shear flow magnitude compared to the analytical results.

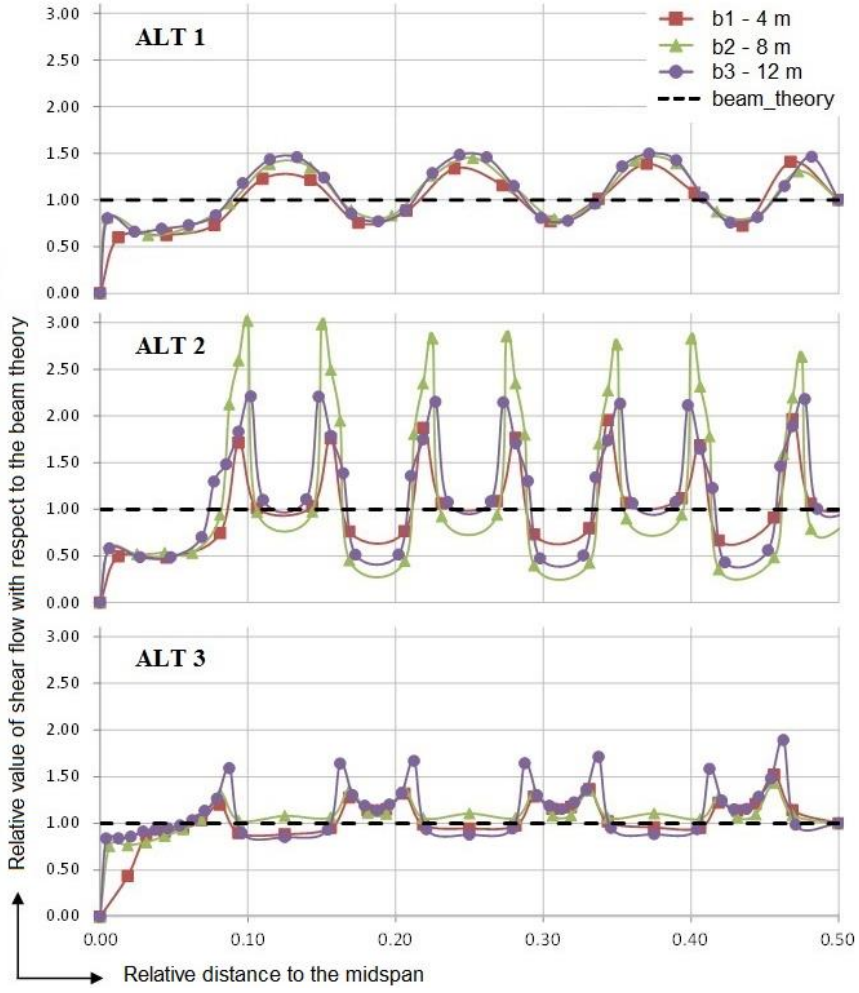

Fig. 3.9 - Shear flow under different layout of shear connectors (relative values).

It shall be concluded; both the presence of openings and the layout of shear studs have a significant influence on the shear flow pattern. As the findings revealed, there might exist an optimal layout of shear connectors enabling more suitable redistribution of forces between individual studs. Possibly, such an optimal state might positively influence not only the load bearing capacity of connection, but also the overall structural response of a composite beam with web openings. The reasoning behind this statement is based on essential ability of connection allowing advanced development of plastic potential of combined materials.

3.4 On Influence of Web Openings Presence on the Structural Performance of Steel and Concrete Beams

This study continuously extends the previous one (section 3.3) focused on the shear flow magnitude at the bond interface. In contrast, this study contains suitably adjusted dimensions of samples and improved numerical model. Although, the basic principles of the samples' design remained unmodified.

In addition to the previous study, an influence of gradual reduction in number of openings considering two different alternatives was investigated. Speaking of the first alternative - Alternative 1, the openings were reduced in a direction from the centre to the outer edges of a beam sample. Based on that, the number of openings for this group of beams was 7, 6, 4, 2 and 0 (beam without any opening). Conversely, Alternative 2 used direction from the supports towards the midspan. Therefore, this group of samples had 7, 5, 3, 1, and 0 openings. The mentioned alternatives are depicted below (Fig. 3.10).

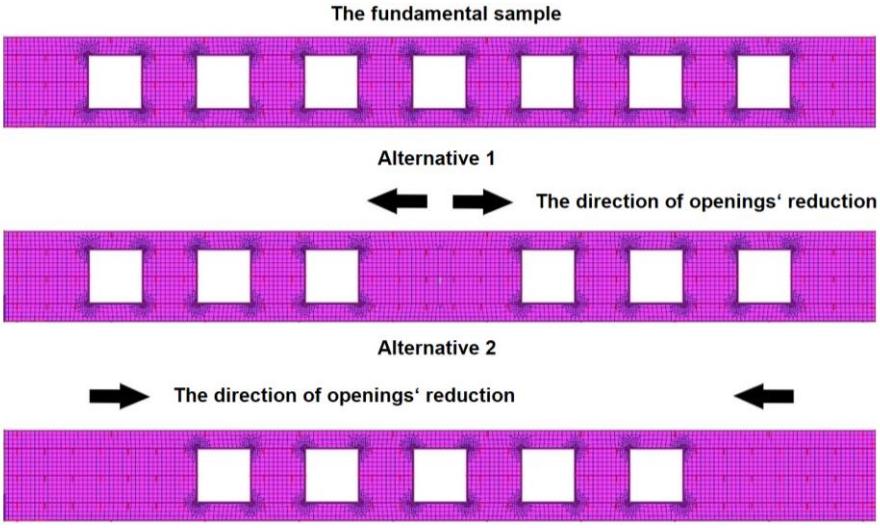

Fig. 3.10 -Alternatives of openings´ number reduction.

Compared to the former study using similar FE model, behaviour of elements discretising shear studs, was refined using bi–linear character in shear loading (Fig. 3.11). This non–linearity was introduced for the contact between the heel of the shear stud and the top surface of the steel flange, whereas the force–slip relationship was derived from the experimental evidence published in [22].

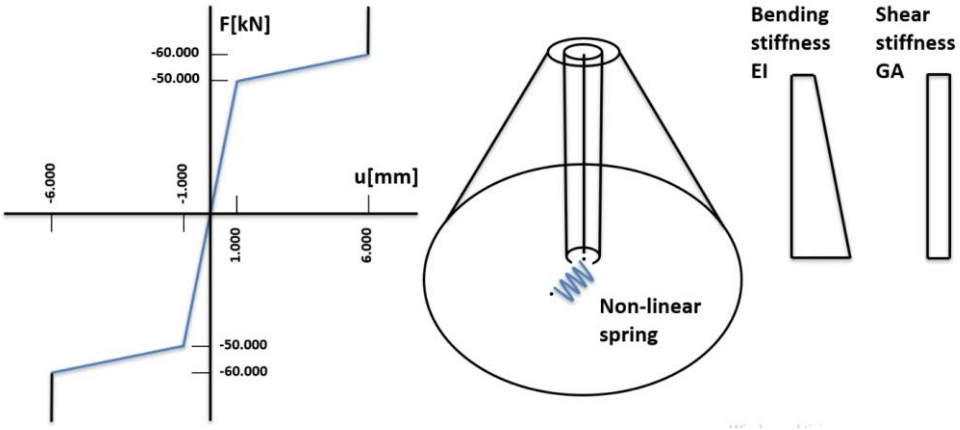

Fig. 3.11 - Discretization of a shear stud in the FE model.

To illustrate the influence of the web openings presence on the structural performance of composite beams, the total strain diagram for two limit cases having either 7 or no openings is shown in Fig. 3.12. As can be seen, the strain distribution in the beam with no openings has a typical behaviour. On the contrary, the strain diagram for the sample with 7 openings is affected significantly. Periodical deviation of strain magnitude is visible.

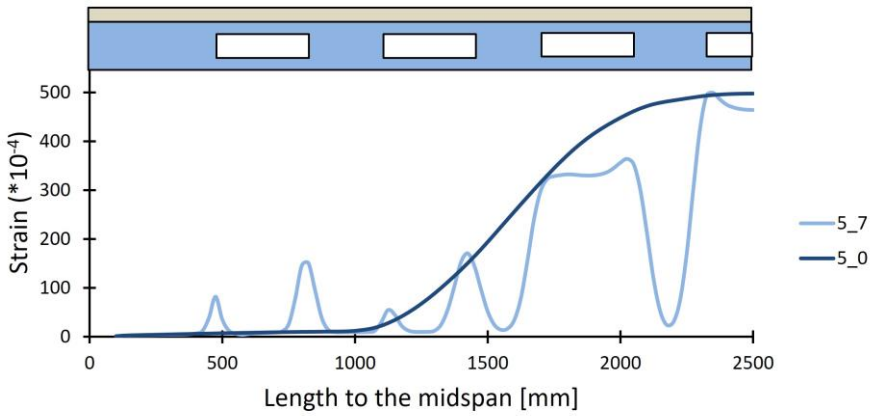

Fig. 3.12 - Diagram of total strains for the fundamental samples.

The following figure (Fig. 3.13 a) and b)) represents results for 4 m long specimens. The curves demonstrate a change in the strain behaviour under modification of the openings' number resulting in relocation of the most stressed regions.

a)

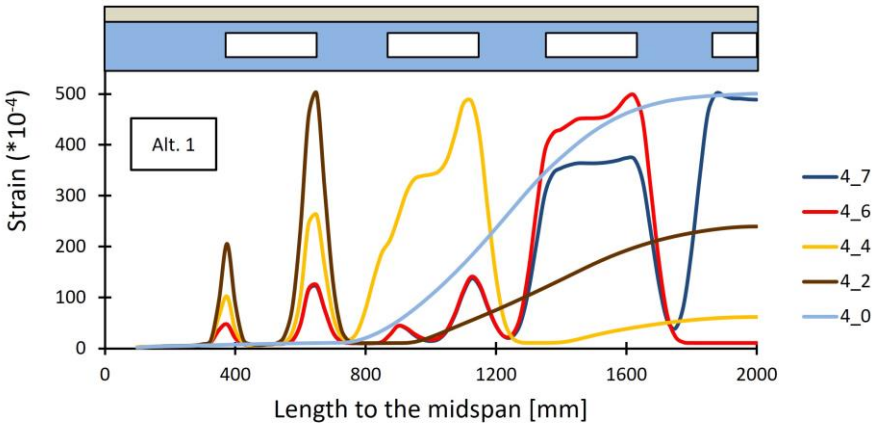

b)

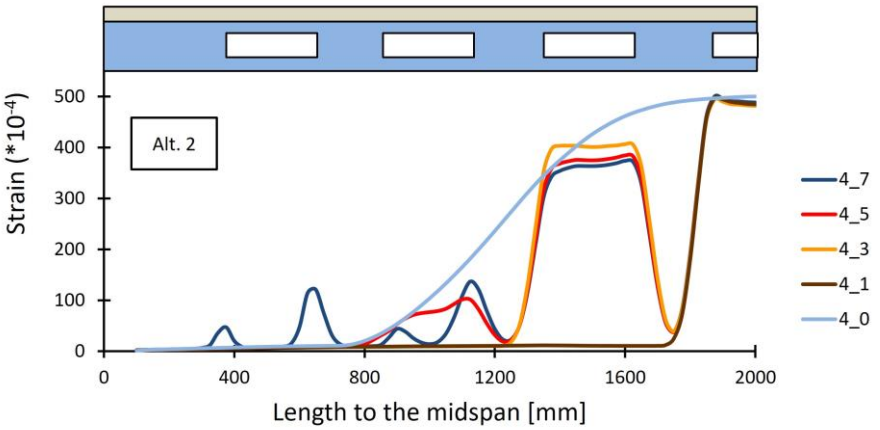

Fig. 3.13 - Total strains in the bottom flange for the span of 4 m.

Results of a) part of the graph correspond to Alternative 1 of the openings' reduction. With the decreasing number of openings, the strain concentration near the support has increasing tendency. In comparison to the sample containing 7 openings, continuously rising character of strain magnitude approaching the midspan remained as in the case of sample having no openings. This outcome indicates a better utilization of the bearing member capacity compared to the beams with openings concentrated close to the support.

In b) part of Fig. 3.13 can be found results for Alternative 2. As this option has adopted a reduction of openings in the direction from the support, the highly stressed regions are located primarily at the midspan. It is worth noting, the samples with 1 and 3 openings experienced main strain concentration near the openings, but the values of strains at the rest of the specimen are negligible.

Furthermore, the overall change of the strain magnitude is captured in Fig. 3.14 a) and b), where behaviour of strains at the locations of the low (LME) and high moment end

(HME) of the openings can be observed. The terms of LME and HME relate to the value of the primary bending moment at a particular side of an opening.

a)

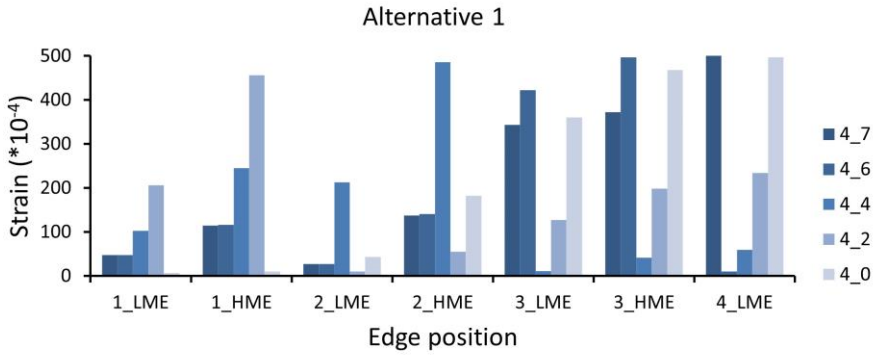

b)

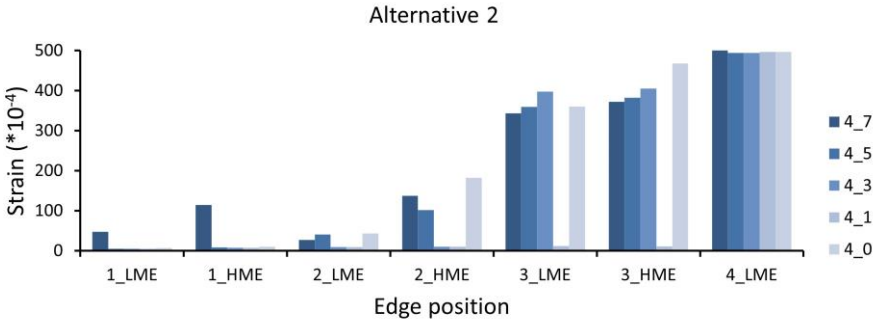

Fig. 3.14 - Diagram of total strains' rate at LME and HME of openings.

The a) part of the graph shows results for beams employing Alternative 1, while the b) represents Alternative 2. As can be noticed, this depiction only emphasizes the conclusions from the previous:

- an increase of strains near the support (Alt. 1),
- continuous rise of strains approaching the midspan (Alt. 1),
- regions having enormous stress gradient are located at the midspan (Alt. 2),
- values of strains beyond openings are negligible (Samples with 1 and 3 openings of Alt. 2).

As the previous results have represented the total strain distribution at the level of bottom flange, the next two graphs analyse the maximum load level for an individual sample. So, in Fig. 3.15, a cumulative change of the maximum applied load in a percentage rate for beams employing Alternative 1 of web openings' reduction is presented.

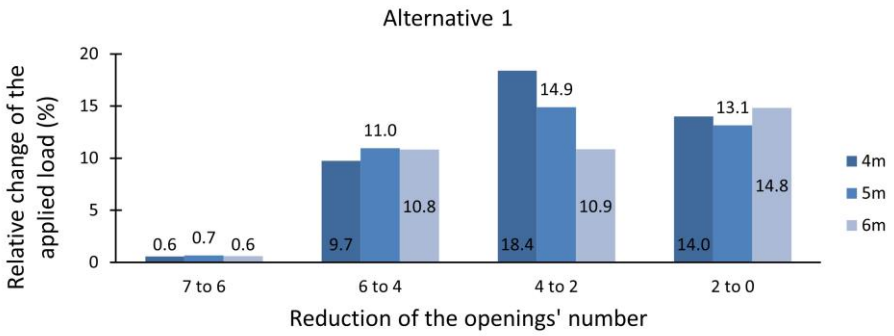

Fig. 3.15 - Change of the maximum applied load rate owing to the different openings' number.

The investigation indicated, when the openings' number is reduced from 7 to 6, almost no influence on the value of the applied load is observed. However, for the other cases, an evident increase is present. In addition, the samples having a span of 6 meters experienced a consistent growth of the load magnitude, while for the rest of samples is such nature not so visible. Nevertheless, an instant cumulative rise in the composite beam resistance is observed.

Inspecting Alternative 2 (Fig. 3.16), samples experiencing the reduction of openings from 7 to 5 and 5 to 3 showed a negligible influence on the beam resistance. Controversially, when the opening number declined from 3 to 1 a slight decrease in the resistance has appeared. This unexpected occurrence might have a source in more intense concentration of stress at the critical region.

Lastly, from the apparent reasons, the extensive rise of the bearing member resistance occurred when no openings are present.

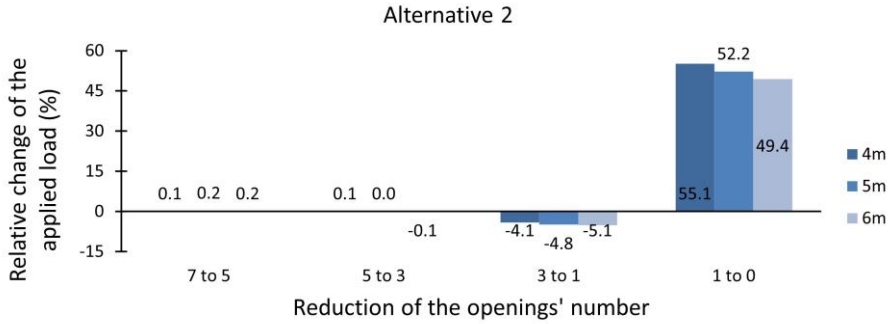

Fig. 3.16 - Change of the applied load rate owing to the different openings' number.

To finalize this discussion, the following graphs represent the strain response for samples differing in span lengths but assuming the same number of openings.

As can be observed in Fig. 3.17, the outline of all curves has the same nature. Despite it, focusing on region between LME and HME, a sudden drop of the strain magnitude

can be seen. This phenomenon has diminished in the area nearing the centre of the beams. Other findings indicate that strains for openings close to the support have almost the same magnitude for LME and HME, respectively. An increasing character approaching the midspan may be thus expected.

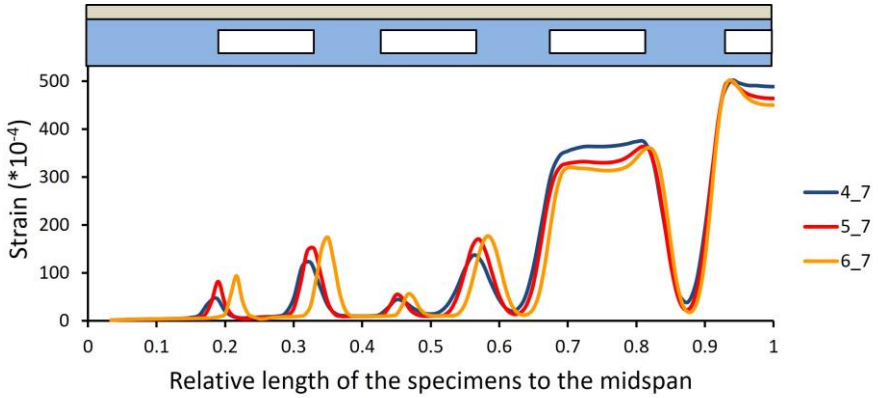

Fig. 3.17 - Strain behaviour of specimens having seven openings and different spans using relative distance to the midspan.

Furthermore, in the region of greater magnitude of strains, there is a slight change in behaviour for specimens having the shortest span (4 m). The curve declination is not so noticeable as for the other samples. Similar tendency was observed for beams with 4 openings employing Alternative 1 (Fig. 3.18). This phenomenon can be referred to the opening to span length ratio. That means, as the length of the span contracts, the length of opening does the same. Consequently, this might lead to a stiffer response of weakened regions by openings and different distribution of strains.

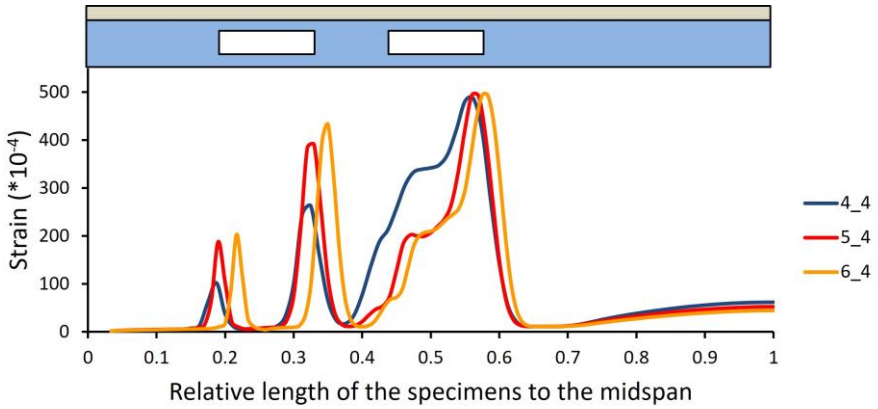

Fig. 3.18 - Strain behaviour of specimens having four openings and different spans using relative distance to the midspan.

Summing up, for composite beams having multiple openings can be recommended:

- omitting an opening in the centre of a beam with multiple openings trying to achieve savings does not represent an effective solution,

- an ideal position of the openings´ region should be bounded at a distance of one opening length from the support area and having the same distance from the midspan.

3.5 Composite Beams with Web Openings Employing Alternative Layout of Shear Connectors

As the previous chapters were concentrated on the investigation of the shear flow behaviour and impact of the opening presence on the overall load response of composite beams having openings, separately, the following study complements both principles and simultaneously deepens an insight into this field.

This objective is accomplished by an alternation of two main parameters. Firstly, the change of openings' number emphasizing the process of opening formation considering the direction of their reduction was examined (Fig. 3.19). To reveal the influence of this aspect, the redistribution of strains and shear flow, respectively, was observed. The strains were measured at the level of the bottom flange, whereas the shear flow was captured at the bond interface. As basic samples, the composite beams with seven and no openings were considered. Following this treatment, two alternatives has arisen. Alternative 1 has contained samples having 7, 6, 4, 2 and 0 openings while Alternative 2 has encompassed samples with 7, 5, 3, 1, and 0 openings. In this case, the beam samples had only continuous distribution of connectors.

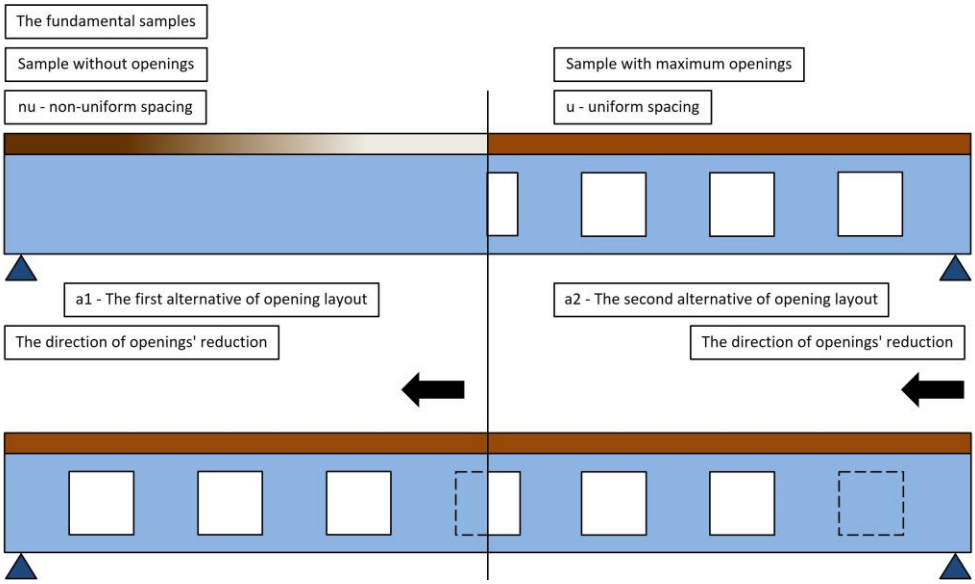

Fig. 3.19 - Fundamental samples and process of openings' number reduction.

Secondly, the influence of shear connectors' layout on the behaviour of longitudinal shear at the level of coupling was observed. Respecting this attribute, several

alternatives of layout were employed, where the matter of examination lays in enhancement of samples´ load response with the same number of shear studs. In particular, shear connectors were distributed along the specimens continuously or in groups. These groups were located above the web-post or opening region. For both alternatives, uniform and non-uniform spacing was assumed.

In more detail, the principle of non-uniform distribution followed the nominal elastic shear diagram. For samples with continuous layout of couplers along the beam, the consistent decrease in shear studs' spacing length was designed. In comparison to the samples employing group spacing, the non-uniformity was presented by a change of shear studs' number for particular group. This yielded into positions having high, normal, or low density of shear connectors. The demonstrative description of investigated beams shows Figure 3.20.

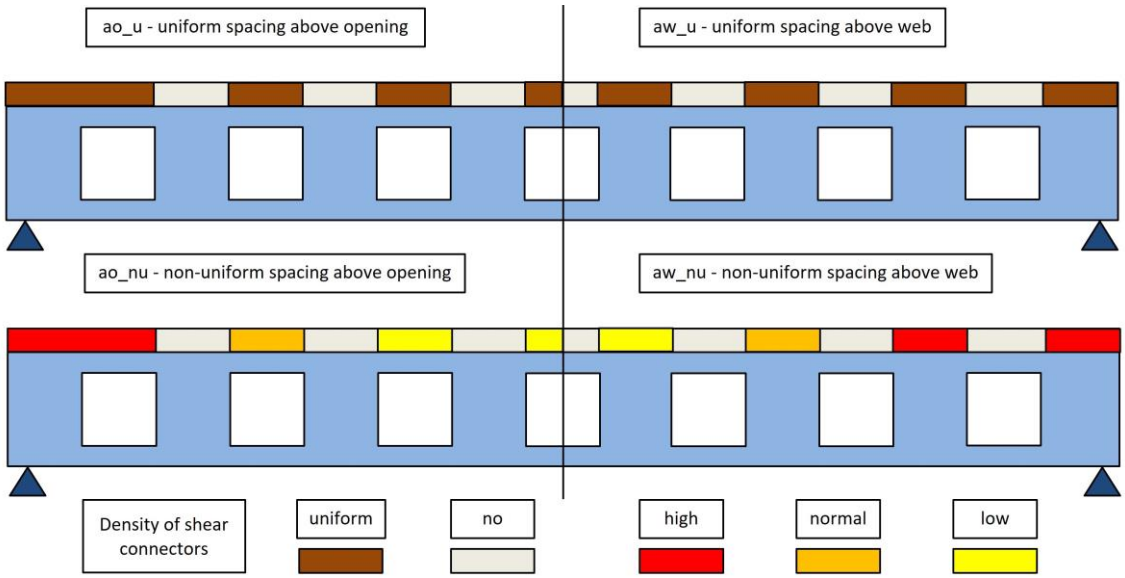

Fig. 3.20 - Samples having grouped connectors.

The first set of evidence discusses the relation between openings' manner formation and shear flow behaviour at the concrete-steel contact for samples having the uniform layout of shear connectors. As illustrated below, the results indicate that difference not only in the opening number but also in the progress of opening removal takes a critical place in mechanical response considering the shear flow magnitudes.

This significance is demonstrated by dependence of total strains at the bottom flange and shear flow distribution, which are visualized in (Fig. 3.21). As can be seen, the curve of the shear flow mirrors the behaviour of strains. This character is observed for both alternatives.

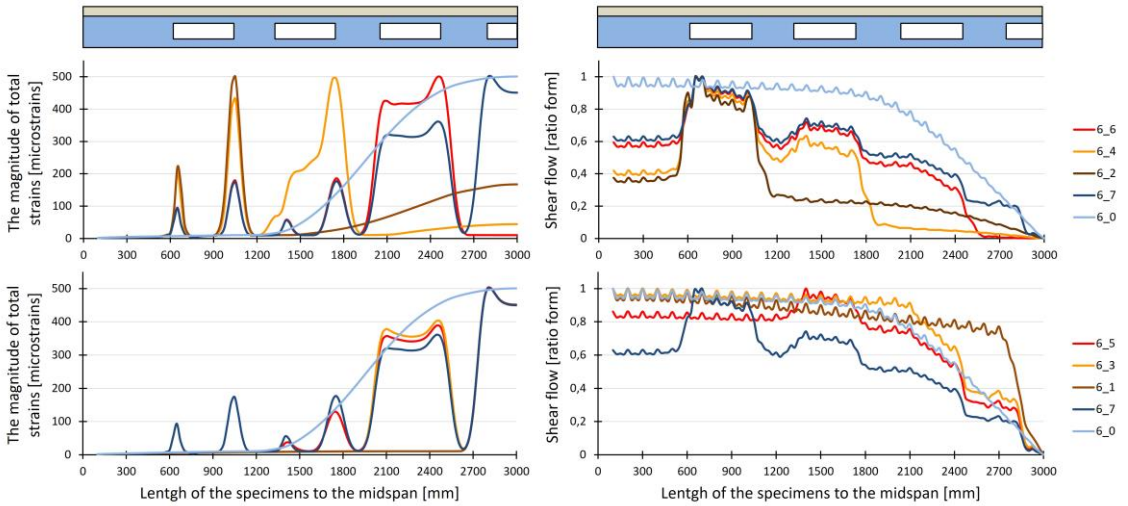

Fig. 3.21 - Structural response of 6m long samples caused by openings' manner formation.

The next set of results is focused only on the variation of shear connectors' distribution and its influence on total strain evolution and shear flow change. In this case, just samples having seven and no openings were investigated. Regarding the shear connectors' layout, both uniform and non-uniform spacing was employed. Based on that, a slight change of data referring to the strain behaviour is observed (Fig. 3.22). Assessing samples having no opening, a shift of the strain curve occurred. While for samples with multiple openings, a decrease in strain magnitude at the opening regions was present. The data relating to the longitudinal shear indicate, in the zones where a decrease in strain magnitude appeared, an increase in the shear flow values is present.

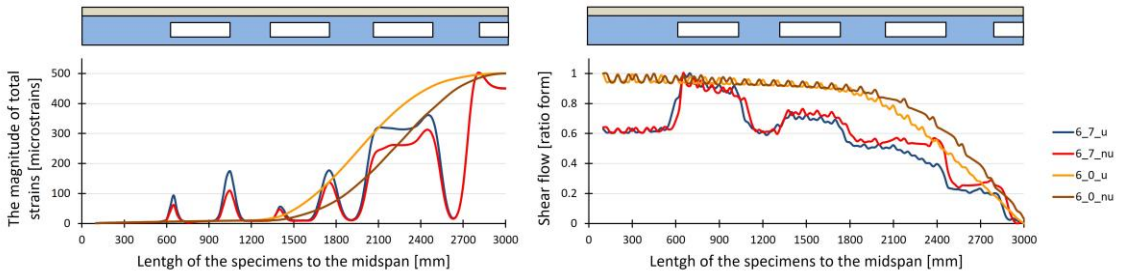

Fig. 3.22 - Structural response of 6m long samples with 7 and 0 openings considering variation of shear studs' layout.

As mentioned before, the beams using connectors concentrated above the web-post or opening region were analysed as well. Hence, the results obtained from this group of specimens will be presented and compared to the reference sample employing continuous distribution of shear studs.

Firstly, beams using uniform spacing are compared (the upper part of Fig. 3.23). Considering the strains, the concentration of connectors above the web caused an increase of developed strains, whereas an opposite effect for samples having studs at

openings is captured. Assessing the shear flow behaviour, a rapid rise followed by a plateau part occurred as a consequence of connectors grouping. Contrary to the previous findings, the reduction of strain magnitude yielded a reduction of shear flow as well.

Secondly, findings covering the beams' response with continuous increase of shear studs' density are presented (the lower part of Fig. 3.23). Comparing samples having a uniform and non-uniform layout of connectors, it can be seen a general decrease of strain magnitude except the centre of a beam. From the shear flow viewpoint, almost the same nature of load response was obtained for samples designated as 5_7_nu and 5_7_aw_nu, while sample 5_7_ao_nu experienced more visible discrepancies.

Assuming both principles, the specimens restrained with connectors at the web-post exhibited a higher value of strains in comparison to samples having shear studs at openings. Moreover, a general decrease of shear flow magnitude is notable for beam 5_7_ao_nu apart from highly stressed locations.

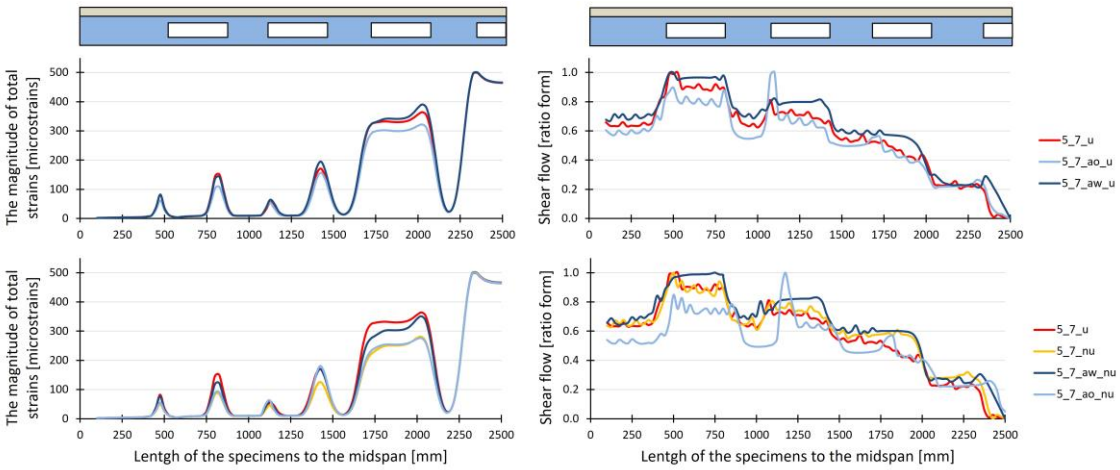

Fig. 3.23 - Structural response of 6m long samples with 7 and 0 openings considering variation of shear studs' layout.

As a summarization of implemented adoptions, a relative change of applied load for particular samples as a ratio to the reference load value of 200 MPa is presented.

The findings related to the opening formation manner can be seen in Fig. 3.24. It is apparent, the value of applied load for Alternative 1 had an increasing nature for all specimens. However, in the case of Alternative 2, relatively constant response excepting the sample with any opening has occurred. What is a typical behaviour for all the samples, in which an opening is present at the midspan.

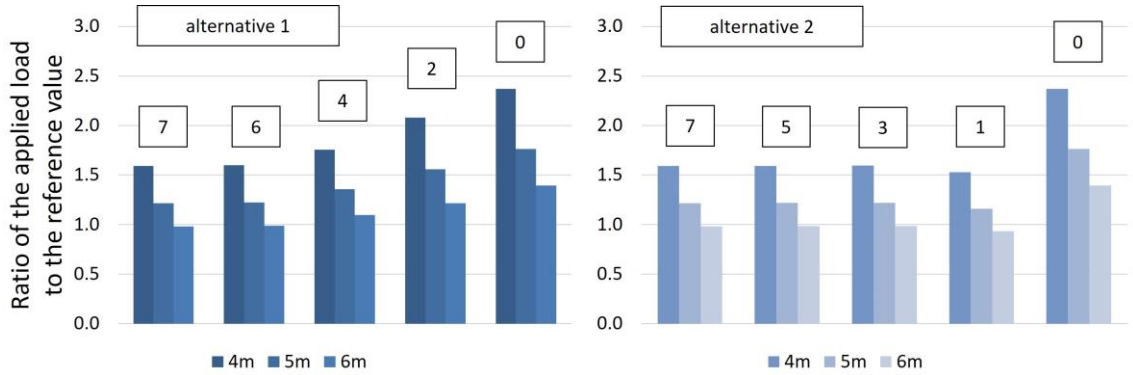

Fig. 3.24 - Comparison of effectiveness considering direction of openings' removal.

The analysis also brought out evidence covering the shear connectors' layout modification. The left part of (Fig. 3.25) revealed, there is no significant increase in applied load magnitude. The detailed comparison is depicted in the right-hand side of (Fig. 3.25), in which the range of values is determined as a ratio of applied load for individual type of sample to the basic sample using a uniform spacing of connectors. It is demonstrated, the introduced variations of shear connectors' layout caused negligible enhancement of carrying capacity even slight loss of it.

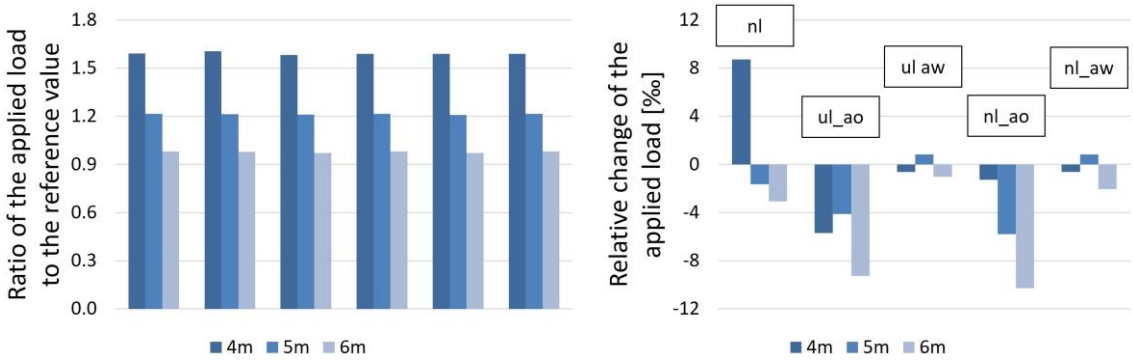

Fig. 3.25 - Overview of final effect of shear studs' distribution change on the maximum applied load.

Based on the analytical procedure and finite element investigation several conclusions can be drawn.

Discussing the importance of opening existence on the strain distribution at the level of bottom flange and shear flow at the steel-concrete interface, respectively, the findings showed, Alternative 1 experienced an increasing nature of load capacity with a reduction of openings in the range of 1 to 14%. On the contrary, Alternative 2 yielded results showing a negligible increase, even a decrease of resistance, omitting the sample having any opening.

Further, the analysis has pointed out; the shear flow is completely influenced by an opening introduction which changes its character. To restrain these negative effects, various modifications of shear connectors' layout were investigated.

Assessing samples using the change from uniform to non-uniform spacing along the length of a beam, the shear flow character and strain distribution was affected noteworthy. Despite this fact, the change in the overall carrying capacity did not experience a greater enhancement.

Regardless of the presented evidence, a firm relation between openings' existence and total strain distribution accompanied by modification of shear flow was confirmed. In addition, it can be claimed, the layout of shear connectors does not play any role in respect of the overall carrying capacity of composite beams with web openings. In order to bolster these deductions, based on the currently derived evidence, an experimental testing, attempting to confirm these results, will be conducted. Moreover, a full-scale parametric investigation using FE method is also intended.

3.6 On FE Modelling Techniques of Concrete in Steel and Concrete Composite Members

This study reports a complex, multiple-load-step, structural nonlinear static analysis of a composite steel-concrete beams with web openings. Moreover, it serves as an initial step for both the justification of analytically designed samples for the experimental testing and more comprehensive FE model used for the subsequent parametric study.

Discussing the analytical part firstly, the overall design of examined samples was provided according to the corresponding theoretical background, design standards [20, 21] and available literature [6, 8]. The overall length of the investigated beams was 4.7 m having span of 4.5 m. The composite samples consisted of a welded 380 mm deep asymmetric I-section having dimensions of the bottom flange of 270x16 mm, the top flange of 120x14 mm, and a web of 350x12 mm. Mentioning the steel web, multiple web openings were cut-off. These openings were centrically placed in respect of the web depth having a square shape of size 200x200 mm. The reader can find the representative of beam samples in the following figure (Fig. 3.26).

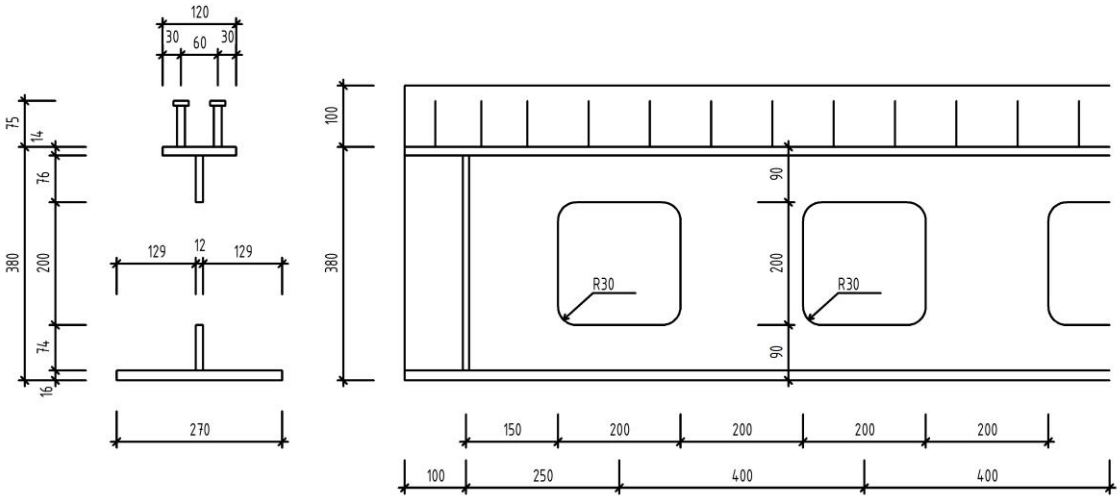

Fig. 3.26 - Cross-sectional dimensions and web opening positioning.

Further, their corners were rounded by radius of 30 mm. Finally, the concrete slab was 100mm deep and 800mm wide. From the material viewpoint, S235 steel class was used for the steel component whereas the concrete strength was of 28 MPa.

In general terms, web opening presence evokes additional stress occurrence in the form of the Vierendeel bending and other failure mechanisms [8]. Hence, a complex design approach is necessary which adopts employment of specific geometry limitations and several limit state assessments. For the purpose of this study, the beams were verified only against the global forces - shear and bending. This verification was performed at the most critical location - at the middle of opening located closest to the place of the force application, where the combination of both, the shear force and bending moment produces the most stressed location.

Moving spotlight to the numerical part of this survey, the FE model of composite steel-concrete beams having web openings was built using two- and three-dimensional elements. Especially, the bottom flange and the web of steel beam were discretized by shell elements while the top steel flange and concrete slab by volume elements. Considering the shear connection, its behaviour was defined in a simplified manner using 2D elements and properties of bonded contact. The decision to use this simplification was based on requirement of simplicity and continuity of the model.

As topology of the model was determined, the material characteristics could be specified. For the steel component, yield strength of 235 MPa, Young's modulus of 210 GPa, and Poisson's ratio of 0.3 was applied. Further, the working diagram was defined as bi-linear with a hardening branch having tangent elastic modulus equal to 210 MPa. For the concrete component, material parameters were defined by Young's modulus of 30 GPa, Poisson's ratio of 0.2, and compressive strength of 28 MPa. As a general assumption,

an idealized stress-strain curve of concrete according to EC2 was adopted. While the concrete load response in the FE model was defined by various constitutive laws, an individual input of required variables was necessary. Moreover, using the Microplane model, in order to estimate the most appropriate load response, the compression test of a cubed specimen was essential to perform (Fig. 3.27).

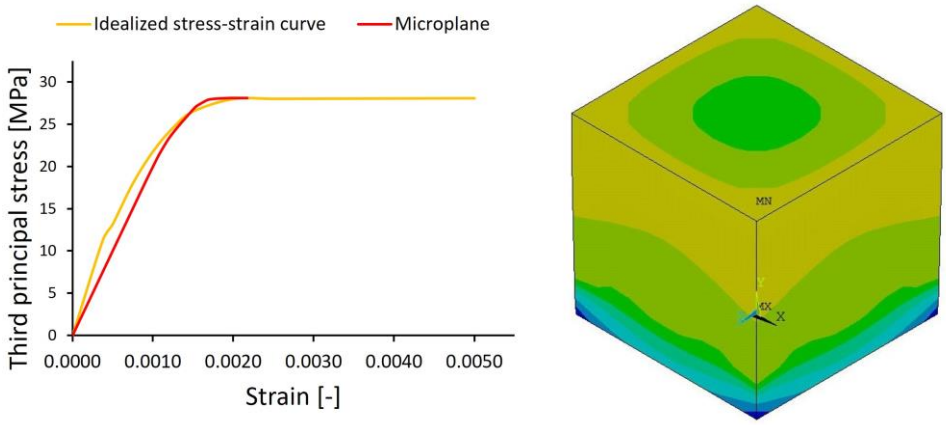

Fig. 3.27 - Stress-strain relation of concrete cube being under pressure.

Aiming to acquire the most reasonable load response, a suitable combination of constitutive laws and element types have to be applied for individual parts of the FE model. Thus, for the steel part, the material constitution using the bilinear isotropic hardening rule was adopted. This was combined with two types of elements. Especially, as the steel bottom flange and web were modelled as 2D objects, four nodded element SHELL181 usually representing moderately thick shell structures, was employed. Whereas the steel top flange was discretized by eight nodded volume elements SOLID 185. These elements were selected for their implemented capabilities enabling to simulate plasticity, stress stiffening, large deflection, and large strains.

From the concrete perspective, the user has the option to choose between four material models which are implemented in ANSYS software environment. However, it should be kept in mind, every material model demands only a certain type of element, as follows:

- Willam-Warnke criterion is linked to 3D element SOLID65.
- Drucker-Prager and Menetrey-Willam criterion uses 3D element SOLID185.
- The Microplane constitution allows usage only of 3D element CPT215.

As all the above-mentioned alternatives represent different material models and use different element types, within this FE survey, their capabilities and deficiencies were investigated.

After the proper modelling of samples´ geometry, definition of input parameters for material models and selection of appropriate FE types, a generation of a relevant mesh was of paramount importance. By doing so, the focus was stressed on regions having susceptibility to development of large plastic strains. This was satisfied by usage of certain mesh density and application of mapped meshing (Fig. 3.28).

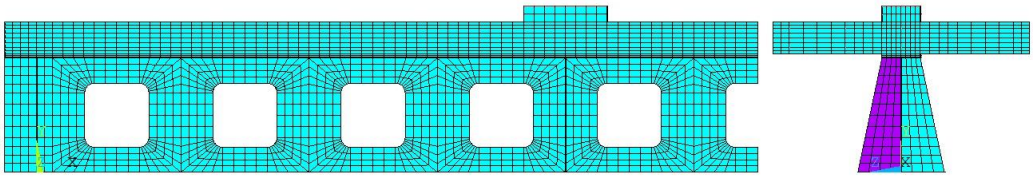

Fig. 3.28 - Meshed FE model.

Speaking of boundary conditions, the load was applied in a form of a pressure acting on the load spreading plates. Based on the modelling practice, these plates have had only one-third of the stiffness magnitude of concrete and Poisson's ratio equal to 0.499. All these provisions were made due to avoiding of local stress concentration leading to divergence even before of attaining the load limit. In order to correctly simulate the boundary conditions of simply supported beam, the deformation constraints were applied only at particular edges of elements. Additionally, the model effectiveness, in respect of time consumption, was improved by application of the symmetry constraints.

As the one of the main objectives of this study was to highlight the versatility of software ANSYS in respect of different constitutive laws for concrete, derived data on the basis of FE model of composite beam with web openings are discussed.

So, turning to the global deflection of the FE samples, the models have yielded almost the same structural performance. Taking the Willam-Warnke as the reference model, discrepancy in deflection at the mid-span has varied from 0.02 % to 8.86 % (Fig. 3.29).

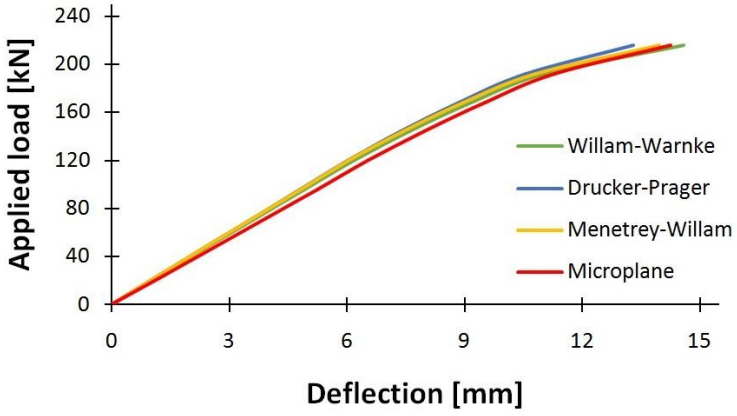

Fig. 3.29 - Load-deflection diagram.

In order to assess the stress response during the multiple load steps, the data from the level of steel bottom flange are depicted in Fig. 3.30. The stress curve signals, the change of concrete material model influences the load response of the steel component negligible, of course, within used range of applied load. The difference between the data diverged on the scale of 0.02% to 6.02% with respect to the reference model.

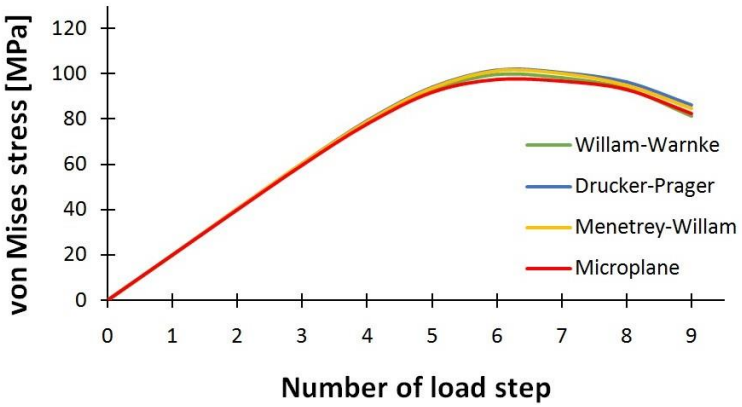

Fig. 3.30 - Stress diagram at the level of the bottom flange.

The next set of results has shown, although within the FE model was applied notable simplification for the shear connection, it has predicted the load response quite credibly. This can be clearly seen from Fig. 3.31. As was expected, the corners of openings experienced a serious concentration of stresses leading to advanced plastic strain development.

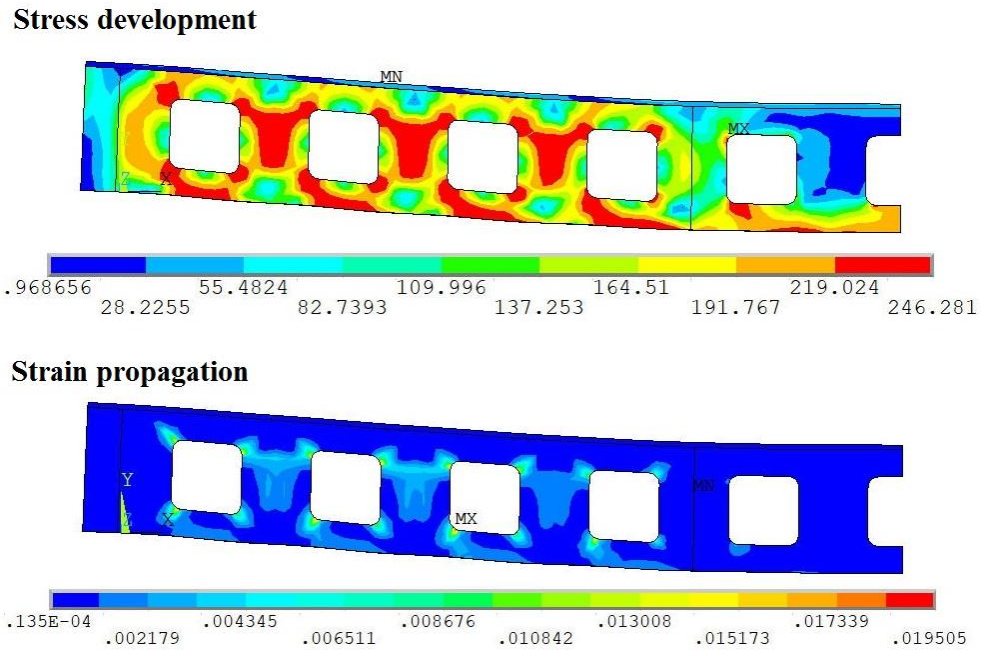

Fig. 3.31 - Stress and strain response of the beam samples, respectively.

Generally, simulation of concrete behaviour in FE models and its realistic load response can be challenging. This might have several roots. The two most striking, causing severe convergence difficulties, are represented by cracking and crushing phenomena which arise after exceeding of its strength capacities. In order to cover this part of loading process, special treatments have to be applied. Unfortunately, three of four herein presented concrete material models are unable to process the mentioned natures of concrete, hence display great computational shortcomings.

Turning back to the scope of this study, as the applied load overcome the 90% of the sample´s resistance against the combination of shear and bending which was determined by the analytical calculation, the non-convergence occurred imminently for all the constitutions excepting the Microplane model. These and other difficulties are demonstrated in Fig. 3.32 where, at the very first sight, several curves diverging in both shape and magnitude are visible.

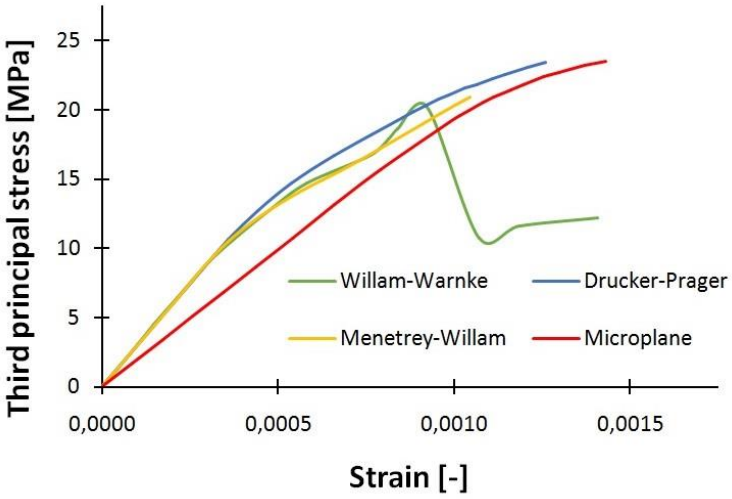

Fig. 3.32 - Stress-strain relation of at the level of the concrete slab.

Considering the Willam-Warnke model, a sudden change in the stress magnitude can be observed. This response implies an advanced development of crushing or cracking phenomenon even before of achievement of the full concrete strength. Thus, the outcome casts a critical doubt on the relevance of usage of this model for the subsequent parametric FE analysis.

Turning to the Drucker-Prager and the Menetrey-Willam failure criteria, they produced almost the same results. Moreover, both were able to undergo only about 92% of the applied load before the divergence occurrence.

In order to overcome these difficulties, the Microplane model was implemented in software ANSYS which seems to represent the most precise and effective way for

description of concrete behaviour. Using this model, no convergence difficulties have arisen. Moreover, high stress magnitudes could be developed along the beam (Fig. 3.33). These might be assigned to the existence of the push and pull-out forces acting at the material interface. Due employment of the Microplane model these local effects, important for resistance assessment, could be captured. So, compared to the other constitutions, significant improvement in simulation capabilities is evident.

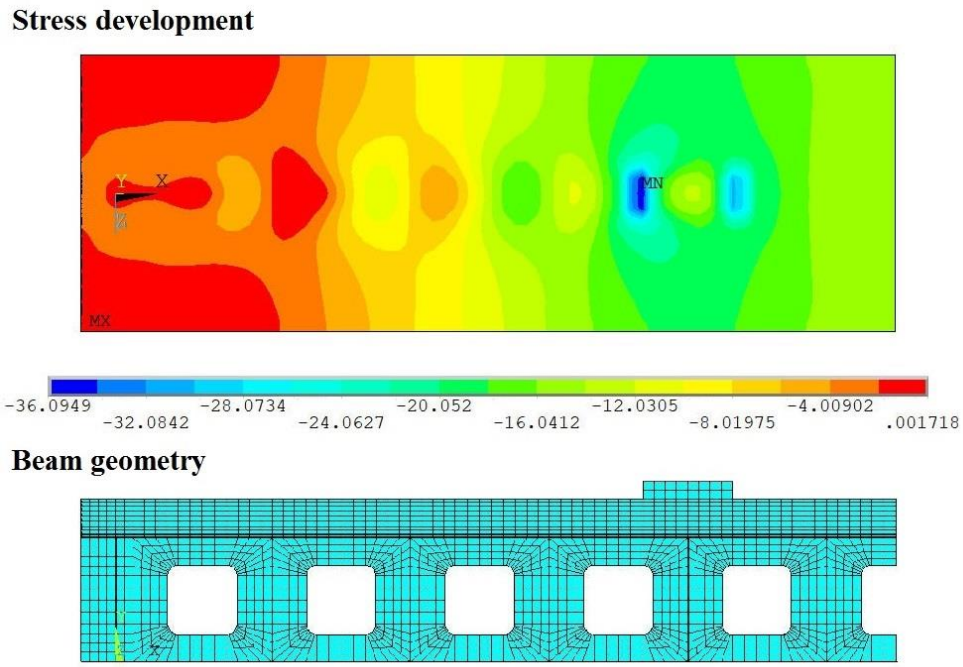

Fig. 3.33 - Stress state at the top level of the concrete slab.

In conclusion, identifying the major failure mechanism of composite steel-concrete beams with multiple web openings is found to be a complex task. So, aiming to deeper an insight in capabilities of the FE simulation for these load bearing members in ANSYS environment, a fundamental FE survey was conducted. In this way, the load response was observed at several locations of the FE model of a composite beam. Furthermore, an impact of four individual constitutive models for concrete was examined. Applying this approach, an attempt was made to find the most capable one.

So, as the results showed, the structural performance of the composite member was influenced just slightly by the variation of concrete constitutive models. However, from the user perspective, the convergence problems experienced by the Willam-Warnke, the Drucker-Prager and the Menetrey-Willam constitutive laws have emerged a solemn problem regarding the convenience of computation. The leading reason behind these computational difficulties lies in their constitution definitions. This subject is addressed in detail in section 5.1.

Nevertheless, it has to be noted, only one of the herein presented constitutions did not undergo the mentioned issues, the Microplane model. Consequently, the Microplane model has a potential to be considered as the most effective alternative. Hence, in section 5.2 an algorithm for an effortless definition of input parameters for the Microplane model, defined under three fundamental load conditions (uniaxial compression, uniaxial tension and biaxial loading), is presented.

3.7 Summary

On the basis of conducted studies, it can be concluded:

- the existence of web openings in steel beams affects the lateral-torsional stability in a great measure,
- both the presence of openings and the layout of shear studs have a significant influence on the shear flow pattern,
- by a change of shear connectors´ layout, the overall carrying capacity does not experience any greater enhancement.

Nevertheless, an experimental testing attempting to confirm or disprove these results, has to be provided. Therefore, our experimental programme will be presented and discussed in the next chapter. Besides, as a comprehensive FE investigation is intended, an appropriate FE model for the experimentally tested specimens has to be built. Unfortunately, as the last study has revealed, several challenges are accompanied by concrete simulation in ANSYS. Hence, broader discussion on this issue is delivered in chapter 5 – Finite Element Model.

With respect to the thesis aims, it could be claimed, the third aim:

3. Conduction of the following parametric studies focusing on:
    a. shear flow at beams with web openings with uneven distribution of shear studs,
    b. effect of the presence of openings on the resistance in lateral-torsional stability of composite beams with web openings in the assembly and operational stages,

was achieved.

4 EXPERIMENTAL PROGRAMME

On the evidence obtained from the previous analytical-numerical studies, the experimental survey was carried out. Reflecting the previously presented, the configuration of experimental tests has met the requirements for a detailed inspection of:

- influence of shear connectors´ layout on behaviour of composite beams with web openings,
- redistribution of shear forces between the Tees aiming to provide simplification of the Vierendeel bending resistance evaluation.

In the following, an elaborate description of the experimental programme is provided.

4.1 Foreword to the Experimental Testing

Attempting to explain the course and limits of our research, the entire process of beam samples composition will be presented. An imperative for this treatment laid in occurrence of several obstacles during the conceptual arrangement of experimental samples. Hence, some of the preliminary concepts had to be rearranged.

For instance, from the manufacturing process viewpoint, one of the very first alternative assumed, the steel cross-section will be manufactured from two T-shaped hot-rolled sections welded together. But, after consultation with the manufacturer, this alternative was assessed as extremely costly. This led to an alternative employing a welded cross-section. Additionally, an asymmetrical beam section was used in order to implement its advantageous properties in the bending.

Further, two alternatives of shear studs' arrangement were considered:

- uniform along the entire beam,
- concentrated above the web-posts.

Also, the openings were firstly designed in two manners having different shape:

- rectangular with rounded corners,
- circular.

However, due to the unexpected dramatic increase of costs of structural steel in 2021, only four samples considering the first alternative of openings´ shape were tested in laboratories at the University of Žilina. So, on the basis of the previous analytical-numerical studies, the specimens´ configuration was designed in a way which allows us to observe:

- deflection at the critical positions,
- strains at the level of:
    - the bottom Tee,
    - the top Tee,
    - the web opening edges,
    - and slip at the material interface.

By dint of a prudent procedure during the preparation stage of the experimental programme, the pivotal objective of this experimental inspection, that means, properly capture the load-response of composite beam having web openings, was accomplished.

4.2 Configuration of the Test Specimens

The steel part of the composite beams was designed as a fabricated section. That means, the steel-section was formed from three steel plates by welding to form an asymmetric I-section. In general terms, this asymmetry is typically characterised as the ratio of the bottom to the top flange area ranging from 3 to 1. In our case, this ratio was at level of 2.6. Turning to the openings, they were squared in a shape having their corners rounded off. They were centrically placed with respect to the web depth. The solid parts of the steel web between openings, the web-posts, were of the same length as openings excepting the end web-post. Considering the concrete part of composite samples, the slab was designed as a solid one having relevant reinforcement. The basic representation of the samples´ configuration is illustrated in the following figure (Fig. 4.1).

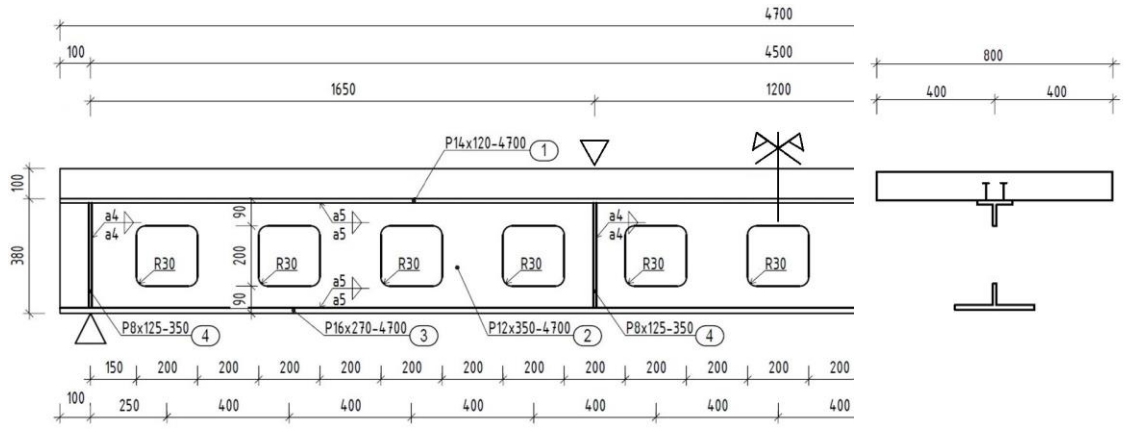

(a) (b)

Fig. 4.1 - Side view a) and cross-section b) of the tested beam samples.

Additionally, the geometrical parameters of investigated samples are summarized in Tab. 4.1

Tab. 4.1 - Overview of geometrical parameters of investigated samples.

component	width [mm]	depth [mm]	strength [MPa]
concrete slab	800	100	46.18
top flange	120	14	280
web	12	350	276
bottom flange	270	16	304

opening	200	200	-

shear stud	diameter [mm]	depth [mm]	strength [MPa]
shank	13	67	327
head	25	8	

Further, the connection at the steel-concrete interface was formed by headed shear studs. These connectors were designed to withstand both the horizontal shear loading caused by interface slip and the tension forces initiated by the Vierendeel bending existence. Furthermore, in the light of contribution of composite action to the Vierendeel bending resistance, the layout of shear connectors has varied across the samples. Two alternatives of connectors´ layout were under examination. The first one employed the uniform distribution of studs while the second one used non-uniform spacing, wherein the connectors were omitted above the openings.

By so configuration (Fig. 4.2), connectors´ contribution to the Vierendeel bending resistance might be minimised, thus leading to more extensive deformations in the regions of the openings´ corners and the web-posts.

a)

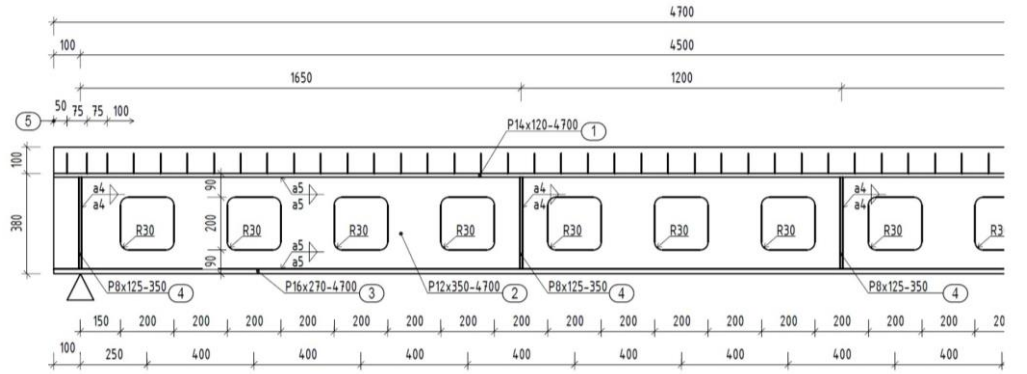

b)

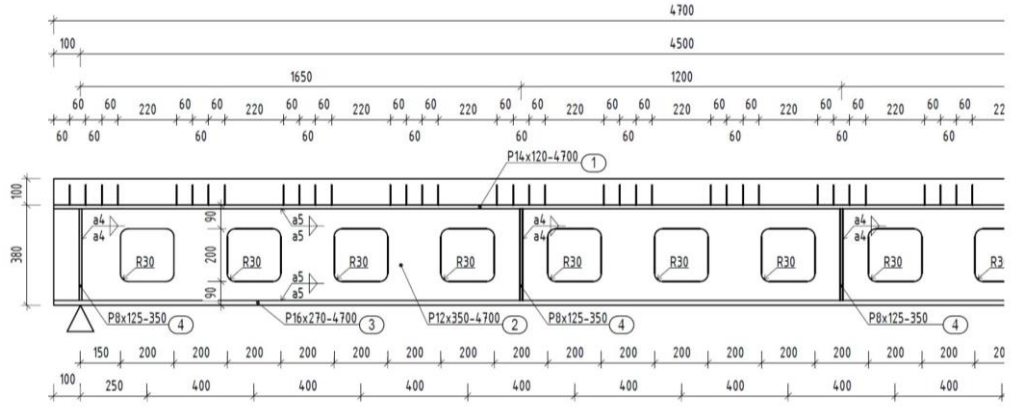

Fig. 4.2 - Side view of the beam samples differing in shear connectors´ layout – a) uniform and b) non-uniform.

The overall configuration of beam samples was based on the design rules given in [8]. These rules constitute not only material aspects, loading conditions and shear connection natures, but specify particular size limits for individual beam components as well. The overview of applied rules for investigated samples is summarised in Tab. 4.2.

Tab. 4.2 - Overview of applied geometrical rules.

opening shape	samples
max. depth of opening	$0.57*h_w$
min. depth of Tee	$0.26*h_w$
max. opening length	$1*h_o$
min. width of web-post	$1*l_o$

In addition, the beam design was approved by the preliminary FE analysis, which has only underpinned the Vierendeel bending as the major failure mode for this particular beam configuration (Fig. 4.3).

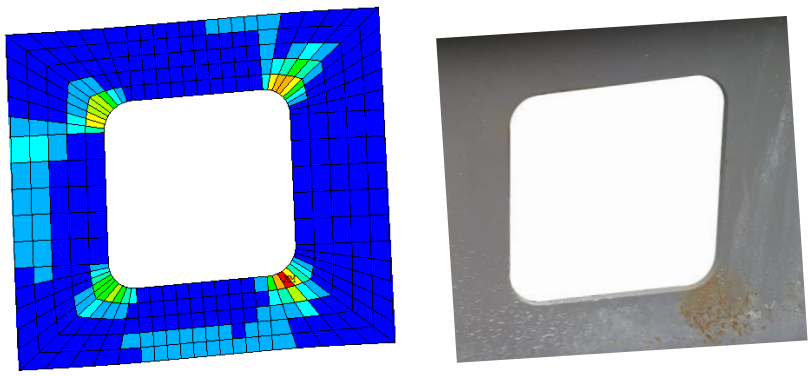

a) b)

Fig. 4.3 - Failure mechanism representing the Vierendeel bending in the steel web from a) the preliminary FE analysis and b) the experimental sample.

After meticulous deliberation, as the most appropriate load form, the configuration of four-point bending test was determined. Two main roots were behind this decision. In fact, these were the laboratory conditions and the structural efficiency. Considering the latter, by existence of the constant shear force spanning from the support to the location of the force induction, the effects of the shear connection alternation on the Vierendeel bending and the horizontal shearing of the web-posts can be recognised more easily.

By usage of this load configuration, one has to always bear in mind, preventing of the local failure of the steel web under the applied force and above the supports is paramount of importance. This requirement was warranted by the application of web stiffeners at the already mentioned critical positions. Additionally, a load spreader with elastic fillet have been installed between the hydraulic jack and the concrete slab to avoid excessive local stresses.

The samples configuration can be seen in Fig. 4.4.

Fig. 4.4 - Samples configuration.

In the view of applied conditions, the final part of the preparation stage of experimental testing was necessary to perform - application of measuring devices.

4.3 Measurement Devices

Within this experimental programme, a set of linear variable differential transducers (LVDTs) has been used for displacement recording. Generally, these devices use a linear displacement sensor which records variation of the magnetic properties as the ferromagnetic bar moves. Consequently, this process is conveyed by electrical signal, which is subsequently compiled to a certain number of data sets of measured quantity. As displacement is recorded only at a certain point of specimen´s surface and only in one direction, the measurement can be defined as of global scale. In our experimental programme, their main function was to capture vertical deflection and slip. While vertical deflection was measured at two positions - at the midspan and under the applied force, the measurement of a slip was recorded at the material interface using a unit-distance manner of configuration along the specimens.

Turning our aim to the measurement of deformation, strain gauges has been applied at certain locations as well. In fact, the quantity what is really being measured is the electrical resistance of a wire. So, as the strain gauge is fixed to a surface of a sample and undergoes deformation, the electrical resistance varies based on the change of wire´s cross-section. Before final definition of the local deformation of the specimen, the recorded values have to be multiplied by the gauge factor. Speaking of the strain gauge

attributes, several parameters play a crucial role by proper choice of their size, type and gluing. The main of these are:

- size of a specimen,
- size of material heterogeneities,
- scale of measured deformation,
- temperature,
- humidity,
- and test duration.

The strain gauges can be located individually or in groups. Using an individual gauge, the load response is measured only in one direction. In contrast, the strain gauges concentrated in a group called rosette allows to define the whole deformation tensor. This simplifies the process of data correlation between the real ones and numerically obtained. Hence, both principles were applied within our survey.

In particular of the configuration of strain gauges within this experimental programme, positions for these devices were cautiously determined using the record & control principle. That means, a certain number of devices were just recording and storing data for further usage, for instance for validation of the FE model. Hence, the gauges located at positions where the excessive strains are not present facilitated picture of the overall stress state during the loading. Opposed to that, the strain gauges having the control function have been measuring and controlling the entire process of loading, because they were applied at locations where the desired failure (the Vierendeel bending) should have occurred. That means, these locations should have been exhibited to yielding caused by extreme shearing occurring near opening edges. Accordingly, during the experimental testing, the strain gauges were applied as:

- set of individual gauges to record the strain in particular direction,
- as biaxial rosettes (0 - 90) in a shape of T or V.

In this way, the configuration of measuring devices can be envisaged according to the following table.

Tab. 4.3 - Assignment of record and control principle for individual components.

	Beam component				
Principle	Concrete slab	Material interface	Top flange	Web	Bottom flange
Record	X	X	X	X	X
Control				X	

Further, the locations of strain gauges relating to the material can be split, as follows:

- at the concrete level,
- at the steel level.

At last, the locations were defined in respect of the longitudinal position as well. Hence, the devices were fixed near the support and at the centre of beam samples.

The arrangement of both, the strain gauges and LVDTs, is simply depicted in Fig. 4.5. Their detailed description and illustration can be found in section 5.8 and in Appendix B.

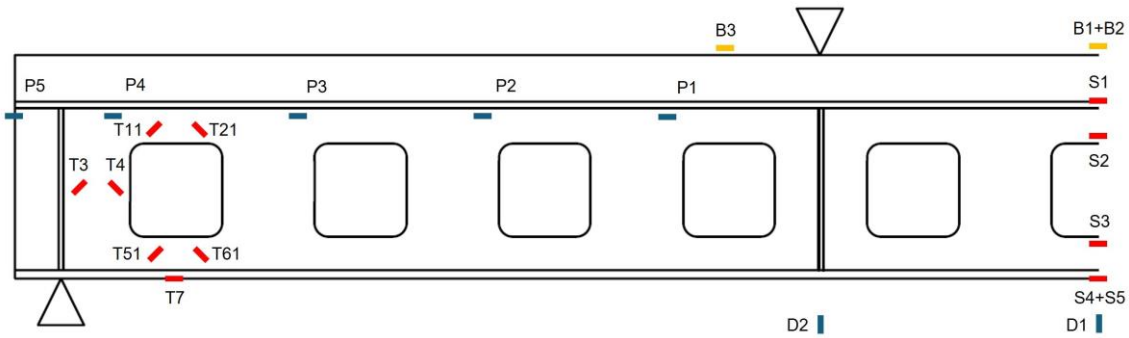

Fig. 4.5 - Configuration of the measurement gauges.

All the measured quantities were simultaneously recorded throughout the entire loading process (Fig. 4.6) aiming to obtain the most exact stress projection for the subsequent parametric FE-based investigation.

Fig. 4.6 –The loading process.

4.4 Experimental Procedure

After execution of the primary steps of experimental survey (rig set up, dial and strain gauges application), the load was introduced by controlled deformation using a low displacement gradient. After that, it was applied in a stepwise manner, that means, at certain load levels, the loading process was interrupted in order to consider the load relaxation effects.

The stated can be clearly seen from Fig. 4.7, which represents the force-deformation relation of a representative sample recorded at position D1.

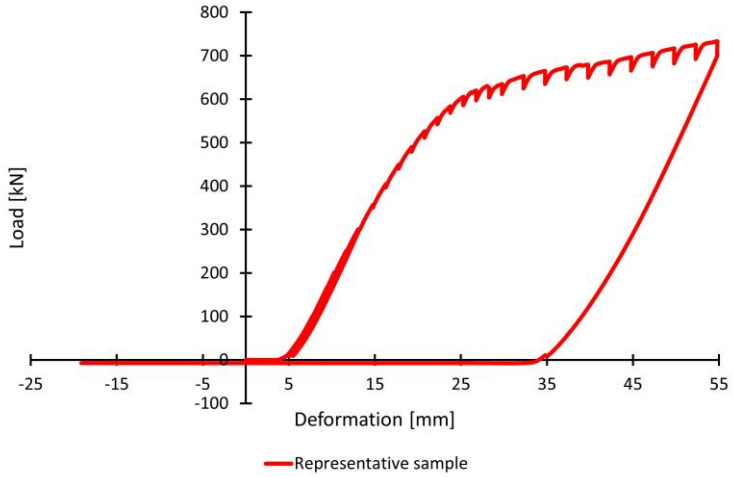

0

Fig. 4.7 - "Raw" load-deflection relation of a representative sample.

To be specific, the samples were loaded gradually using 50 kN increments up to the first occurrence of yielding. That means, the linear capacity was drained at the level of 600 kN. At this phase, the web next to the outermost opening experienced the very first yielding. That means, the Vierendeel bending was taking the place. Subsequently, the increments were reduced to 25 kN per a load-step. At the load of 650 kN, the yielding process occurred at the level of bottom flange at the mid-span as well. By subsequent loading, the process of advanced yielding without any significant change was observed. Hence, the ultimate failure mode was represented by locally yielded web owing to the Vierendeel bending effects limited by a certain magnitude of deflection. So, the process of loading was determined as accomplished at deflection of 32 mm at position D1. As the last stage of loading, the unloading process was initiated which yielded the curve parallel to the other one obtained from the linear elastic stage of deformation.

To demonstrate agreement between evidence recorded from individual samples, the load-deflection curves from all the investigated specimens are depicted in Fig. 4.8. It has to be noted, the presented data are cleaned out of the relaxation effects.

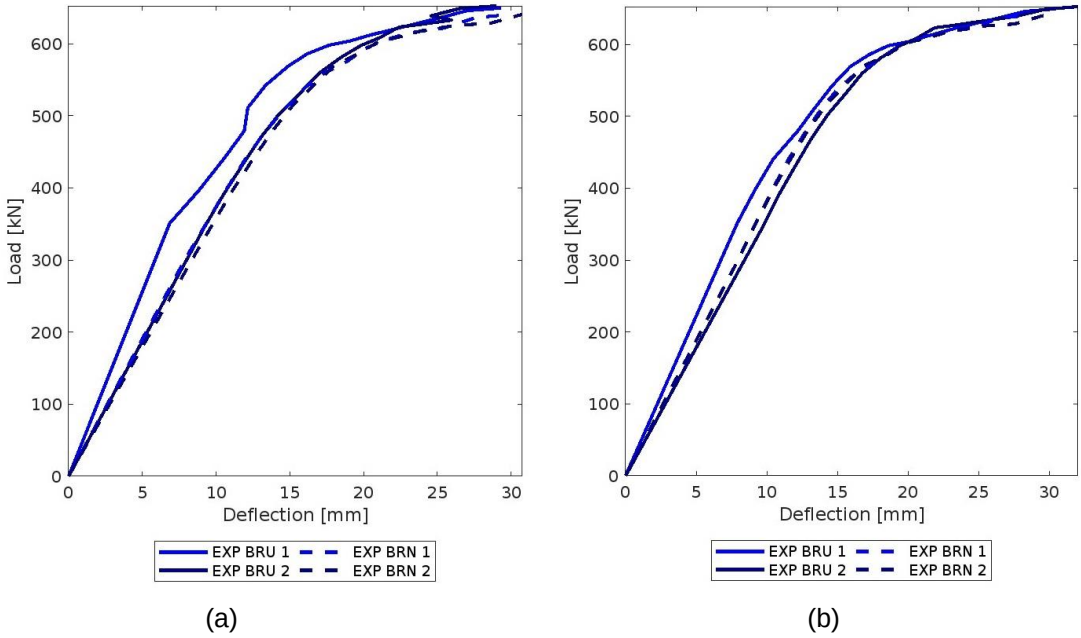

Fig. 4.8 - Load-deflection relations of the investigated specimens at positions a) D1 and b) D2.

A detailed discussion regarding the experimental data will be delivered in section 5.8, which is concerned with validation of the FE model. Hence, in the following only the fundamental evidence with respect to the material properties definition is about to be presented.

4.5 Tension Testing of Steel

Fundamentally, determination of properties for metallic materials represents a crucial aspect regarding the structural analysis and design. Hence, in order to interpret the experimental tests properly and to ensure appropriate material input for a FE investigation, the tensile strength testing of individual parts of the steel part of the composite beams was conducted. These tests, namely coupon tests, were carried out in accordance with EN ISO 6892-1: 2019, which represents the most commonly adopted testing standard for the tensile testing of metallic materials at ambient temperature.

The samples for coupon tests were extracted from un-yielded regions of composite beams at the level of bottom flange and web. From either part, three samples were made. Before testing, the protective coating on samples´ surfaces was mechanically removed and the cross-sectional dimensions were measured. The mean values of measured quantities can be found in Tab. 4.4.

Tab. 4.4 - Mean values of measured quantities.

beam component	depth [mm]	width [mm]	yield strength [MPa]	ultimate strength [MPa]
web	12.00	13.65	276.16	423.49
bottom flange	15.83	13.40	304.00	424.51

By conduction of tests, the tensile loading machine having 500 kN capacity was deployed. The specimens were fastened by gripping at either ends with a pair of clamps. The load was applied by displacement control of a stroke during the test procedure which could be divided into 4 stages:

- elastic range - from the outset to proportional limit,
- yielding range - from proportional limit to yield strength,
- strain hardening range - from yield strength to ultimate strength,
- post ultimate range from ultimate strength to fracture.

The averaged stress-strain response and obtained quantities of individual steel parts loaded up to the ultimate strain are depicted in Fig. 4.9.

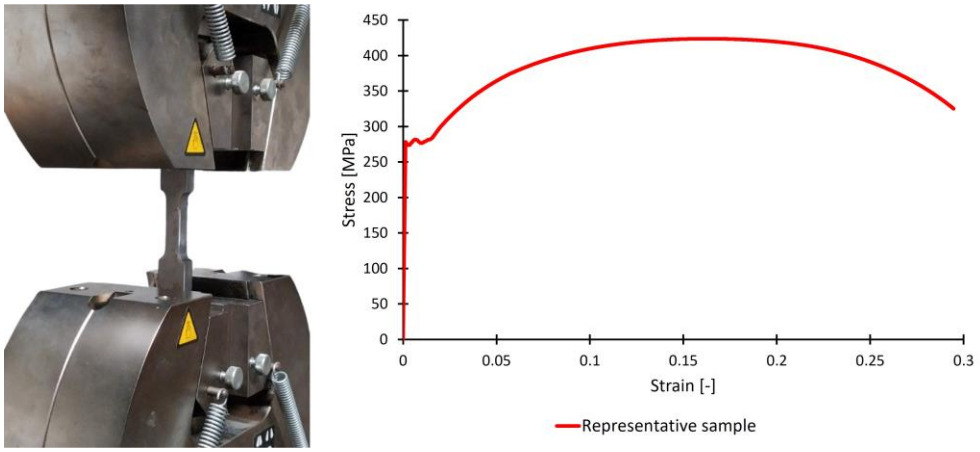

Fig. 4.9 - Coupon testing.

4.6 Uniaxial Testing of Concrete in Compression

In general, a detailed experimental analysis of concrete has always been a complex task. This complexity arises due to the variability of the material caused predominantly by its composition. For concrete components of the investigated samples, the mixture of concrete was made of particular volume of water, granular skeleton having constant grain size and a binding agent (commercially available cement without any particular properties). The samples used for uniaxial compression test were cylindrical in a shape having standardized dimensions. These cylinders were obtained by two fashions,

namely by moulding when the concrete slab was casted, and by core drilling after the experiment. Concrete as a material, which mechanical properties evolve in time and depend on environment, must be cured under stable conditions. That ideally means, the cylinders are for 28 days long cycle preserved in water until the testing is conducted. During this experimental investigation, these conditions were accomplished. The nominal sample is illustrated in Fig. 4.10.

Fig. 4.10 - Concrete testing.

The axial deformation measurements were carried out by a machine using deformation control, in which is the sample commonly placed between two heavy steel plates (punches). With the help of displacement sensors and software for data acquisition, the averaged axial deformations of the specimen were recorded. The limiting strength of concrete specimens under compression was defined at the level of 46.18 MPa.

4.7 Summary

Within the presented experimental programme, it was provided:

- Design and configuration of the experimental samples and testing apparatus.
- Description of loading process.
- Reasoning behind layout of measurements gadgets.
- Basic illustration of the load response of investigated samples displaying almost excellent agreement.
- Additional experimental testing identifying a set of material parameters necessary for building of a reliable FE model.

Concentrating on completion of the thesis aims, the first one:

1. Proposal and realisation of the experiment focused on the resistance and behaviour of composite beams with web openings,

could be assessed as accomplished.

In addition, as the alternation of layout of shear connectors conveys one of the main objectives of this investigation, its influence could be directly observed. Based on the load-deflection relations, it can be concluded, this parameter did not cause any significant change in relation to the overall load response. This implies; the configuration of shear connectors might have local significance, especially at the level of individual shear connectors.

To complete the other aims of the thesis, the reference FE model has to be built. However, since several issues related to concrete simulation in ANSYS were identified in section 3.6, their rigorous treatment shell be addressed. Respecting said, quite broad description of material laws for concrete implemented in ANSYS is delivered at first. As a side result, a calibration procedure defining input parameters for the Microplane model is developed. Furthermore, partial attention is paid for material constitution of steel and FE contact. By doing so, not only deeper comprehension of studied problem is attained, but also the second aim of the thesis:

2. Creation and calibration of a numerical model based on the FE method,

can be successfully completed.

5 FINITE ELEMENT MODEL

In general, physics' problems are characterized by integrals or partial differential equations. However, if the investigation deals with a complex task, problems with corresponding mathematical formulations can arise. For this reason, the numerical methods are employed. Recently, the FE method is one of the most exploited numerical techniques for solving these mathematical challenges.

So, by building of a FE model, a rigorous approach should be employed ensuring proper geometry description, usage of suitable material models, appropriate meshing, and cautious application of boundary conditions. Aiming to fulfil these ambitions within the scope of this research work, the FE calculation of highly non-linear structural problem of composite beams was covered by software ANSYS.

Unexpectedly, several challenges regarding achievement of a proper load response, especially for concrete, was needed to surmount. Attempting to solve this problem, a calibration procedure for definition of input parameters for the Microplane model using ANSYS parametric design language was developed. Additionally, partial attention is also paid to material constitution of steel and to properties of FE contact representing a simplified form of shear connection discretization.

Completing picture of the entire process of the reference FE model building, solution process configuration, structure of the finite element model and mesh sensitivity study are delivered.

As the last step, validation of the finite element model is provided.

Following this course, a corner stone for the credible parametric FE investigation has been laid.

5.1 Review of Material Modelling of Concrete in ANSYS

In ANSYS, there are several constitutive models which define multiaxial stress-state of concrete elements under application of a force. These models work on fundamentals of theoretically defined relations controlling development of stress-strain rates upon the ultimate performance defined by the failure surface.

In recent decades, several approaches defining the complicated stress-strain behaviour of concrete under various stress states were formulated. The most important of them with respect to the extent of our investigation are:

- linear- and non-linear-elasticity theories,

- perfect- and work-hardening plasticity theories,
- microplane-based theories.

Even though the two first of constitutive relations satisfy the salient concrete natures and rigorously formulated mathematical requirements, their usage is limited. An employment of these stress-strain-rate-based models might tend to convergence difficulties and several shortcomings, especially in the region of post-peak behaviour for both compression and tension. During entire loading process, concrete tends to experience continuous development of multidirectional micro-cracks within the cementitious matrix. This concrete feature makes its load-response highly complex even during the low stress levels. Despite this fact, concrete is treated like an initially isotropic material. Nevertheless, this treatment is sufficient within the elastic deformation zone.

Considering the high stress levels, by a usage of constitutive laws predominantly based on the plasticity theory for FE analyses, it is possible to load an investigated sample merely up to the peak load experiencing any or minor convergence difficulties. However, the fact is, although the global resistance of a sample is not passed, the local effects present in a FE model in the vicinity of regions prone to the stress concentrations might produce divergence of a solution. These critical regions tend to form near areas of:

- sudden cross-section-size change,
- supports,
- joints,
- application of load,
- application of pre-stressing.

From the practical perspective, this obstacle can lead to enormous time consumption caused by seeking for an appropriate analysis refinement. The most widely spread refining methods are:

- reduction of a load increment,
- application of a coarser mesh in critical regions and vice versa,
- replacement of selected set of elements by only-linear-defined ones,
- surrounding a concrete component with a layer of soft linear defined material,
- using of a hardening branch instead of a softening one above a specific portion of the softening region.

As visible, the mentioned practices contravene some of the essence characteristics of concrete behaviour and basic rules of FE modelling. One has to be always careful when applying these refinements in respect of calculation correctness.

However, the light of hope for more convenient FE analysis and more flexible material model covering major aspects of concrete complex stress-state exists and is represented by the following possibilities:

- the nonlinear-elastic fracture model (ATENA),
- the coupled damage-plasticity model (ABAQUS),
- the Microplane model (ATENA, ANSYS).

Respecting fact that our FE investigation was conducted in ANSYS, concept of the Microplane model will be reported.

The most significant difference compared to the constitutive relations working on the plasticity theory principles originates in the mathematical concept itself. Instead of typical definition of stress-strain evolution based on the tensorial approach, the Microplane model vigorously exploit vectors representing both the magnitude and direction of developing strains or stresses. In addition, the hidden brilliance of this method lies in an employment of microplanes, which track the crack patterns within the cementitious matrix as precisely as numerically and practically possible.

As a dominant interest of a general FE analysis is to be sufficiently accurate and time effective, several options were studied in order to find the most appropriate manner for simulation of concrete behaviour. The following chapters describe available constitutive models for concrete in ANSYS.

5.1.1 Concrete as a Part of the Theory of Plasticity

Generally, the constitutive equations trying to describe behaviour of concrete using the flow theory of plasticity (Fig. 5.1) consist of the following parts:

- yield criterion,
- flow rule,
- strain-hardening rule,
- loading–unloading conditions.

Speaking of the first, the yield criterion defines the limiting stress state for yielding occurrence. Commonly, it is determined by a three-dimensional failure surface. The material's behaviour within space of this surface displays only elastic natures. However, when this surface is passed, the flow rule specifying growth of the inelastic strains´ onsets.

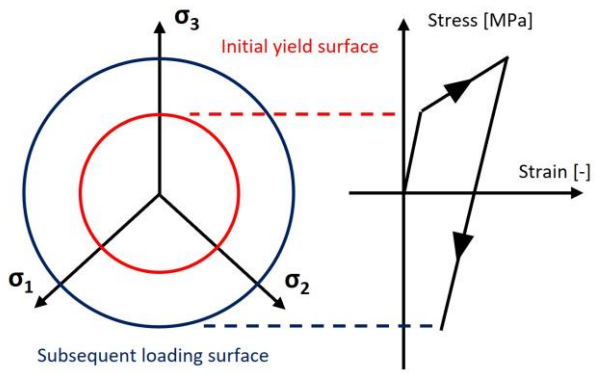

Fig. 5.1 - The basic principles of the plasticity theory.

Two major kinds of the flow rule can be distinguished - associated and non-associated. The very difference between these rules comes from a yielding direction after passing the strength limit (Fig. 5.2).

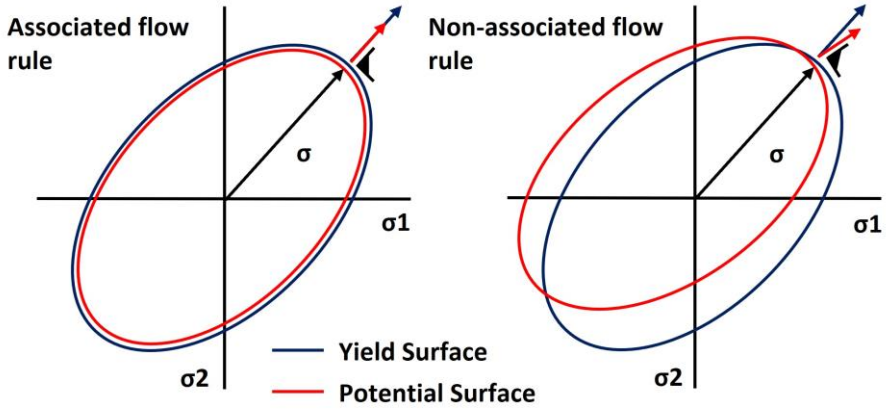

Fig. 5.2 - Flow rule theories.

Being specific, the associated flow rule is being defined through the normality principle - the plastic strain-rate vector is normal to the total vector stress and is well established within the metal plasticity. The main reason for that lies in the volume preserving ability of metals after the yielding process initiation displaying no energy dissipation until attainment of the ultimate strength. However, this scenario is not applicable for concrete, so an employment of the non-associated plasticity is adequate. The ground for this treatment lies in the residual shear capacity of concrete coming from the aggregate interlock which is responsible for a change of the yielding angle.

Also, compared to steel, concrete as a granular material type exhibits eminent volume changes associated with the shear distortion of individual internal particles. This aspect is characterized by dilatancy angle which represents the ratio of a plastic volume change over plastic shear strain (Fig. 5.3). Curiously, it remains constant solely for a short range of strains - near and at the peak strength. That means, it changes mainly in the pre- and

post-peak region. Of course, concrete cannot dilate infinitely, that means the dilatancy vanishes by loading and any further volume changes are restricted. This behaviour only bolster significance of dilatancy angle and complicates the correct description of concrete behaviour indeed.

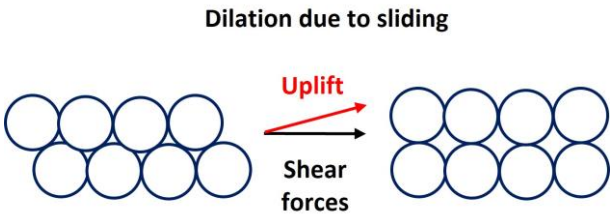

Fig. 5.3 - Dilation of particles in concrete.

Turning to the hardening rule, which controls the form of subsequent yield surface, the strain-softening is being generally thought as the most suitable for concrete. Despite this fact, the perfectly plastic hardening having isotropic expansion of the initial yield surface was commonly applied. So, in order to eliminate this defective behaviour, various damage models accounting for a gradual reduction of a material strength were developed.

Unfortunately, in ANSYS software environment, the majority of constitutive models of concrete are based on the mentioned principles, even though they display some sort of bounded mechanical performance. The roots of their shortcomings could be assigned to the following two factors.

The first one conveys difficulty to formulate a generally applicable constitutive law for concrete, which has easily identifiable material constants. This is due to the complex heterogeneous nature of concrete, which results in very distinct responses under different stress states and loading histories.

The second one embodies certain numerical instabilities encountered by an onset of softening regime and localization of strains. But as will be shown later, this repulsive state occurs solely when a constitutive model is formulated phenomenon-logically, that means not incorporating material microstructure and using stress and strain invariants for description of the inelastic phenomena.

Hence, to picture the main drawbacks of material models implemented in ANSYS software package, their fundamentals will be presented.

5.1.2 The Willam-Warnke Model

The Willam-Warnke constitutive model describes behaviour of concrete under an arbitrary triaxial stress state limited by a certain failure surface. This constitutive model works on principles of the theory of plasticity and work-hardening law, so not incorporating the softening. Hence its capabilities are quite limited. To be specific, this constitution is able to determine concrete stress working diagram only upon the ultimate load performance. Regarding the stress limits, in tension, the constitutive model incorporates the tension cut-off, while in compression, the stresses are hindered solely to the low-compression regime. That means, the failure envelope has straight meridians and non-circular cross-section (Fig. 5.4). Moreover, whether the compression or tension regime arises, the normality principle defines the inelastic deformation direction. These facts are in a great controversy to experimental evidence of the concrete load response.

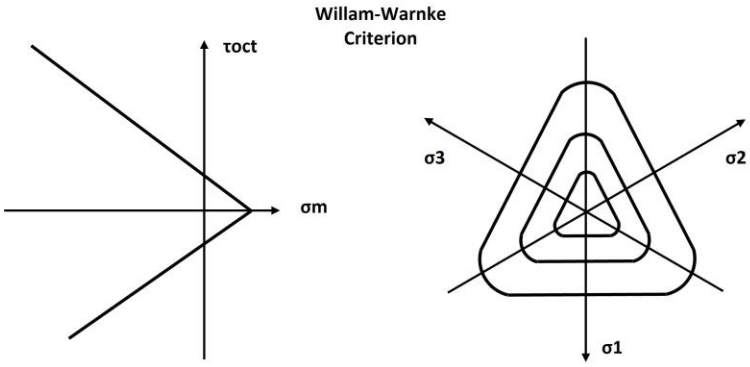

Fig. 5.4 - Simplified depiction of meridian and deviatoric section of the Willam-Warnke criterion.

From stated, evident deficiencies regarding this concrete model can be identified. More detailed description of further drawbacks will be discussed later.

5.1.3 The Drucker-Prager Model

In general, the Drucker-Prager failure criterion is a three-dimensional pressure-dependent model defining the ultimate structural performance of brittle materials. The very first applications were addressed to describe the inelastic deformation and failure of soils. Besides that, this constitution is competent to simulate concrete behaviour as well. This criterion has emerged on the basis of the outer cone of the Mohr-Coulomb law. Additionally, it is combined with the tension cut-off incorporating the Rankine theory (Fig. 5.5).

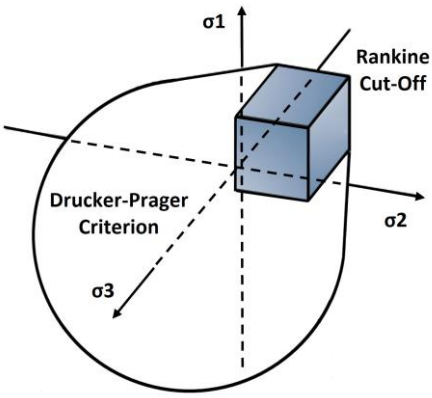

Fig. 5.5 - Simplified depiction of the Drucker-Prager criterion combined with the Rankine cut-off.

Paying more attention to relation between the Mohr-Coulomb and the Drucker-Prager model, the latter one represents an enhanced version of the former one from the mathematical perspective. Illustrating said by deviatoric plane projection, the Mohr-Coulomb failure surface contains sharp edges which firmly ruin smoothness of the failure function and its subsequent differentiation. In other words, at the point of a function where a "corner" exists, does not exist its derivation. Therefore, the Mohr-Coulombs failure function is not differentiable at entire of its domain, what results under particular stress-states in pathological numerical instabilities (Fig. 5.6).

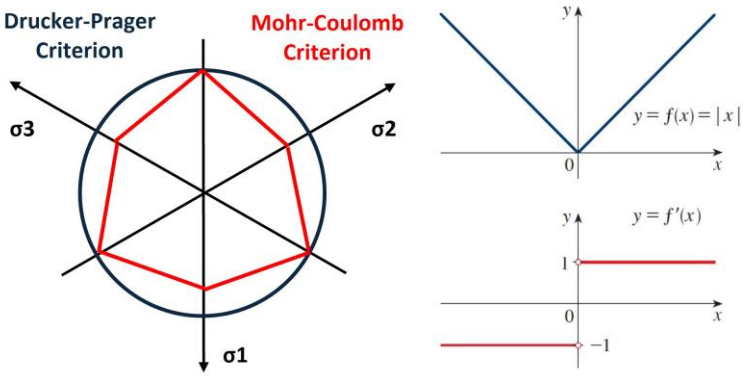

Fig. 5.6 - Deviatoric section of the Drucker-Prager and the Mohr-Coulomb criterions with example of non-differentiable region.

Turning back to the Drucker-Prager model, here the circular shape of the failure curve violates experimental evidence describing the failure curve as continuously shape-changing from nearly triangular for tensile stress to convex - typical for high compressive stresses.

Nevertheless, this constitution provides compared to the previously presented model one remarkable enhancement. To be specific, the softening load response is covered by the fracture. More about this is delivered in the one of subsequent sections (5.1.5).

5.1.4 The Menetrey-Willam Model

The Menetrey-Willam constitutive (Fig. 5.7) model represents a refined adaptation of the Willam-Warnke model incorporating dependence on three independent stress invariants. It shares also some features with the Drucker-Prager model, thus is suitable for FE simulations of similar materials. The Menetrey-Willam model, however, seems to be generally better than the previously mentioned.

For instance, the main difference between the Ducker-Prager failure criterion and the Menetrey-Willam can be easily discern from their deviatoric sections. Where the latter one incorporates the continuous change of failure surface from almost a circular to almost a triangular shape by virtue of the out-of-roundness parameter advocated by relevant experimental evidence. whereas the former one retains having a circular shape within entire load-level extent. In addition, the flow potential is being defined as non-associated.

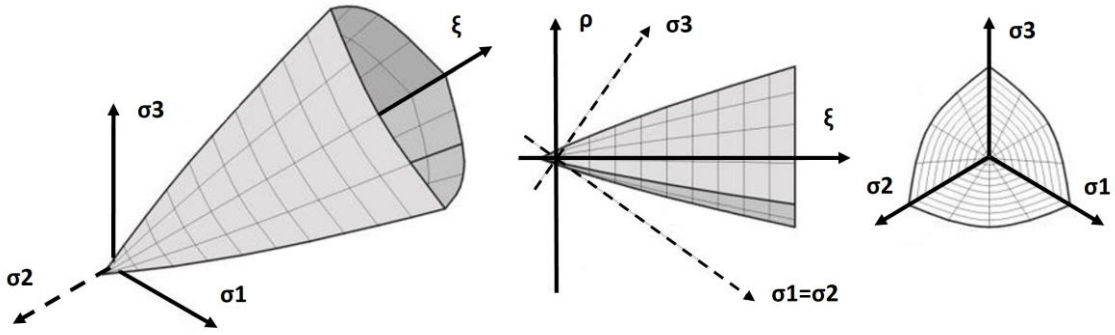

Fig. 5.7 - The Menetrey-Willam surface in the Haigh-Westergaard space.

However, the striking point refers to the extension of simulation capability beyond the strength limit, so to the softening zone of deformation. Detailing the stress-strain load response for both, the Drucker-Prager and the Menetrey-Willam concrete model during the softening process, the fracture theory considering the micro-cracking phenomenon for a heterogeneous aggregate material, what concrete exactly is, was implemented into ANSYS (detailed in section 5.1.5).

In conclusion, compared to the other concrete models implemented in ANSYS, one has to accept a noteworthy advance. Despite it, still some capability abridgements have remained. On this basis, a deeper insight regarding the numerical difficulties during FE computations is generally discussed in the section.

5.1.5 The Main Drawbacks of the Fundamental Material Models in ANSYS

Concentrating on capabilities of the presented concrete models in relation to a general limiting state represented mostly by formation of a crack, the smeared cracking model is used. So, if the purpose of an analysis attempts to capture only the total load-deflection state instead of tracing a realistic crack pattern, the smeared cracking approach seems like a sufficient formulation.

In more detail, the cracking process for both material models the Drucker-Prager and the Menetrey-Willam is simulated by the fictitious crack model developed by Hillerborg (Fig. 5.8). However, in this case, it should be kept in mind, this fictitious crack model is capable only of Mode I fracture simulation. On this basis, behaviour of tensile stresses is controlled by the fracture energy which is based on the crack opening width. This energy represents a certain type of material property required to propagate a crack. The gradual loss of the tensile strength is defined by a virtue of a cohesion reduction, which triggers when the material is no longer intact. So, within the limited fracture zone, as the stress decreases, the deformation increases. This unloading scenario arises after passing the criterion of maximal tensile stress at the beginning of a crack tip. Furthermore, at the end of cracking zone, after reaching a limiting width of crack rupture, the crack end becomes stress-free. Consequently, complete loss of cohesion leads to creation of a total fracture behaving as granular cohesion-less materials. Regrettably, as was mentioned before, only Mode I capturing an opening of the crack tip orthogonal to the surface exhibited to the maximal stresses for both compression and tensile regime is considered. So, if the simulation which the matter of issue addresses shearing of concrete, an alternative solution must be found.

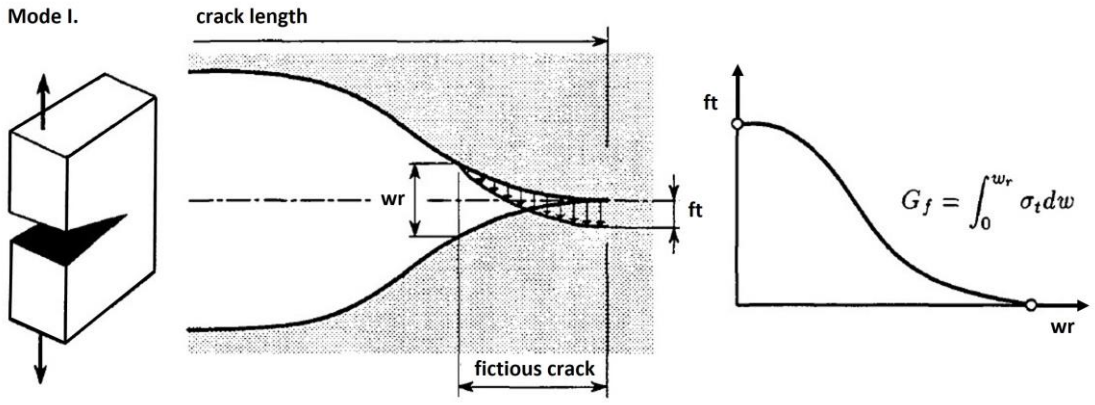

Fig. 5.8 - Factious crack model by Hillerborg.

Among other phenomena present by the cracking process, the stiffness degradation plays one of the most important roles. A simplified model for gradual degradation of

concrete strength using an elastic relation proportional to the cohesion is implemented for the aforementioned two constitutions. The complete loss of strength is characterized by negligible elastic module and Poisson's ratio equal to zero.

Unfortunately, despite this implementation the softening process, these models are able to capture the main failure mechanism at the peak load, but unable to properly report the rest of the softening process. Thus, many difficulties arise during the FE computation as consequence of local stress concentrations, so even before achieving the ultimate load limit of an investigated sample. So, no matter how intense the effort and range of applied adjustments are (reduction of load increments, change of equation solver or an application of numerical stabilization), the computation is not able to obtain the force equilibrium. This repulsive state is predominantly caused by the loss of uniqueness of a solution. That means in terms of the uniqueness theorem, as the strain energy function is defined by relation of deformation to force, its value respecting thermodynamic laws has to be positively definite, if it is not, it would produce heat. Consequently, within the concept of plasticity theory, variety of numerical instabilities having roots in non-existence of one-to-one function (two strains correspond to the same stress) might occur (Fig. 5.9).

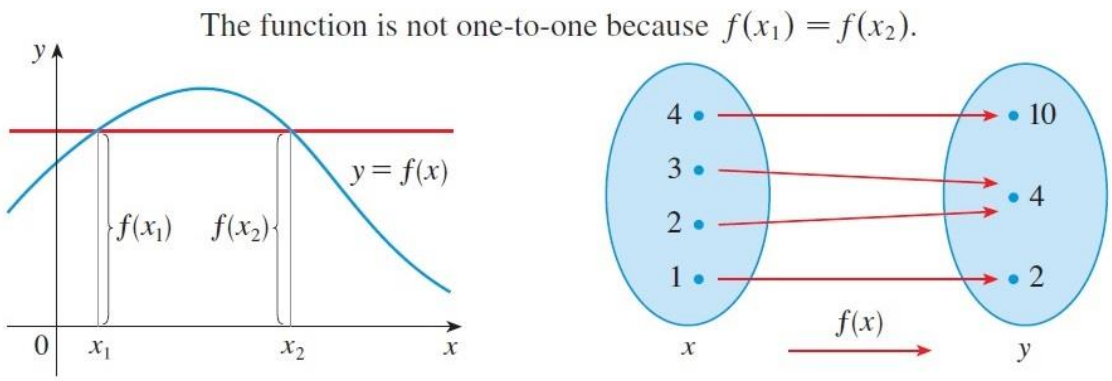

Fig. 5.9 - Simplified example of the uniqueness theorem.

As a result, the global stiffness matrix is not defined as invertible anymore. Thus, during the solving procedure, the computation is abruptly ceased and convoyed by an error message addressing matrix singularity problem.

Similar problems might by encountered by damage laws implemented in classical continuum models, wherein damage is considered as isotropic and linked to the evolution of inelastic strains. Generally, if a simply supported bar of a length L under uniaxial tension not incorporating any initial defects is taken into account, the problem with non-uniqueness of a solution arises as a consequence of uniformly distributed stresses along the sample. In this case, there are many outcomes likely to occur, but the situation is

clueless with respect of the correct solution. Further, turning to the stiffness loss description of quasi-brittle materials, a great caution should be paid to the inelastic deformation localisation which might produce significant discrepancies compared to the experimental evidence. The origin of this localisation lies in development of material defects resulting in subsequent reduction of effective load-bearing area just at particular positions of a FE model. Consequently, during the softening, concentration of inelastic deformations just for certain elements at certain location is expected. So, if the element size changes from greater to smaller, the deformation zone behaves likewise. That means, for a certain mesh density, only particular solution can be obtained. In addition, compared to general numerical computation by which a decrease of element length leads to more accurate results, by the stiffness degradation process the same approach produces the exact contrast. This state is widely known as pathological mesh dependence or spurious mesh sensitivity (Fig. 5.10).

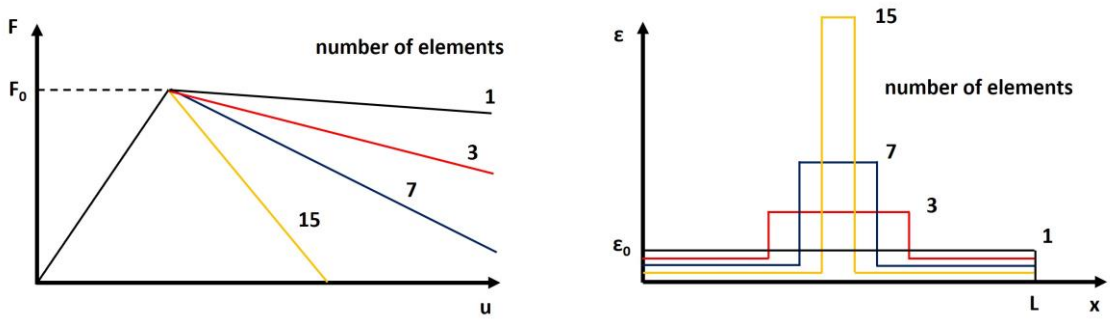

Fig. 5.10 - Pathological effects of mesh refinement on the numerical results.

Fortunately, there exists several possible solutions for proper description of strain softening phenomenon spanning from the endochronic theory, the plastic-fracturing theory, plasticity with decreasing yield limit, the bounding surface theory, and most recently continuum damage theory. However, relevant applicability of damage models is strongly conditional upon absence of localization phenomena. Therefore, a high demand for additional techniques such as crack band approach or non-local methods within the context of the smeared approach to damage has been witnessed in the last decade. On this account, a brief description of other software and their constitutions for concrete, highlighting their strengths and weaknesses, will be delivered.

5.1.6 Material Model in ABAQUS

As the next generation of material laws capturing complicated concrete behaviour, the classical work-hardening plasticity theories were replaced by the plastic-damage models. This vital enhancement advanced the bounds of previous constitutive principles beyond the level of peak-stresses capturing the stiffness degradation and opened new

dimension for cyclic loading. Consequently, many scientific studies were conducted using elegance and simplicity of this material constitution [17].

However, exploring the input material parameters in more detail, especially dilatancy angle deservers an increased attention. So, as was mentioned before, its value varies during the entire loading process and, what is more significant, it affects behaviour and spread of plastic zones. Thus, a worth considering obstacle arises. If this constitution uses constant value for so dynamic parameter, this simplification subverts the fundamental principles of granular material natures and might produce controversial results. Hence, aiming to attain adequate concrete response, conduction of a parametric study using different values for dilatancy angle seems to be an imperative before every single FE analysis differing in concrete class, loading and structural type (Fig. 5.11). Regarding this matter of issue, more details can be found in [23].

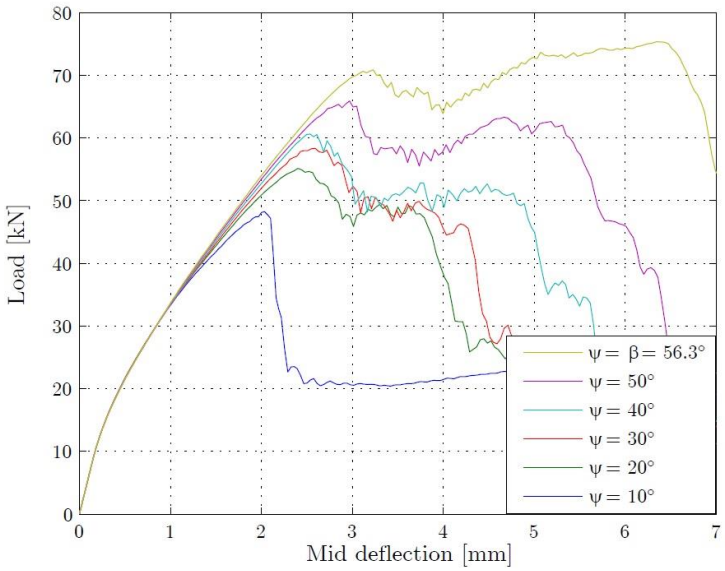

Fig. 5.11 - Influence of dilatation angle in concrete damaged plasticity model (ABAQUS) [23].

Albeit this evident drawback, this model is widely spread not only in the commercial civil-engineering community but also in the scientific one. The main representative of this constitutive model is implemented in ABAQUS software package.

Concluding, as this constitution is able to capture more-less the major of concrete natures not only for static but also for transient structural problems, the relevance of its usage signals no doubts.

5.1.7 Material Models in ATENA

Basically, three major principles for modelling of concrete behaviour are implemented in ATENA software environment.

The first one is represented by SBETA concept. This approach exploits fundamentals of the nonlinear hypo-elastic constitutive model. Interestingly, different laws are used for loading and unloading conditions. This treatment allows to smooth continuation of a calculation even by appearance of energy dissipation processes, in this case, the gradual damage of concrete.

The second one - Fracture-Plastic Constitutive Model combines constitutive models for compressive (plastic) and tensile (fracturing) behaviour. Where, the plastic response is based on the Menetrey-Willam criterion, which permits exponential softening by usage of return mapping algorithm for the integration of constitutive equations. Hence, this model warrants the solution for all magnitudes of strain increments. Turning to fracturing, the model employs Rankine failure criterion with classical orthotropic smeared cracking formulation and crack band model enabling rotated or fixed crack approach.

The third one uses principles of the microplane formulation. Debate on this subject will be brought up in the following section.

5.1.8 The Microplane Model in ANSYS

Picturing the composition of concrete mixture under certain magnitude of a load (Fig. 5.12), previously intact material displays highly oriented patterns exhibiting non-uniformly distributed inelastic deformations which can be thought as a function of normal stresses and strains across the planes.

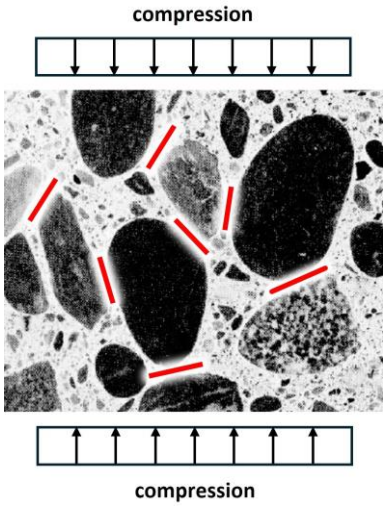

Fig. 5.12 - The fundamentals of the Microplane model principles.

Attempting to realistically express this complex stress state, a fundamental concept for genesis of the Microplane model has arisen. The corner stone of this approach was laid on the pivotal idea of Taylor [24], who proposed the constitutive law for polycrystalline metals. The fundamental development of this model was undertaken by Bazant and

Gambarova [25]. As this material model manifests significant benefits compared to the classical models based on the theory of plasticity, there are, of course, some important differences. The typical constitutive models employ tensorial invariants, which operate with stress and strain tensors. By doing so, evaluation of second and fourth order tensor functions enters, what significantly complicates the process. Contrariwise, the Microplane model is defined through stress-strain laws assign to several individual planes. These planes represent thin contact layers between adjacent aggregates producing sharp extremes of stresses with subsequent micro-cracking initiation. This phenomenon is the main cause for development of inelastic strains, which can be hardly described by constitutions using macroscopic strains. Therefore, the microplane approach does not introduce these tensorial relations at individual microplanes but exploits vectorial relations on randomly oriented planes of a small unit sphere describing deformation state along weak surfaces of cementitious matrix to establish the constitutive laws. The tensorial invariance restrictions are then satisfied using integration of responses estimated at the unit sphere to macro-level by the principle of virtual work (Fig. 5.13).

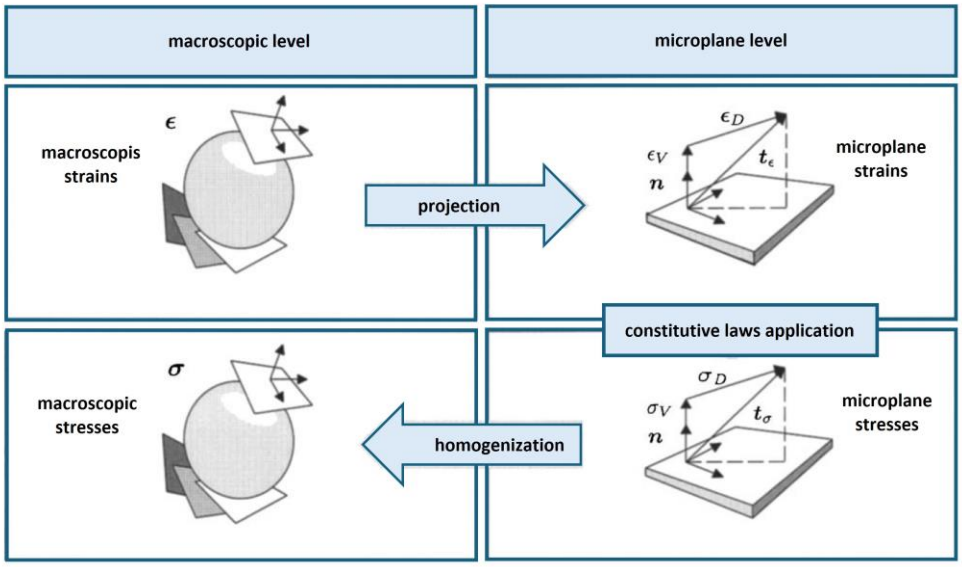

Fig. 5.13 - Simplified depiction of the Microplane theory.

Furthermore, by virtue of vectors acting on the microplanes, it is able to account for anisotropy induced by the inelastic strains resulting in multiaxial damage expressed in relatively simple manner. So, to model these strain-softening processes of concrete, the microstructure is constrained kinematically, not statically, as was postulated by Taylor. The reasoning behind this treatment lies in character of the inelastic behaviour of concrete, which is predominantly strain- not stress-controlled. Practically it means, the strains acting on microplanes having different orientations represent the resolved

components of the same macroscopic strain - projection of its components. As a result, this approach with additional employment of non-local theories warrants avoidance of spurious localization of damage - one of the greatest challenges in description of concrete strain-softening process. What in comparison to the previously mentioned material models, based on principles of the plasticity theory, significantly outperforms their simulation capabilities.

Hitherto, two main methods regarding formulation of the microplane material laws exist. The first one works on principles of stress-strain boundaries. This approach is implemented in software ATENA and follows the research work by Bazant et al. On the other hand, the second approach introduces laws which combine principles of the microplane theory and invariant-based plasticity and damage models and is implemented in ANSYS software package. Herein, the constitutive laws emerge on the fundamentals of the Drucker-Prager cap model enabling to cover a variety of stress states acting on the microplanes under static or cyclic loading conditions. Moreover, as an effective remedy regarding the spurious mesh sensitivity problems, an implicit gradient regularization scheme exploiting the nonlocal approach has been implemented within the FE code as well.

However, as the Microplane model works on principles of strain decomposition of the global strain components to the individual microplanes using vectorial basis, its properties using typical stress-strain relations cannot be defined. On that account, a calibration of material parameters for the Microplane model in the form of an algorithmic code was developed. The entire course of this calibration procedure is presented and discussed in chapter 5.2.

5.1.9 Cap Model as a Yielding Criterion

For the Microplane model in ANSYS, the yield function considers the undamaged stress space displaying linear behaviour under angle α between the caps for compression and tension regime. In addition, under this angle, a linkage to the Mohr-Coulomb model can be found, wherein it represents coefficient of friction.

Although simplicity and versatility of these cap models, convergence difficulties were encountered by their usage. Hence, a multiplicative formulation between individual functions of the yield surfaces aiming to define a smooth (continuously derivative) failure surface was implemented. As being typical for yielding functions covering the load response under all possible stress triaxialities, also this volumetric-dependent cap surface using a three-stress invariant implementation is defined under hydrostatic compression. Albeit not so clear definition of stress-strain relations for concrete as in the

case of classical material models, the physically measurable quantities relevant for concrete (for instance - uniaxial and biaxial strengths) can be easily demonstrated by the meridian section of the yield surface (Fig. 5.14).

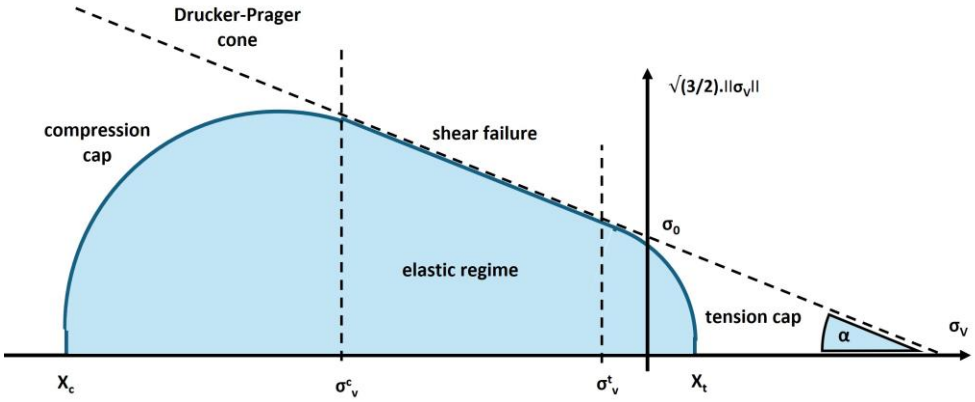

Fig. 5.14 - Depiction of elastic regime of the Drucker-Prager cap model.

5.1.10 Damage Model

As was stated earlier, in order to cover the post-peak strain softening behaviour, in other words the gradual damage, the initial idea of static constraints was replaced by employment of kinematic constraints. By dint of this enhancement, the very first fundamental for directional-dependent stiffness degradation incorporating damage laws on individual potential failure planes has been laid. This is followed again by the homogenization process of responses over the unit sphere in order to quantify macroscopic anisotropic damage.

Reflecting the aforementioned material models, wherein solely the simplest form of isotropic damage was adopted, the Microplane model offers an evident advantage. By dint of this treatment, more realistic reproduction of microcracks during the inelastic regime of concrete was able to capture. While on the other hand, attempting to incorporate anisotropic damage into classical models causes severe difficulties resulting in complex definition of three-dimensional material formulations using higher order damage variables. Hence, the microplane approach conveys more natural and simpler manner.

Despite this great enhancement, the pathological mesh sensitivity aspect remained unsolved. Therefore, a suitable regularization scheme employing a length scale parameter via the nonlocal formulation was adopted into the Microplane model.

5.1.11 Non-Local Effects

Taking on account classical continuum theory, material behaviour at arbitrary node of a sample is typically governed by constitutive relations considering basically elastic

constants, stress-strain relation, and other necessary properties. The linkage between these nodes is warranted by the equilibrium equations and the stress tensor. However, these classical material models do not consider the microstructure of simulated material in respect of the specimen size, what in the case of samples made from concrete represents an alarming shortcoming. That means, there is no length scale, although the material heterogeneities influence the material load response in a great measure. Considering this fact, it seems vital to implement some sort of length scale parameters into the material model. This demand has provided a fertile ground for genesis of the nonlocal continuum models.

In more depth, the nonlocal constitutions respect the influence of a neighbouring domain of the material point. As the real stresses and strains experience at critical points of load patterns sharp extremes, which are hardly to describe by the classical continuum models, this phenomenon is expressed by weighted average of inelastic strains over a certain representative volume. In addition, by averaging of responses within the neighbouring domain, the deformation field remains smooth not displaying any discontinuities (Fig. 5.15), which in general brings about an ill-posed boundary value problem.

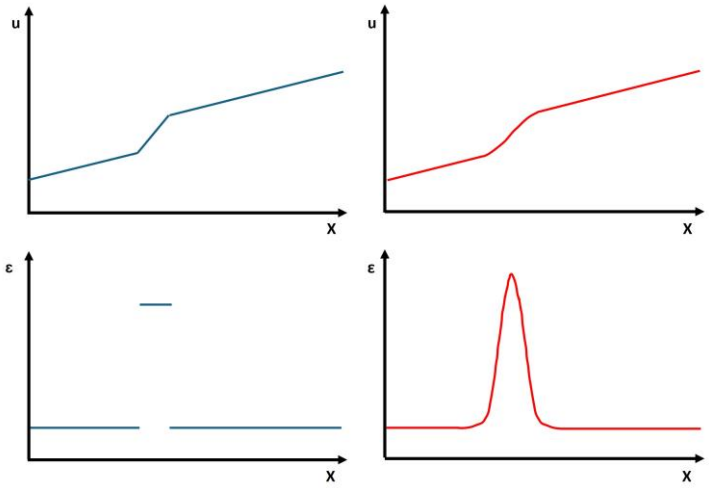

Fig. 5.15 - Examples of dis- and continuous description of narrow band width formation.

To be specific, as the strain-softening damage tends to localize in a zone of vanishing volume, not using the non-local approach might produce an incorrect convergence by gradual refinement of an element size. That means, the location of crack bands is mesh dependent. This conflicts with general objectivity in reference to the realistic load response. So, these weight functions work with special input parameters, for instance a characteristic material length, aiming to embody size effects and provide more realistic simulation of strain concentration resulting in formation of narrow crack bands. Fortunately, this sort of a problem is also lessened using the non-local approach,

especially for ANSYS, by the implicit gradient regularization, which is incorporated into the FE procedure as an extra degree of freedom.

5.2 Algorithmic Calibration of the Input Parameters for the Microplane Model in ANSYS

Despite indisputable enhancement of concrete simulation capabilities by development of the Microplane model, two practical issues have arisen, namely:

- higher demand for computation performance,
- additional expertise of the user for proper definition of input parameters.

Trying to solve the latter issue, calibration procedure of the input parameters for the Microplane model will be provided.

So far, the Microplane model cannot be defined by typical stress-strain relation as by classical concrete constitutions, thus the user needs to identify 16 material parameters in total. However, some of them could be easily defined from uniaxial concrete tests, some derived from literature, and some identified on the basis of mutual relations. On grounds of the preliminary studies, it was revealed, only 4 parameters display a great potential to significantly influence the stress-strain behaviour under variety of loading conditions. Consequently, a calibration code within the environment of ANSYS was developed. Herein, the material parameters are verified by optimum fitting with respect to fundamental stress-strain relations for concrete in uniaxial compression and tension, and under biaxial pressure.

5.2.1 Algorithm Structuring

Firstly, a scale of deformations and a primal range of values for input parameters are essential to define. Secondly, the entire FE model, covering volume modelling, material definition, element selection, model meshing and boundaries application, is built. Thirdly, solution controls are specified. Fourthly, a procedure defining adequate value for Young´s modulus of concrete is performed. Then, the remaining parameters are identified by algorithm process and optimum fitting with the reference stress-strain laws. Finally, an outcome in the form of 4 meticulously identified parameters is obtained.

Detailing the first part:

- Considering load ranges used in experimental tests for uniaxial compression and tension, and biaxial pressure, the load limit was determined in the form of strain having value of 0.005. In the FE model, this treatment has met condition of

deformation at the level of 0.005 mm in relation to a 3D cube model of size 1x1x1 mm (Fig. 5.16).

- Loads passing this limit within the previous experimental measurements have yielded slightly unreliable results having root in complexity of measurement procedure and concrete response within the fracturing zone, therefore the limit.
- Further, a primal range of values for 16 parameters is required to be specified. Their brief overview including relation between individual parameters and also span of applicable values is summarized in Tab. 5.1.

- *Tab. 5.1 – General values of the input parameters for the Microplane model.*

Parameter type	Parameter	Note	Value
Elasticity	E	Modulus of elasticity	21000 - 40000 MPa
	v	Poisson´s ratio	0.18
Plasticity	f_{uc}	Uniaxial compressive strength	defined from the compression cylinder test
	f_{bc}	Biaxial compressive strength	$1.15*f_{uc}$
	f_{ut}	Uniaxial tensile strength	$1.4*(f_{uc}/10)^{(2/3)}$
	σ_{vc}	Intersection point abscissa between compression cap and Drucker-Prager yield function	$-2/3*f_{bc}$
	R	Ratio between the major and minor axes of the cap	(1.5-3.5)
	D	Hardening material constant	10000 - 300000
	R_T	Tension cap hardening constant	1
Damage	γ_{t0}	Tension damage threshold	0
	γ_{c0}	Compression damage threshold	(1 - 10)*10E(-5)
	β_t	Tension damage evolution constants	1000 - 10000
	β_c	Compression damage evolution constants	1000 - 10000

Non-local	*l*	Characteristic length of an element	up to the mesh
	c	Nonlocal interaction range parameter	4*l**2 < c (mm^2)
	m	Over-nonlocal averaging parameter	(1-4)

The author would like to refer the reader for more detailed description of the mentioned parameters to [26].

Moving to the second part:

- A cube of size 1x1x1mm is modelled via volume command.
- Material parameters are specified by commands allowing the Microplane model abilities to be fully exploited.
- Element type is selected. In this case, only element CPT215, activating two extra degrees of freedom for the regularization technique, can be employed.
- Meshing of modelled cube is performed.
- Boundaries are applied. Noteworthy, they are flexibly adjusted to a configuration of applied load (uniaxial or biaxial).

Within the third part, specific solution options were applied:

- Analysis type was specified as a static structural analysis.
- Large deformation effects were included.
- Number of sub-steps was equal to 50.
- Maximum number of equilibrium iterations was specified as 25.
- Automatic time stepping was applied.
- Convergence limits for force and deformation were defined.

Discussing the fourth part:

- Trying to identify a suitable value for Young´s modulus *E* and a primer value of hardening material constant D, only a half of the limited load (0.0025 mm) is used for the uniaxial compression test simulation. The reason for this extraordinary approach - not respecting the standardized values of Young´s modulus for individual concrete classes, lies in finding the most optimum fitting with the reference load response. In fact, 600 computations are performed.
- After a successful identification of Young´s modulus *E* and a starting value of hardening material constant *D*, the full scale of load is applied under uniaxial compression and tension, and biaxial pressure. By doing so, change of load

response under combination of 3 parameters (*D*, *βt*, *βc*) varying in predefined extent is examined by usage of algorithmic process. In total, 7500 calculations are made.

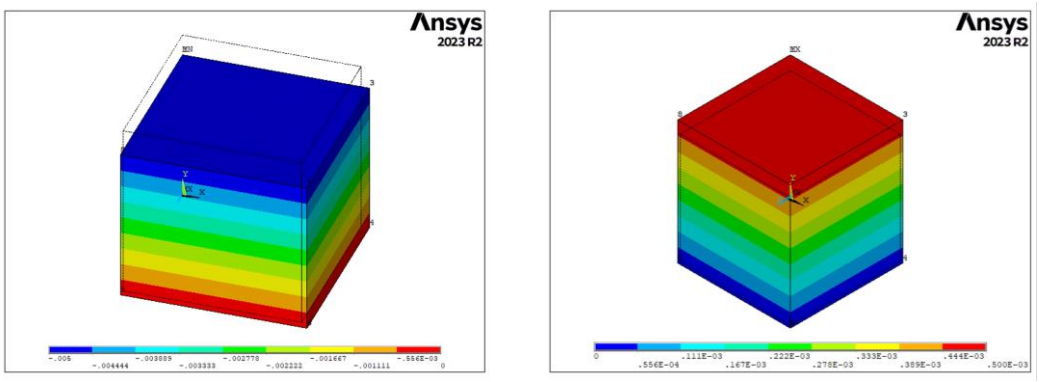

(a) (b)

Fig. 5.16 - FE cube model under a) compression and b) tension.

Ultimately, an outcome in the form of 4 parameters, concretely, Young´s modulus *E*, hardening material constant *D*, tension *βt* and compression *βc* damage evolution constants, is obtained. With respect to our needs, the derived input parameters are summarized in Tab. 5.2.

- *Tab. 5.2 – Derived input parameters for the Microplane model.*

Note	Parameter	Value
Modulus of elasticity	E	21 GPa
Poisson´s ratio	v	0.18
Uniaxial compressive strength	f_{uc}	46.18 MPa
Biaxial compressive strength	f_{bc}	53.11 MPa
Uniaxial tensile strength	f_{ut}	3.88 MPa
Intersection point abscissa between compression cap and Drucker-Prager yield function	σ_{vc}	-35.41 MPa
Ratio between the major and minor axes of the cap	R	2
Hardening material constant	D	80000
Tension cap hardening constant	R_T	1
Tension damage threshold	γ_{t0}	0
Compression damage threshold	γ_{c0}	1*10E(-4)
Tension damage evolution constants	β_t	6000
Compression damage evolution constants	β_c	2000
Characteristic length of an element	l	50
Nonlocal interaction range parameter	c	4500 mm^2
Over-nonlocal averaging parameter	m	2

However, it should be kept in mind, the correlation between stress-strain laws and FE results is an imperative before any succeeding usage of identified parameters.

5.2.2 Correlation with Stress-Strain Laws

The results obtained from the previous FE calculations has been calibrated by fitting against generally accepted stress-strain laws defined for uniaxial compression and tension, and biaxial pressure. Especially, these relations were selected for determination of suitable values for the free parameters (*E*, *D*, *βt*, *βc*). As a consequence of applied methodology, a sound credibility for the intended FE investigation is warranted.

Turning to uniaxial compression, the formula defined by Popovics [27] was based on the former relations but having ability to estimate the complete stress-strain diagram of concrete. Additionally, it provides more relative curvature, which in the end guarantees a better fit of experimentally derived data within wider limits than the similar formulas available in literature. This relation is defined by the formula:

$$f = f_o \cdot \frac{\varepsilon}{\varepsilon_o} \cdot \frac{n}{n - 1 + (\varepsilon / \varepsilon_o)^n} \tag{9}$$

where

f = *axial stress*

f_o = *ultimate stress*

ε = *unit strain*

ε_o = *unit strain at the ultimate stress*

n = *constant expressed as a function of the compressive strength of normal weight concrete defined as follows:*

$$n = \frac{4}{10} . 10^{-3} . f_o + 1 \tag{10}$$

Consequently, agreement between data can be seen in Fig. 5.17.

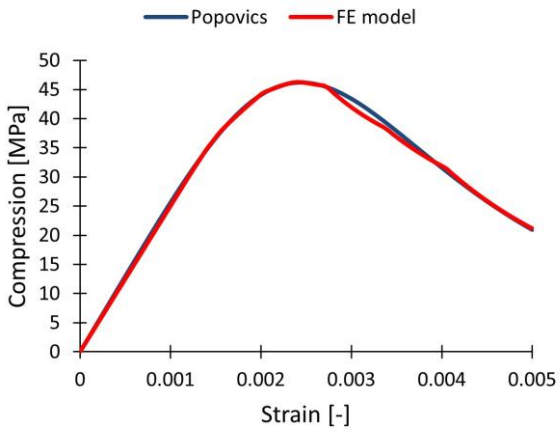

Fig. 5.17 - Comparison of the reference stress-strain law and FE outcome under uniaxial compression.

Further, as a reference relation for uniaxial tension, the formula based on the investigation of Cintorina [28] was chosen. The root behind this selection laid in high credibility of experimental evidence describing the softening response of concrete under direct tension. To be specific, within this study a strain-controlled testing method was used, therefore the post-peak curve could be more easily recorded.

Thus, a unique formula for normalized load vs. deformation curve has been proposed taking form of:

$$\sigma = \sigma_{\max} \cdot \frac{A}{(\delta / \delta_{\max})} \cdot (1 - e^{B.(\delta/\delta \max)^C}) \cdot (1 - \delta / \delta \max)^D \qquad (11)$$

where

σ = *tensile stress* $A = 0.075$

σ_{max} = *maximum tensile stress* $B = 400$

δ = *displacement* $C = 1.95$

δ_{max} = *maximum displacement* $D = 0.50$

In Fig. 5.18., analytical and numerical data are illustrated.

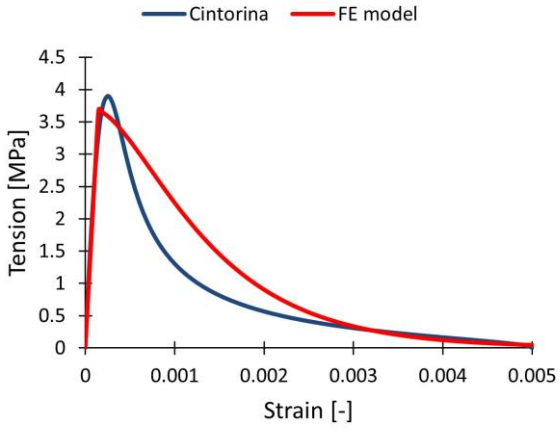

Fig. 5.18 - Comparison of the reference stress-strain law and FE outcome under uniaxial tension.

As the last one, the load response of concrete under biaxial pressure was justified using criterion based on the research of Kupfer [29]. This experimental study has yielded following description of concrete stress state in:

- compression - compression regime as:

$$f_{cb} = \frac{1 + 356/100.a}{(1+a)^2} \cdot f_c \qquad (12)$$

where

f_{cb} = *biaxial strength*

f_c = *uniaxial compressive strength*

a = *ratio between principal stresses in concrete*

- compression - tension regime as:

$$f_{ctb} = f_c . r_{ec} \tag{13}$$

where

r_{ec} *= factor describing almost linear behaviour between the ultimate strengths in compression and tension, respectively, thus reducing* f_c *by value ranging from 0.99 to 0.01*

- tension - tension regime as:

$$f_{ttb} = f_t \tag{14}$$

where

f_t *= uniaxial tension strength*

Finally, correlation between the criterion of Kupfer and results from the FE calculation using the Microplane model are reported in Fig. 5.19.

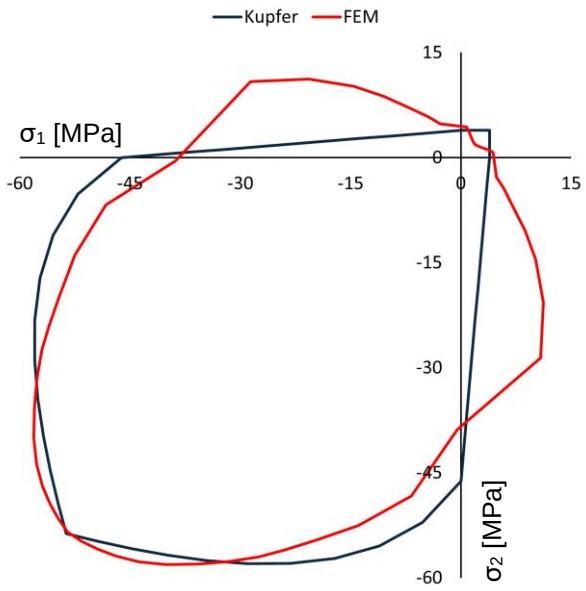

Fig. 5.19 - Comparison of the reference stress-strain law and FE outcome under biaxial pressure.

5.2.3 Discussion

In conclusion, the FE model predictions could be labelled as quite precise with respect to the reference criterions. Using the calibration procedure, instead of guessing the values for required parameters of the Microplane model in ANSYS, a rigorous methodology was defined.

Although, some burning questions, for instance expressing a paucity of verification extent in comparison to calibration procedure of the Microplane model M7 [30, 31] might arise. Hence, as the picture of the concrete load response seems to be incomplete, more detailed study devoted to this subject is of wider interest.

Moreover, a noteworthy discrepancy under biaxial loading in both compression - tension and tension - tension regimes were revealed. Detailing this phenomenon, results from different strength classes of concrete were evaluated. This has yielded evidence illustrated in Fig. 5.20, which implies possible pathological behaviour of this material model in the mentioned loading zones.

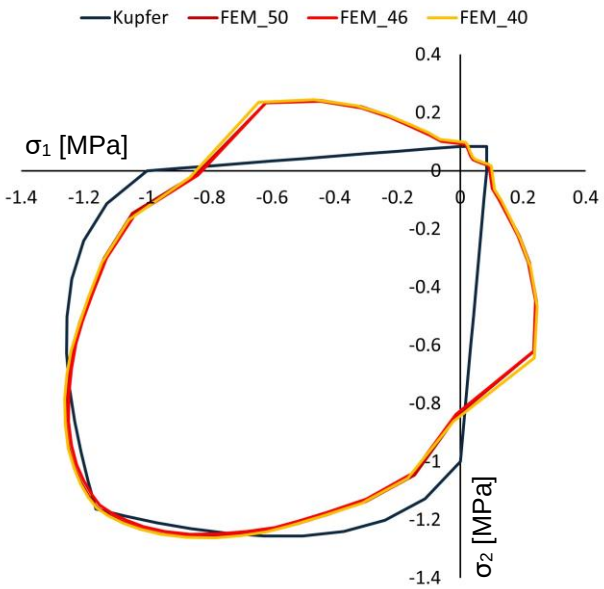

Fig. 5.20 - Comparison of the reference stress-strain law and FE outcome under biaxial pressure employing different strength classes.

Considering fundamentals of this material subroutine, root behind this issue might origin in formulation of the cap yield surface. Especially, its smoothness is ensured by multiplication of different formulas expressing individual loading regimes. Despite declared, scale of the impact needs deeper inspection.

5.3 Steel as a part of the FE model

In contrast to the material models for concrete, any incorporation of the material microstructure for steel is unnecessary, so constitutive models, which are defined only locally are able to capture the most important part of the load response.

The basic concept suggests steel behaves in a linear fashion up to the initiation of yielding. Within this range, the slope of stress-strain relation is equal to the elastic modulus E_s. Passing the yield criterion expressed commonly by the yield strength,

plasticity initiates. However, there are different definition of the yield criterion for different materials. For metallic materials, the yield surface is independent of the hydrostatic pressure and is commonly defined in the principal stress space. One of the most prevalent yield surfaces of this type is the von Mises yield criterion, which can be envisaged as a cylinder with the axis along the hydrostatic line (Fig. 5.21). In addition, it also defines the plastic flow potential.

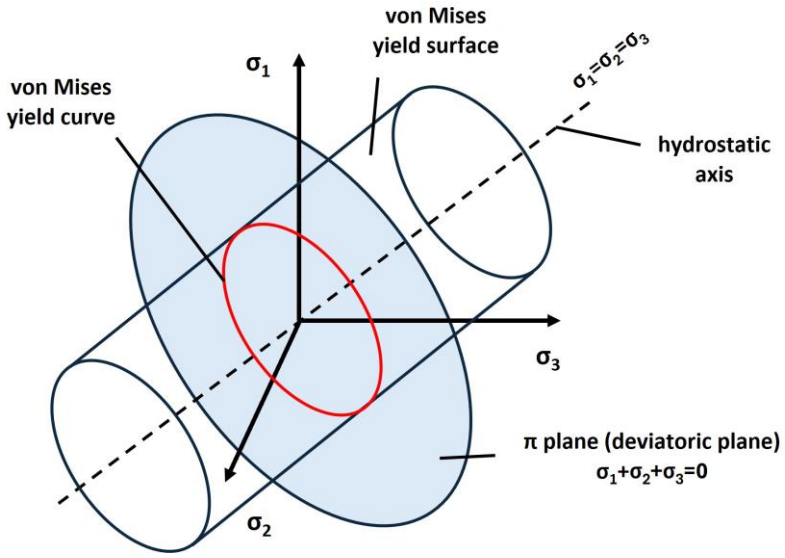

Fig. 5.21 - Von Mises yield criterion.

As was mentioned before, the plasticity models can be divided into two fundamental families using associated and non-associated flow rule. The associated plasticity models properly capture the plasticity of crystalline metals. In more detailed terms, the direction of the plastic strain rate tensor remains normal to the yield surface (normality hypothesis of plasticity) which leads to the uniqueness of the solution. This is being quite important factor for convenience of an arbitrary FE computation containing steel elements with reference to the solution divergence. Based on this, the evolution of inelastic strains can be evaluated by the flow rule.

After passing the initial yield surface, the inelastic deformation (irreversible strain state) is governed by the hardening rule. Considering the isotropic hardening model, it is characterized as an expansion of the yield surface without any distortion or translation. Basically, it is defined by a hardening parameter which is a function of the plastic strain. Different relations can be considered between the hardening parameter and effective plastic strain. Commonly, for the von Mises criterion, the linear relation is selected expressing the simplest relation. So, when the inelastic deformations enter, the model

experiences a uniform increase in the size of the yield surface resulting in a certain increase in a stress.

For this material model, the input quantities, in a form of stress and strain measures, corresponds to each other. That means, they are defined as one-to-one function, they are unique. This only emphasizes simplicity of the FE computation for steel elements in comparison to FE models containing concrete components.

For the sake of preciseness, an accurate description of stress-strain behaviour for steel elements in the reference FE model was paramount of importance. Ergo, constitutive equations [32] describing almost the full engineering stress-strain response of steel were employed. Even though this constitution is predominantly designated for the hot-rolled carbon steels, it has been applied in the FE investigation for a welded steel-section not displaying any notable disparities.

This model conveniently covers elastic response up to the yield point, followed by a yield plateau and strain hardening up to the ultimate tensile stress. Noteworthy, as the onset of strain hardening and attainment of the ultimate stress are not so easily defined, predictive expressions solving this issue were developed and calibrated against stress-strain data collected from literature. Even though this constitution is built only on three fundamental input parameters (young´s modulus *E*, yield strength f_y and ultimate strength f_u), it shows more accurate predictions than other widely used models. Formulation of the presented model can be formed as follows:

$$f_{(\varepsilon)} = \begin{cases} E.\varepsilon & for\ \varepsilon \le \varepsilon_y \quad (15) \\ f_y & for\ \varepsilon_y < \varepsilon \le \varepsilon_{sh} \quad (16) \\ f_y + E_{sh}.(\varepsilon - \varepsilon_{sh}) & for\ \varepsilon_{sh} < \varepsilon \le C_1.\varepsilon_u \quad (17) \\ f_{C_1\varepsilon_u} + \dfrac{f_u - f_{C_1\varepsilon_u}}{\varepsilon_u - C_1.\varepsilon_u}.(\varepsilon - C_1.\varepsilon_u) & for\ C_1.\varepsilon_u < \varepsilon \le \varepsilon_u \quad (18) \end{cases}$$

where

$$\varepsilon_u = \frac{6}{10}.(1 - \frac{f_y}{f_u}), \qquad C_1 = \frac{\varepsilon_{sh} + \frac{25}{100}.(\varepsilon_u - \varepsilon_{sh})}{\varepsilon_u}, \qquad (19), (20)$$

$$\varepsilon_{sh} = \frac{1}{10}.\frac{f_y}{f_u}.\frac{55}{1000}, \qquad E_{sh} = \frac{f_u - f_y}{\frac{4}{10}.(\varepsilon_u - \varepsilon_{sh})}, \qquad (21), (22)$$

The author takes the liberty of referring the reader to the reference [32] for more detailed explanation of the individual relations and offers at least a graphic explanation of some of them in Fig. 5.22.

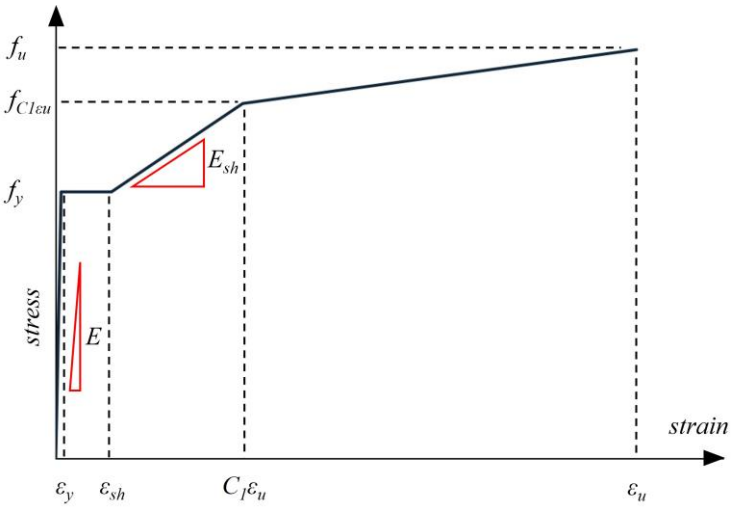

Fig. 5.22 - Quad-linear model of stress-strain behaviour for steel components.

Furthermore, stress-strain relations demonstrating suitability of applied constitution on the basis of experimentally obtained data from coupon tests are illustrated in Fig. 5.23.

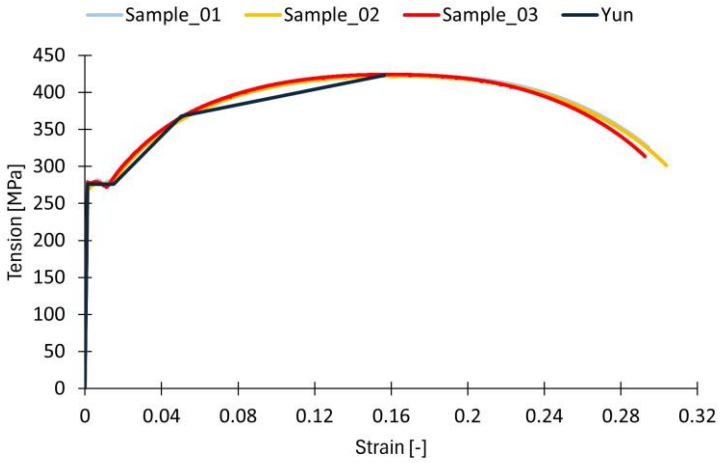

Fig. 5.23 - Stress-strain relations of steel from coupon tests and applied constitutive model.

5.4 Shear Connection as a FE Contact

Commonly, as the simplest description of the shear connection in FE models of composite beams, a spring element is used [33]. On one side, this alternative offers an easy application, on the other side, it can lead to a serious underestimation of axial capabilities of connectors and concentration of unrealistic large strains in the area of application.

Seeking for more appropriate FE discretization, a 3-D model of a shear stud seems to represent the right one. In this way, a shear stud is modelled as a volume object commonly meshed with higher order elements [34]. Then, a contact between elements forming shear studs and surrounding concrete must be somehow defined. Hence, a set of different variables, for instance normal stiffness, tangential stiffness, general characteristics of underlying materials and their constitutive descriptions, have a great potential to significantly affect or even limit the structural performance of this shear connection alternative. Respecting said, this method appears to be quite challenging.

As the last alternative of a shear connection discretization (Fig. 5.24), a 2-D model working on principles of surface-to-surface contact will be addressed. Particularly, this model represents the golden mean of previously discussed alternatives. It exploits spring model simplicity and preserves partially the 3-D model complexity. Even, a formation of the typical bearing cone is somewhat warranted.

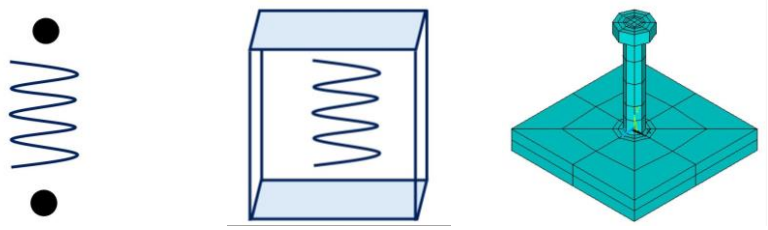

(a) (b) (c)

Fig. 5.24 - Alternatives of a shear connection discretization in FE models a) 1-D spring element, b) 2-D contact, c) 3-D model of shear stud.

Basically, as the Hertz theory [35] creates the bedrock of contact problem analysis, contact surfaces deform on principles of elastic half-spaces. If one of the contacting bodies is significantly stiffer than the other, then the rigid-to-flexible contact accompanied by the unsymmetric (pair-based) option shall be used in ANSYS. By doing so, all the contact elements belong only to one specific surface and all target elements to the other. On this basis, the contact surface properties were assigned to the concrete slab whereby the steel top flange was treated as the target surface [36].

As the next step, a particular type of contact regarding its structural response had to be defined. Considering the mechanical properties of a shear headed studs, the no-separation contact was selected as the most suitable one. Detailing behaviour of this contact, the typical load response of a shear connector was governed by suitable values of normal (FKN) and tangential (FKT) stiffness, and the maximum frictional stress constraint (TAUMAX). It must be noted, these characteristics were firstly evaluated for an individual shear connector and subsequently transformed to two-dimensional domain by division of sum of individual shear connectors´ resistances by the relevant area (Fig. 5.25).

To be specific, the axial stiffness of a shear connector was defined in accordance with [37, 38] as:

$$k_{axial} = \frac{E_s.A_s.h_{ef}}{h_{ef}^2 + \frac{115}{10}.n.A_s} \tag{23}$$

where

E_s = *Young's modulus of steel used for a stud connector*

A_s = *cross-section area of a stud shank*

h_{ef} = *effective height of a shear stud embedment*

n = *ratio between* E_s/E_c, *where* E_c *is Young's modulus of concrete*

Further, the initial tangential stiffness was defined in reference to [6] by formula:

$$k_{\tan} = \frac{D_{\max}}{d_{sh}.(16/100 - 17/10000.f_c)} \tag{24}$$

where

D_{max} = *strength of a shear stud*

d_{sh} = *diameter of a stud shank*

f_c = *concrete strength in compression*

Finally, aiming to incorporate the typical plateau part of the force-slip curve expressing slip behaviour of the shear connection, a criterion of the maximum friction stress (TAUMAX) was defined from equation describing characteristic shear connector resistance [21]:

$$P_{Rk} = (8/10).f_u.\pi.d^2/4 \qquad (25)$$

where

f_u = *ultimate tensile strength of a shear stud*

d = *diameter of a stud shank*

As for the beam samples were applied two alternatives of shear connectors´ layout (BRU, BRN), the same framework must be somehow included in the reference FE model. So, by employment of a FE contact, body of the FE was divided into a certain number of contact areas at the material interface aiming to convey both uniform (BRU) and non-uniform (BRN) layout of connectors. Hence, domains having full, or no interaction were specified, see Fig. 5.25.

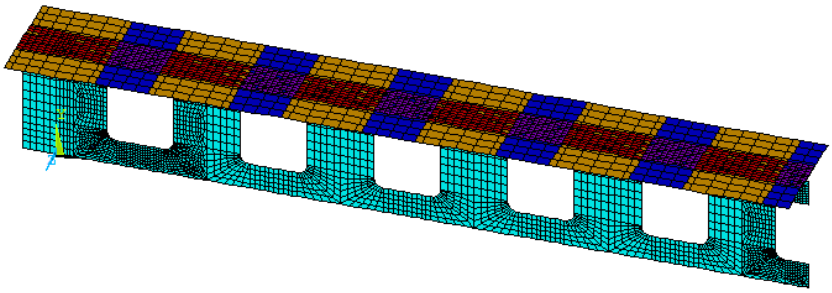

Fig. 5.25 - Illustration of area division at the material interface for application of uniform (BRU) and non-uniform (BRN) layout of shear connectors.

In this context, the contact areas having full interaction were defined as effective areas under individual groups of shear connectors, which have represented the exact part of contact resisting the longitudinal shearing. Contrariwise, the contact areas where no shear connectors were applied, displayed characteristics of no interaction. That means, the contact had almost no tangential resistance, thus allowing almost instant sliding.

5.5 Solution Process Configuration

Having intentions to attain reliable results combined with time efficiency, an appropriate solution process configuration had to be engaged. Hence, several options attempting to accomplish this aim will be discussed.

During the solution stage of a numerical analysis a set of equations, which are generated on the basis of FE method, needs to be solved. Therefore, the solver shall be carefully

selected. In ANSYS, several options are available. Respecting conditions of this FE investigation, the sparse direct solver (SDS) was chosen as the most suitable one. The main motive could be found in solver ability to combine computation robustness and speed required predominantly for nonlinear analysis.

Moreover, the additional advantage of SDS comes from availability of the parallel processing. This enhancement allows solving of a large or medium-sized models having more than millions of DOFs with decreased simulation time using multiple processors (also known as cores). So, for the purpose of this research work, shared-memory parallel processing was employed as well.

Further, the FE computation was performed as a static analysis considering only steady loading conditions (loads varying slowly with respect to time). In addition, our FE analyses have considered three types of nonlinearities - by means of:

- material natures,
- contact properties,
- large deformations.

The author does believe, the reason behind adoption of the first two effects is obvious. Speaking of the last one, after meticulous consideration, it was decided to incorporate this sort of geometrical non-linearity in the reference FE model in order to stay on the safe side. That meant, in the case of large straining existence producing notable local distortions, these effects would be taken into account.

Finally, the full Newton-Raphson procedure was chosen for an iterative solution process required for attainment of the force equilibrium during a nonlinear analysis. To be specific, this option specifies how often a tangent matrix shall be updated during the solution process. In this case, the stiffness matrix was updated at every equilibrium iteration.

Additionally, thus our FE model represents a complicated nonlinear problem not only from the material view but also for a reason it involves a surface contact, adaptive descent technique was activated automatically, which usually enhances program's ability to obtain a converged solution.

5.6 Structure of the Finite Element Model

For discretization of real samples, a combination of two- and three-dimensional elements was used in the FE models, concretely:

- Bottom flange and steel web were modelled with 2-D element SHELL181, which is suitable for analysing thin to moderately thick shell structures. SHELL181 is a four-node element having six degrees of freedom at each node allowing translations in the nodal x, y, and z directions, and rotations about the x, y, and z-axes. In addition, there is a membrane options which reduces degrees of freedom only to the translational (used for web). The element is well-suited for both linear and nonlinear applications. In the element domain, both full and reduced integration schemes are supported. However, as the reduced integration approach eliminates shear locking phenomenon, which could cause irrationally stiff response in bending and has a potential to reduce the computational time, exactly this option was adopted in our FE analyses.
- Top flange was discretized by 3-D element SOLID185, which is defined by eight nodes having only three translational degrees of freedom in the nodal x, y, and z directions at each node. SOLID185 is able to cover plasticity, stress stiffening, large deflection, and large strain effects. So, it is perfectly tailored for simulation of steel structural elements.
- Concrete slab was meshed with solid element CPT215 which represents class of 3-D elements having 8-nodes and coupled physics capabilities. It provides the structural implicit gradient regularization using a nonlocal field, which is one of its major capabilities enabling the proper simulation of concrete behaviour beyond the limit of a hardening zone. This ability is constituted by degrees of freedom at each corner node incorporating nonlocal field values (GFV1, GFV2, GFV3). Also as in other solids, translational degrees of freedom are available in the nodal x, y, and z directions. Further, CPT215 has elasticity, stress stiffening, large deflection, and large strain capabilities. Besides, this element can have any spatial orientation what is imperative for the Microplane model usage operating on randomly oriented microplanes.
- Reinforcement was described by LINK180, which is a 3-D spar element enabling to model trusses, sagging cables, springs, and other bearing members under axial loading. LINK180 is a uniaxial tension-compression element with three degrees of freedom at each node allowing translations in the nodal x, y, and z directions. Noteworthy, no bending effects are included, what for simulation of reinforcement poses no problem. Elasticity, plasticity, stress stiffening, large deflection, and large strain capabilities are included.
- Shear connection was defined as a contact, so certain types of contact elements were employed in the FE analyses. We speak especially of TARGE170 and CONTA174. While TARGE170 constitutes the class of target elements,

CONTA174 is a contact element type. To define a contact, these elements have to overlay underlying solid elements of other FE bodies and share with them the same geometric characteristics. Contact is initiated when the contact surface penetrates an associated target surface. In general, CONTA174 is used to describe the main contact properties for sliding and deformation effects. These are generally covered by Coulomb friction, shear stress friction and other user-defined contact interactions.

An illustration of the FE model is depicted in Fig. 5.26.

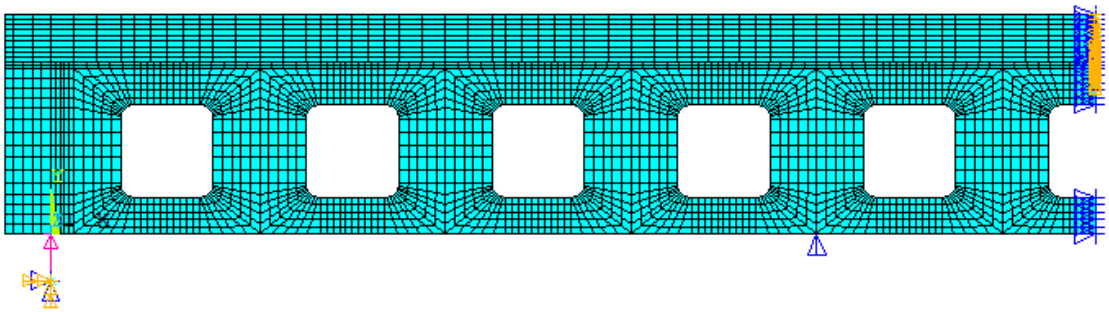

Fig. 5.26 – FE model.

5.7 Mesh Sensitivity Study

The principle of a mesh sensitivity study lies in identification of results´ dependency on the mesh resolution. In this light, three mesh configurations differing in their refinement ratio were examined. Details are briefly summarized in Tab. 5.3.

- *Tab. 5.3 - Configuration of the mesh sensitivity study.*

refinement ratio	1.00	1.35	1.70	2.05
num. of eq.	115309	151183	199173	236383
time (min)	70	120	190	240

To evaluate the results also graphically, both load-deflection and load-strain relations are illustrated in Fig. 5.27.

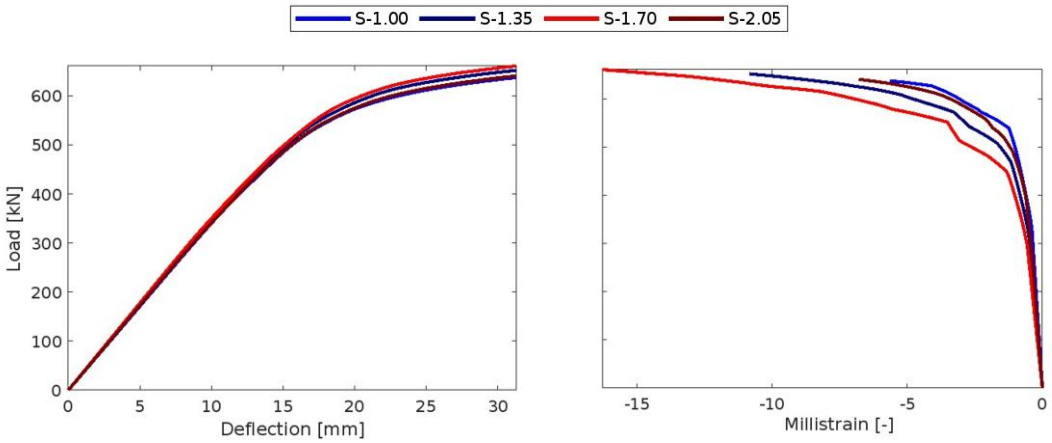

a) b)

Fig. 5.27 – Results from the mesh sensitivity study a) load-deflection relations at position D2 and b) load-strain relations at position T12.

It has to be noticed; strain measurements were taken from one of the most decisive locations (T12) in reference to the limit load. As can be clearly seen, negligible deviations were encountered. In addition, even though samples S-1.00 and S-2.05 largely differentiate in number of finite elements, thus also in number of equations to solve and therefore in computational time, they have produced almost the same response. Based on this, the FE model having ratio of 1.00 was chosen to become the reference FE model for the subsequent parametric FE analyses.

5.8 Validation of the Finite Element Model

Herein, data derived from the experimental and the numerical part of this research work will be presented. In the subsequent will be demonstrated, the differences between these two data sets are within the margin of error expected for a validation stage of a general research survey.

To be specific, within the framework of experimental programme, data were recorded at certain locations (Fig. 5.28) aiming to provide the most relevant reproduction of composite samples´ stress state during the loading. Subsequently, in order to identify the substantial material parameters of individual components of composite beams, small scale specimens were taken from the large ones and tested. According to this, the reference FE model for intended parametric investigation representing the load response of a set of real composite beam samples was built.

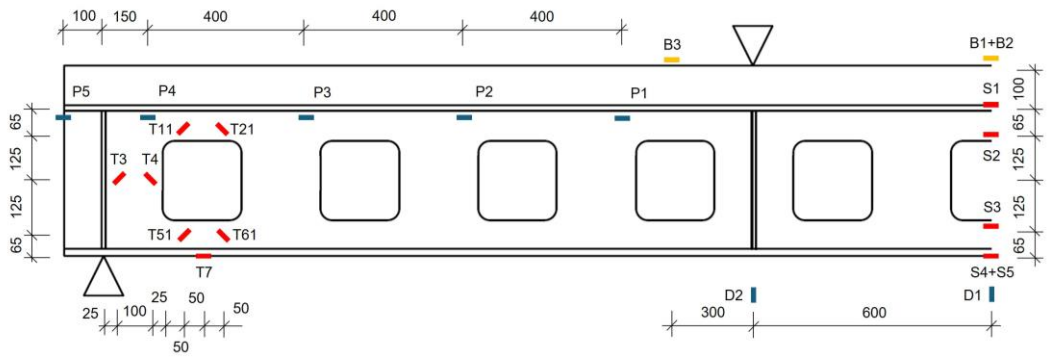

Fig. 5.28 - Location and labelling of measurement gadgets.

On these grounds, the most distinctive graphs corroborating credibility of the reference FE model will be presented. These will show results detailing the load response with respect to different position, material, measured quantity, and its magnitude.

So, firstly, load-deflection curves describing overall behaviour of samples will be demonstrated. Secondly, a set of load-strain relations displaying the most reasonable narrative in reference to data correlation will be addressed. As the last, evidence expressing slip behaviour at the material interface will be discussed.

It has to be noted, the complete evidence regarding the correlation process is summarized in Appendix B.

5.8.1 Load-Deflection Relations

Correlation of outcomes from the experimental testing and the reference FE models using the load-deflection patterns is depicted in Fig. 5.29. Explaining what is presented, the four experimentally tested specimens are blue in colour having solid or dashed line interpreting uniform (BRU) or non-uniform (BRN) layout of shear headed studs. The reference FE models for both alternatives are red in colour.

Speaking of data, they were measured at positions labelled as D1 and D2 (see Fig. 5.28). Being specific, position D1 is located at the mid-span, while position D2 recorded deflection directly under applied load. In all four tested beams, almost the same tendency of the load response can be observed, regardless of the alternative of a shear connector layout. The maximum load equal to 637 kN was defined at a deflection of about 32 mm what represents approximately 1/400 of beams´ span. Beside very good agreement, the FE models behave in a slight softer manner compared to the tested specimens. The main cause behind this laid in maintenance of a certain load-carrying reserve.

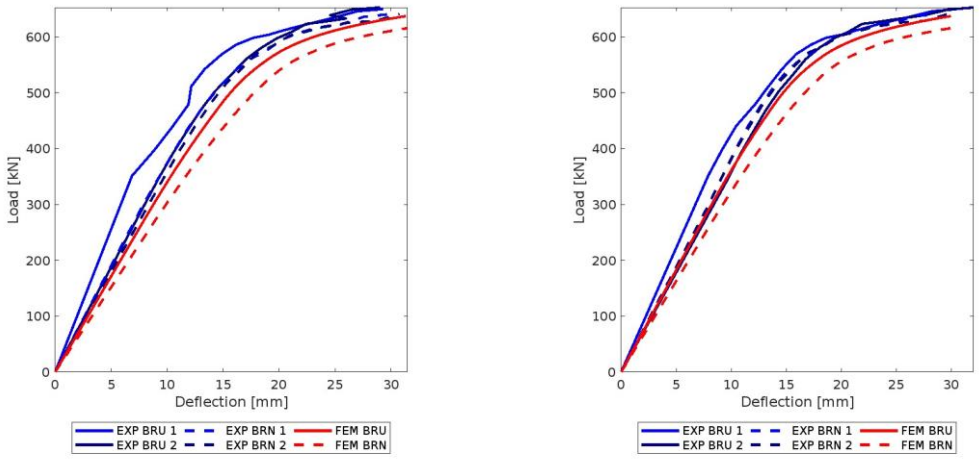

(a) (b)

Fig. 5.29 - Load-deflection relations at positions a) D1 and b) D2.

5.8.2 Load-Strain Relations - Concrete Slab

Moving spotlight to the concrete slab, deformations in longitudinal direction were measured at its top level (position B1, B3). As a result of application of the Microplane model within the FE investigation, negligible discrepancies might be observed (Fig. 5.30). Noteworthy, these measurements were intended solely to complete the picture of complex stress state occurring in the tested samples, so any significant observations were not recorded. As the concrete slab is under compression, the negatives values were documented.

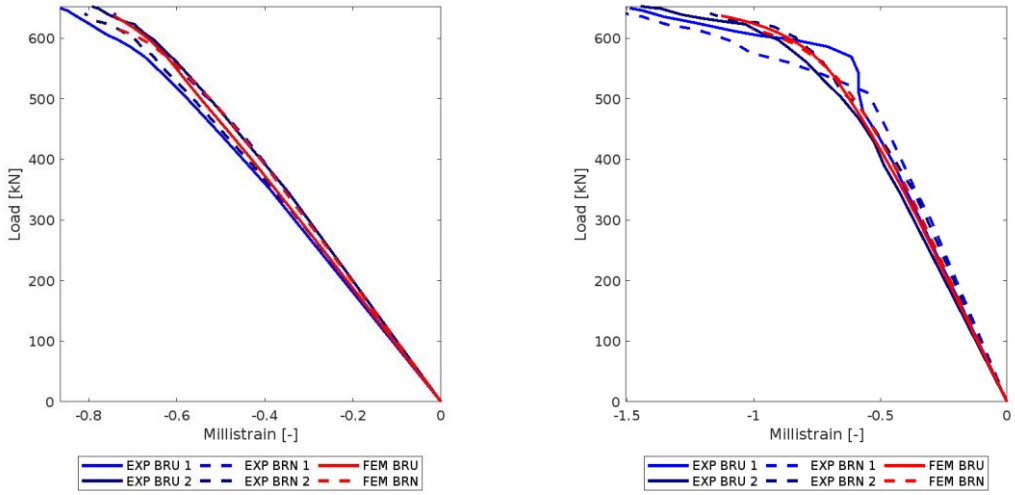

(a) (b)

Fig. 5.30 - Load-strain relations within the concrete slab at positions a) B1 and b) B3.

5.8.3 Load-Strain Relations - Steel Beam, Bending Effects

Considering the steel part of composite samples, the bending effects were recorded by strain gauges applied in the centre of samples (S1, S2, S3. S4), where purely the bending zone was present. So, in order to capture these bending effects, two gauges were applied at the level of the top Tee (Fig. 5.31 a) and b)), while the next two were located at the bottom Tee (Fig. 5.31 c) and d)). It was expected, the top part undergoes compression while the bottom part tension. However, different results were obtained.

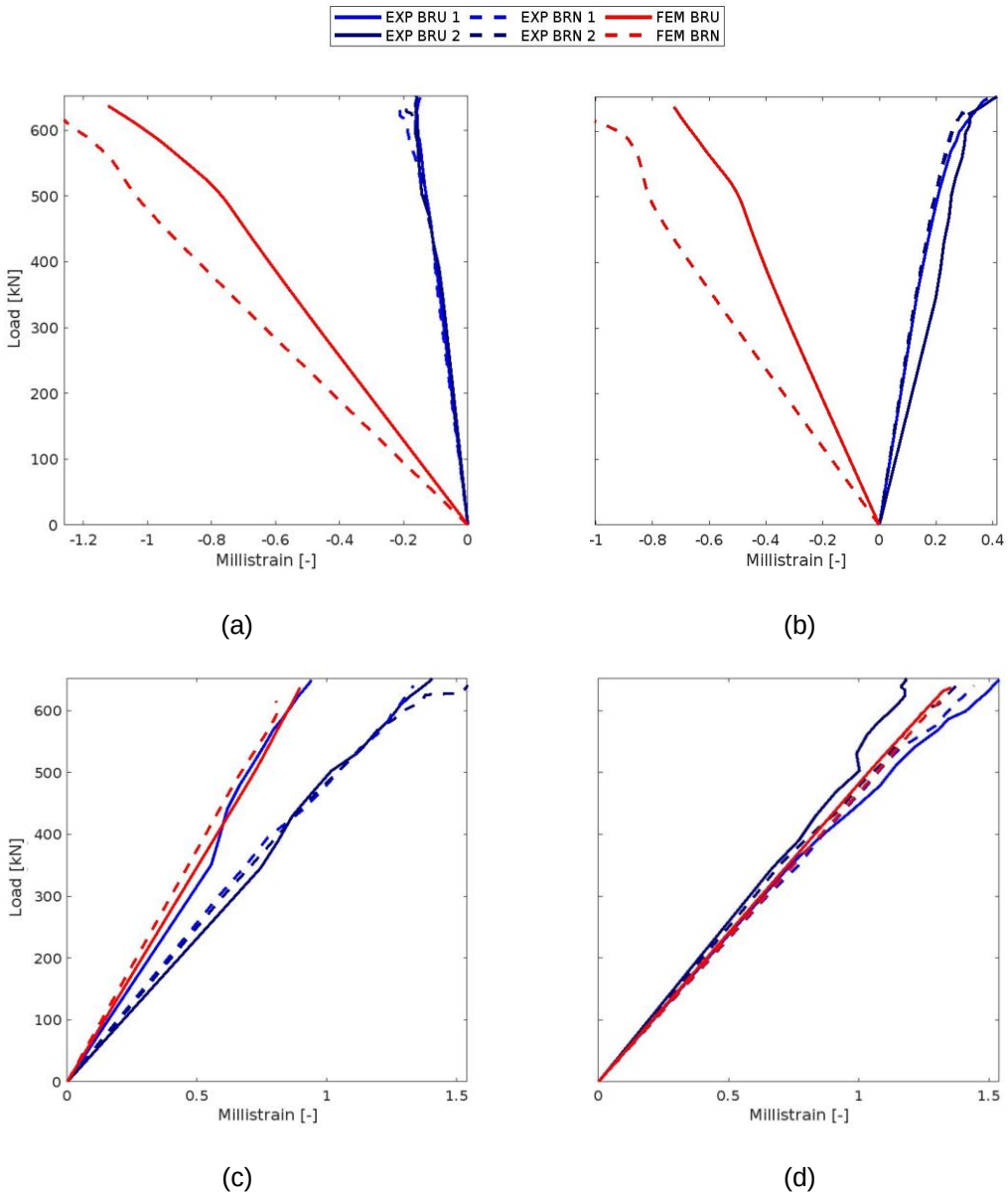

Fig. 5.31 - Load-strain relations at positions a) S1 b) S2, c) S3 and d) S4.

Concentrating on the top Tee (Fig. 5.31 a) and b)), the results unfortunately display notable differences. Especially, there is discrepancy not only in magnitudes but also in pressure state. While for the experimental samples is recorded moderate compression

at position S2, for the FE samples tension is present. The reasoning for this adverse state might be found in two perspectives. Firstly, exactly at this location in the FE models, symmetry constraints were applied. As a consequence, slightly stiffer load response could be produced in this region, so deformations might be somewhat influenced. Secondly, as the 2D model of a shear connection represents a quite important simplification, it might produce into some extent inconsistent results. As shown later, these discrepancies were encountered only in this region, what implies the former suggestion could be correct, or combination of both. In addition, these measurements were made in the vicinity of opening edges, where the yielding phenomenon acts, so the exact description is difficult not only to simulate, but to record as well.

Nevertheless, the outcomes from the bottom Tee (Fig. 5.31 c) and d)) coincide almost perfectly on the entire range of observed deformations.

5.8.4 Load-Strain Relations - Steel beam, Vierendeel Effects

On account of results from the initial FE model, the configuration of measurement gadgets was arranged in accordance to trace the principal strains in the vicinity of the outermost web opening (T11, T21, T51, T61). These measurements are depicted below (Fig. 5.32), wherein some disparities between the experimental and numerical data were experienced. However, after evaluation of these results displaying just a partial occurrence of plastic deformations which are so significant for definition of the desired failure mode, it was decided to rearrange these positions.

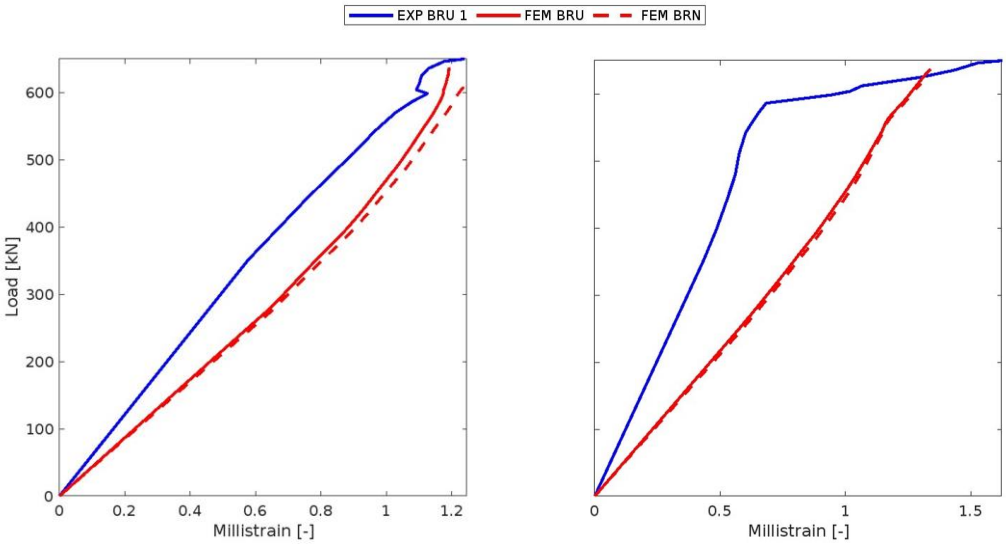

(a) (b)

Fig. 5.32 - Load-strain relations at positions a) T11 and b) T21.

In this case, the gauges were placed under 45-degree angle to horizontal line (Fig. 5.33). This configuration was arranged in accordance to results from the introductory FE model in order to trace the principal strains in the vicinity of the web opening.

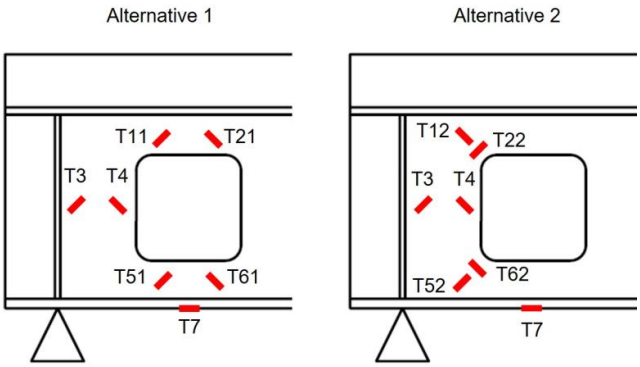

Fig. 5.33 - Rearrangement of strain gauges at location around the outermost opening.

So, as strains have been increasing at these spots after passing the transitional point between low and high deformation response, significant magnitudes of strain were reported. Even though, different shear connectors´ layouts were employed, the rosettes have documented almost identical strain development. As a consequence, after rearranging (Fig. 5.34), more decisive evidence regarding identification of the transitional point between elastic and plastic deformations was able to obtain. Hence, the Vierendeel bending mechanism causing yielding near the corners of openings could be promptly distinguished.

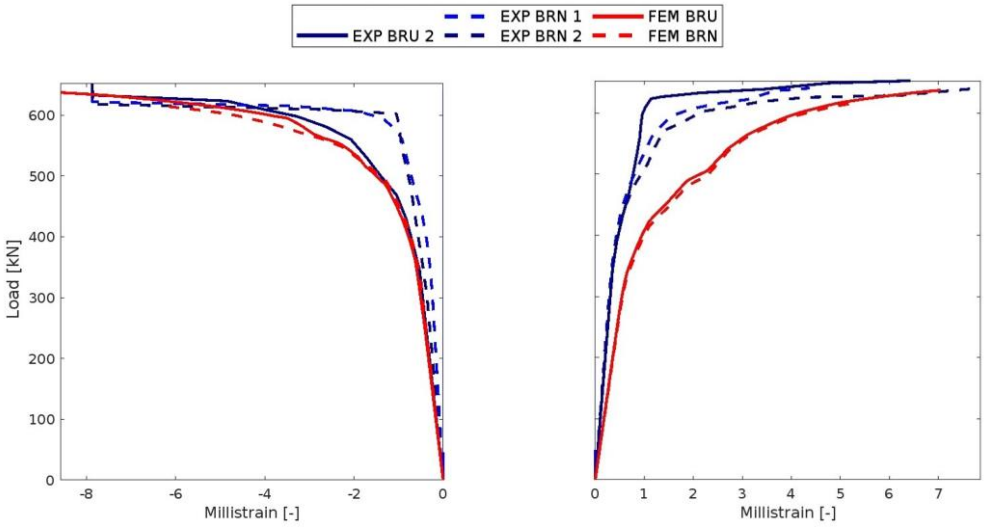

Fig. 5.34 - Load-strain relations at positions a) T12 and b) T52.

Finally, turning our attention to the end web-post located between the support and the outermost opening, the following behaviour of strains was captured (Fig. 5.35).

Considering the complexity of stress-state at this region, certain discrepancies has occurred.

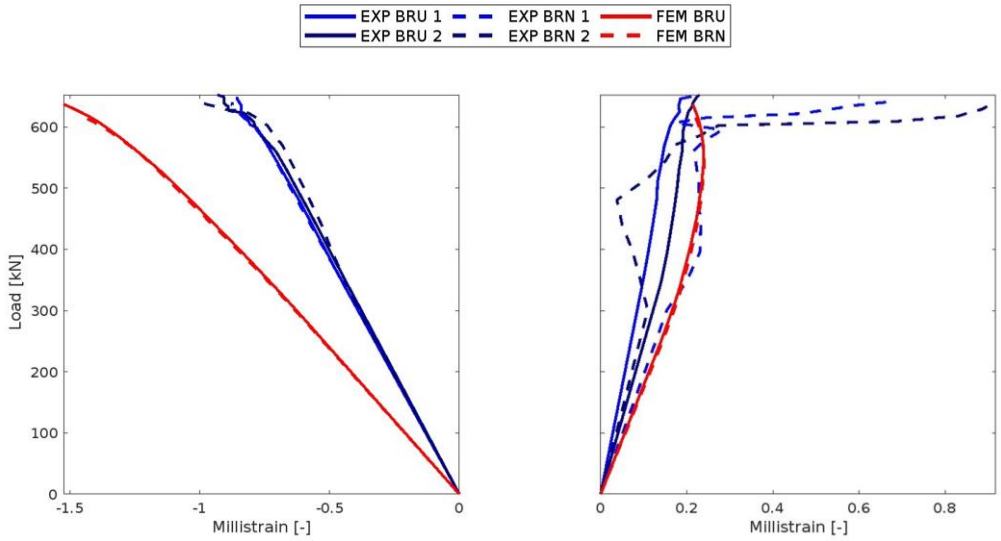

(a) (b)

Fig. 5.35 - Load-strain relations at positions a) T3 and b) T4.

Moving to the last set of data, this was recorded at the level of bottom flange under the outermost opening (T7). A close conformity is clearly visible (Fig. 5.36).

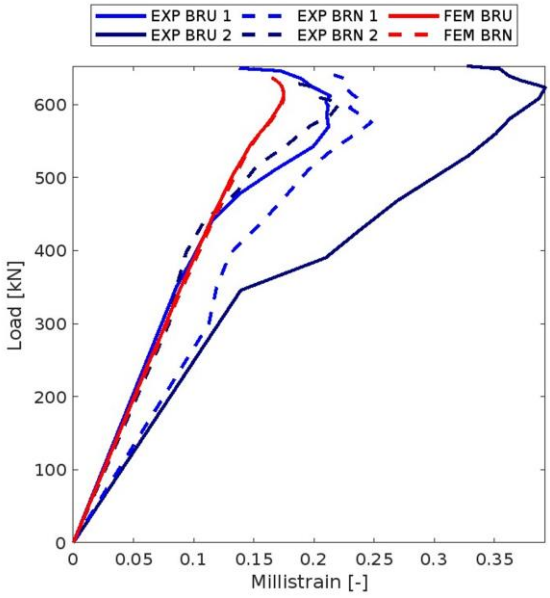

Fig. 5.36 - Load-strain relations at position T7.

5.8.5 Load-Slip Relations - Material Interface

As displacement at the material interface defines the slip behaviour, changes with respect to shear connectors´ layout could be well documented. Moreover, these

measurements might assist to identify an influence of this effect on the overall load response, because they quantify development of strains, especially slip strains.

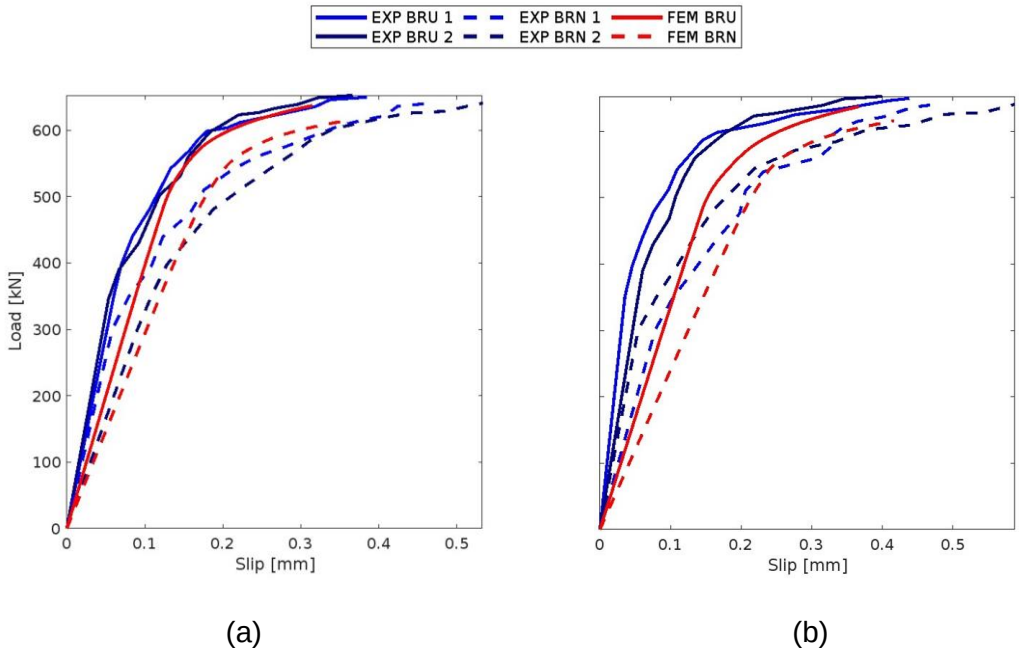

Fig. 5.37 - Load-slip relations at positions a) P2 and b) P3.

So, as Fig. 5.37 documents, the non-uniform layout has led to a softer response and larger values of slip in comparison to the uniform layout. Consequently, one might conclude, the resistance of composite beams with web openings is affected by layout of shear connectors, but its significance is at least questionable.

5.9 Summary

Trough out the previous sections, the following topics were presented:

- discussion on material modelling of concrete,
- calibration code for the input parameters for the Microplane model,
- description and definition of steel material parameters,
- discretization of a shear connection,
- solution process configuration,
- structure of the finite element model,
- mesh sensitivity study,
- validation of the reference FE model.

Following this course, the complex stress state occurring by composite beams with web openings was documented quite precisely. As was intended, the desired failure mode was achieved at the load level of 637 kN and deflection at position D1 of 32 mm.

Focusing on correlation between the experimental and numerical data, the observed discrepancies stayed in acceptable range. Hence, the reference FE model was accepted for the subsequent parametric FE investigation.

On these grounds, the second of the thesis aims:

2. Creation and calibration of a numerical model based on the FE method,

could be deemed as accomplished.

As in the previous summary was stated, the layout of shear connectors displays negligible effects with respect to the global measure, in the following chapter, this statement is challenged by additional inspection. Especially, influence on horizontal shearing at the web-posts and change of shear force proportion between Tees is addressed.

Besides, the second objective of this research work – redistribution of shear forces between the T-sections - will be deeply examined. Various parameters are considered and their impact on the shear force proportions for the Tees is assessed.

6 PARAMETRIC INVESTIGATION

Generally, a FE analysis simplified a process attempting to develop new concepts and methods. By virtue of its universality, deriving of complicated mathematical formulas can be partially avoided and more convenient approach can be applied. The main representative of this advantage is the parametric FE investigation. Of course, to underpin credibility for this sort of analysis, validation of the reference FE model against experimental work has to be provided - as it was documented in the previous chapter. So, if this condition is satisfied, an influence of individual parameters, respecting specific limit performance, could be evaluated in comparison to the reference FE model. In this way, this parametric investigation has been performed and was specially focused on investigation of:

- Horizontal shearing of the web-posts in relation to the Vierendeel action.
- Shear force redistribution between the Tees of a composite beams with web openings.

As is known, for the former subject, a layout of shear connectors represents the key factor, so only this parameter was studied.

But, for the latter one, the crucial factor needs to be identified. Hence, several parameters have been inspected, namely:

- shear connectors´ layout,
- concrete strength,
- concrete slab depth,
- steel strength,
- bottom flange width,
- web thickness,
- web depth,
- opening size.

In relation to the course of the experimental testing, deflection equal to 32 mm at position D1 was established as the limiting state for loading of the FE investigation. The main root behind this decision origin in a great variation of other possible limit states. That meant, under consideration of all the abovementioned parameters, not only the overall resistance is affected and consequently the value of maximal applied load but also location of critical positions with respect to yielding, especially for opening size alternation.

Concerning the up-to-date research [4, 8, 15] focusing on this topic, the following needs to be highlighted:

- Shear force proportion for the Tees is still indeterminate. For the bottom Tee, it ranges from 10% to 40% of the total shear.
- Quite great importance was assigned to the asymmetry of the composite cross-section.
- From the back-analysis of tests on composite beams, it is apparent, the proportion of shear force resisted by concrete slab is much higher than thought.

Hence, a particular attention is paid to these statements in order to confirm or challenge their relevance. So, in the sequel, the impact of individual parameters on shear force redistribution will be studied.

It has to be added, broadcasting the entire volume of conducted calculations would be counterproductive, therefore, only the most distinctive representatives are presented. The remainder ones are condensed in the Appendix C.

6.1 Processing of Results

Before presentation of any outcomes, it is a vital practise to describe methodology behind their derivation. Considering said, the compilation of results can be briefly outlined as follows:

a) carrying out of FE computations considering a set of free parameters,
b) conduction of supplementary calculations within ANSYS,
c) creation of output files from ANSYS,
d) data processing in MATLAB aiming to produce sufficiently narrative outcomes.

Paying attention to part b), the supplementary calculations mean the following:

- mapping results (mostly shear stresses) alongside the particular patterns,
- integrating these results.

By virtue of this concept, shear force magnitudes for the web-posts and individual components of composite samples were able to identify. Afterwards, part c) was applied. That means, the derived results were wrangled for further processing. Finally, conduction of part d) has yielded several graphical outcomes. Hence, in spite of using the most transparent way for broadcasting of findings, a series of graphs using a pair of the fundamental samples (Fig. 6.1) are illustrated. To be specific, the outcomes present data from:

- reference FE sample discretizing the real composite samples labelled as BRU from the experimental programme,
- related alternative from the FE investigation having a solid web-section, thus representing a basic form of the typical composite beam.

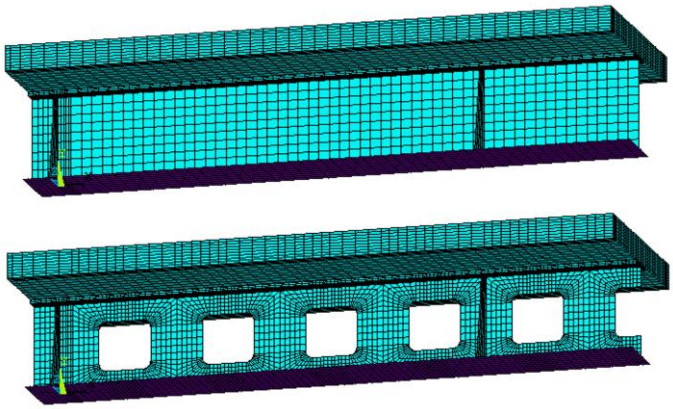

Fig. 6.1 - Fundamental FE models with and without openings.

Behaviour of shear forces along the sample beams corresponding to 4-point load bending test is pictured in two fundamental forms.

The first one (Fig. 6.2) constitutes the results with respect to individual components of composite cross-section (CS - concrete slab, TF - top flange, TW - top part of a web, BW - bottom part of a web, BF - bottom flange).

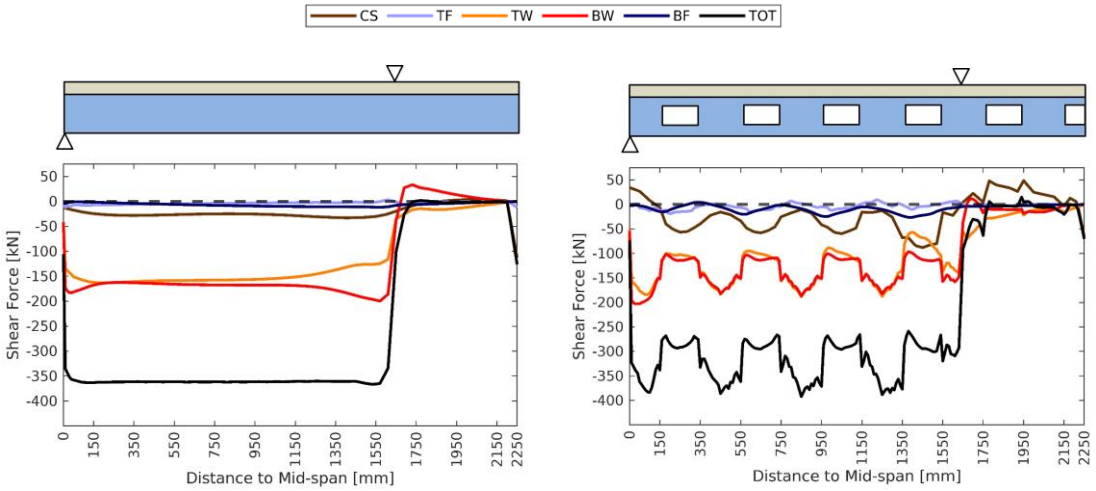

(a) (b)

Fig. 6.2 - Shear force redistribution between individual parts of composite cross-section in composite beams a) without and b) with openings.

The second one (Fig. 6.3) refers solely to redistribution between the top (TT) and bottom Tee (BT). In addition, global behaviour of shear force is captured as well (TOT - total shear force for beam).

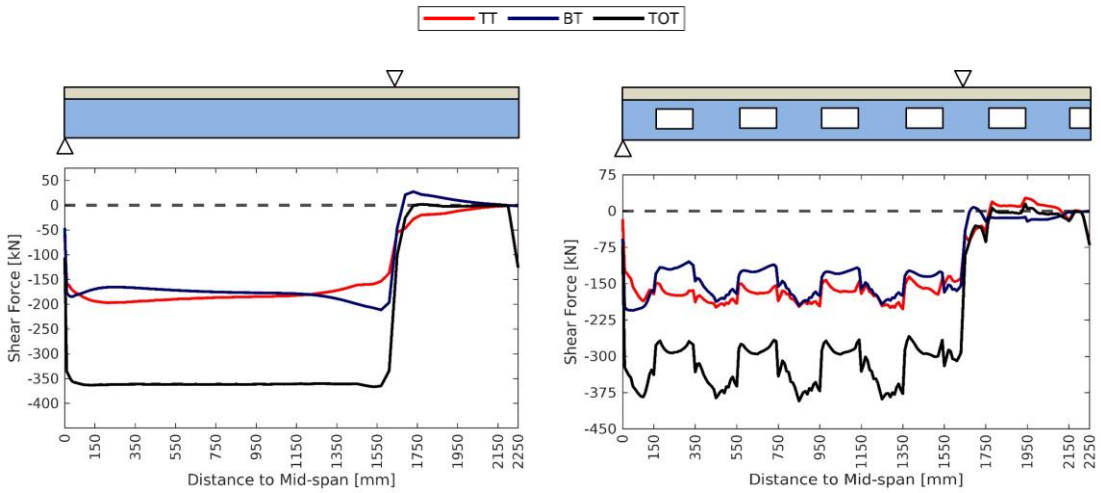

(a) (b)

Fig. 6.3 - Shear force redistribution between the Tees in composite beams a) without and b) with openings.

It can be clearly seen from Fig. 6.2 and Fig. 6.3; the alternative having no openings displays smooth response, while the other alternatives represent the exact opposite. On this basis can be concluded, shear force diagram is significantly affected by presence of web openings.

Aiming to provide more explanatory outcomes, shear force proportions were evaluated only at certain positions. These are given at centres of the openings (red lines) and the web-posts (blue lines), see Fig. 6.4. The same approach was applied for samples having no openings.

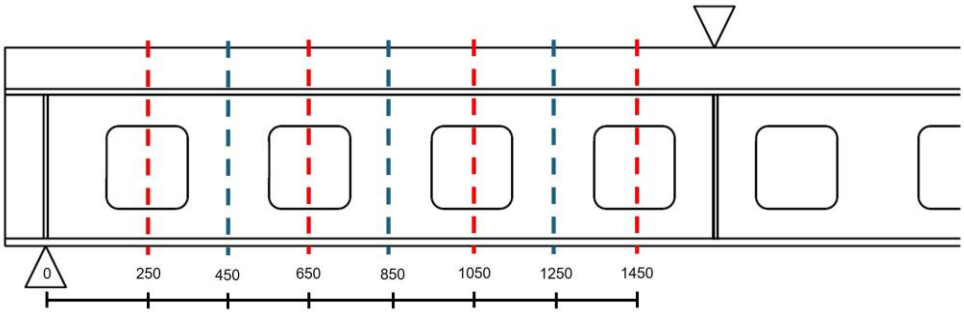

Fig. 6.4 - Locations used for assessment of the shear force proportions.

Application of the above approach has yielded the following results illustrated in Fig. 6.5.

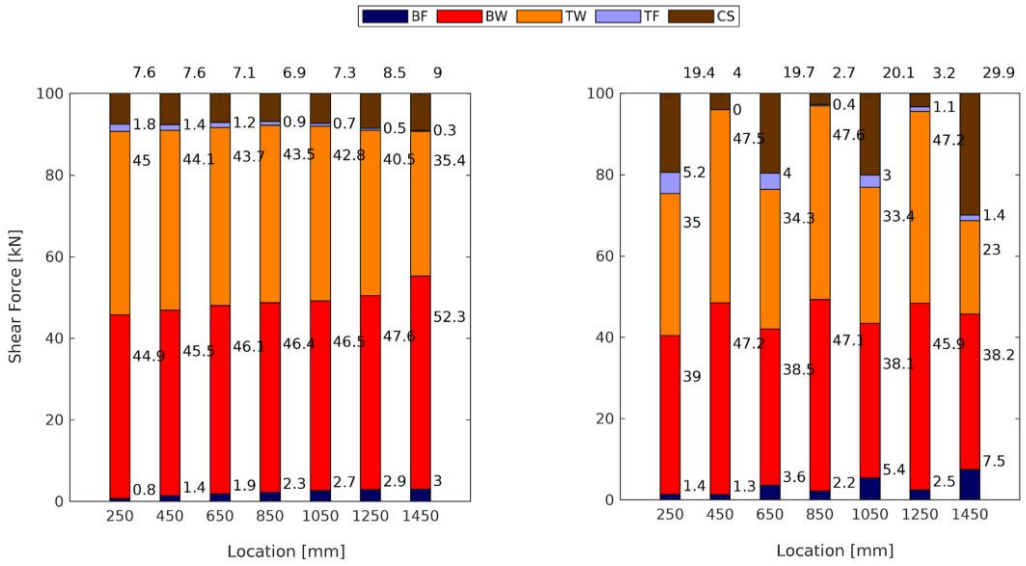

(a) (b)

Fig. 6.5 - Shear force redistribution between individual parts of composite cross-section in composite beams a) without and b) with openings at certain locations.

As can be seen, the sample having multiple openings displays following dissimilarities compared to the sample having solid web section:

- concrete slab contributes to the shear loading capacity at the openings by much greater extent,
- shear forces vary in a periodical manner depending on presence of the openings.

The latter is even more visible from Fig. 6.6, wherein the shear force redistribution is demonstrated again only for the top and bottom Tees.

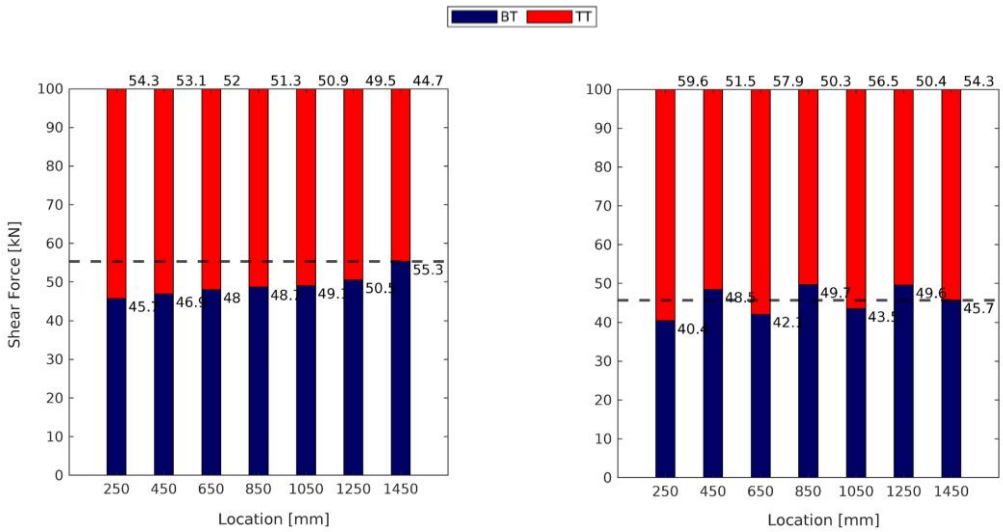

(a) (b)

Fig. 6.6 - Shear force redist. between the Tees of comp. beams a) without and b) with openings.

So, while the sample having solid web section experiences gradual increase of the shear force for the bottom Tee (Fig. 6.6 a)), the other sample displays a periodical character (Fig. 6.6 b)). It seems like the shear force tries to achieve the equilibrium at the centre of web-posts.

On the other side, if behaviour at the opening centres is considered only, especially for the bottom Tee, the following comparison of shear force proportions can be visualized (Fig. 6.7). It has to be noted, the results are in the following visualised only for the bottom Tee due effectivity.

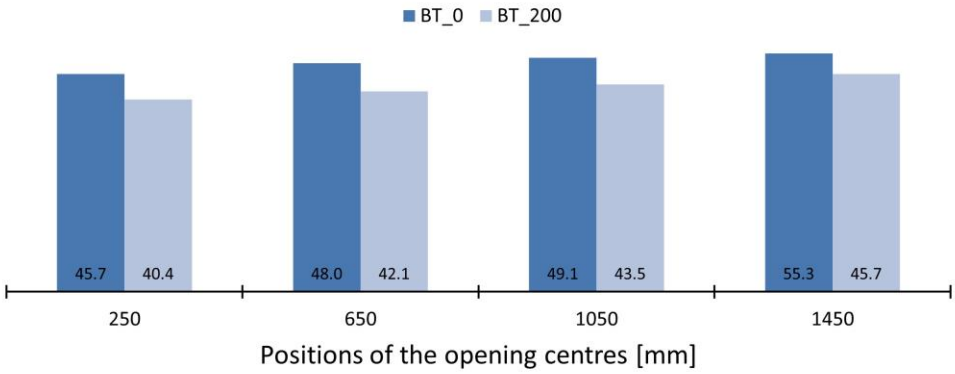

Fig. 6.7 - Shear force proportion for the bottom Tee.

As it can be seen, the bottom Tee of sample having openings (BT_200) experiences a notably lower proportion of shear forces compared to the sample having a solid web section (BT_0). That means, the top part of a composite beam has to exhibit more severe stressing.

The last form in which only the most relevant results are presented, takes the ratio form (Fig. 6.8). In this case, BT_0 is taken as the reference sample to underpin a change of the shear force redistribution as a consequence of introduction of openings.

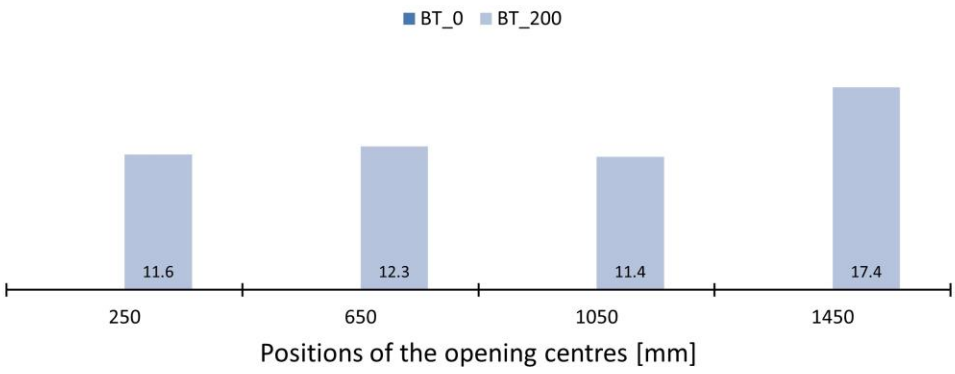

Fig. 6.8 - Shear force change for the bottom Tee compared to the reference sample.

As is visible, the bottom Tee underwent quite large increase of the shear force proportion in the range of 11.6% to 17.4. As this aspect plays crucial role by justification of the Vierendeel resistance, this outcome only emphasizes the need for an appropriate procedure respecting this behaviour.

Using this methodology, it can be easily observed a change of the shear force redistribution between different samples. Respecting the purpose of this investigation, findings from the parametric FE investigation are treated and subsequently demonstrated in this way.

In the following, impact of various parameters is studied.

6.2 Layout of shear connectors

As the Vierendeel resistance at the opening could be classified as highly sensitive to a layout of shear connectors, it was especially this aspect which formed one of the main concerns of our investigation. Furthermore, as the layout of connectors is adjusted, stress state of the web-posts might undergo some changes as well.

On this basis, firstly an impact of change of layout of shear connectors on the shear force proportion assigned to the bottom Tee is of concern. Especially, two sets of samples based on the experimental testing having uniform (BT_BRU) and non-uniform (BT_BRN) configuration of shear connectors were taken into account. Results regarding these beam samples are illustrated in Fig. 6.9.

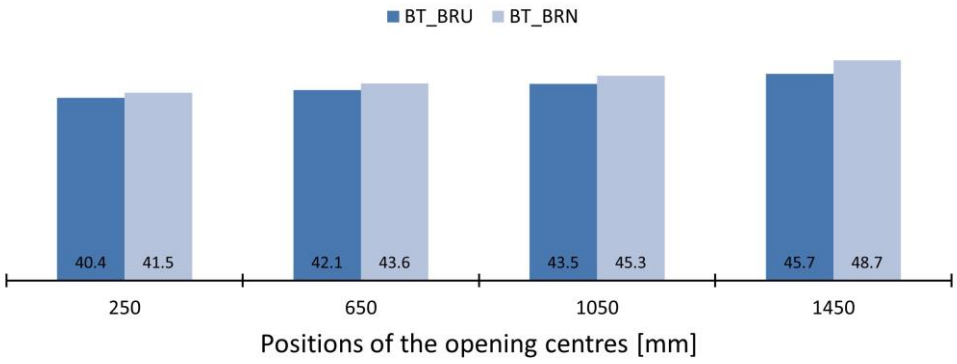

Fig. 6.9 - Shear force proportion for the bottom Tee.

Reflecting firstly the conclusions from the previous research assigning the bottom Tee 40% of total shear force, this value seems to constitute the minimal not the maximal limit in this case.

Considering impact of the shear connector layout, negligible differences (up to 3%) can be observed. Moreover, if BT_BRU sample is taken as the reference, BT_BRN sample

displays increase of the shear force proportion for the bottom Tee only 6.2% (Fig. 6.10). This implies, as the composite action was weakened above the openings, higher utilization of the bottom Tee is present, but its significance is questionable.

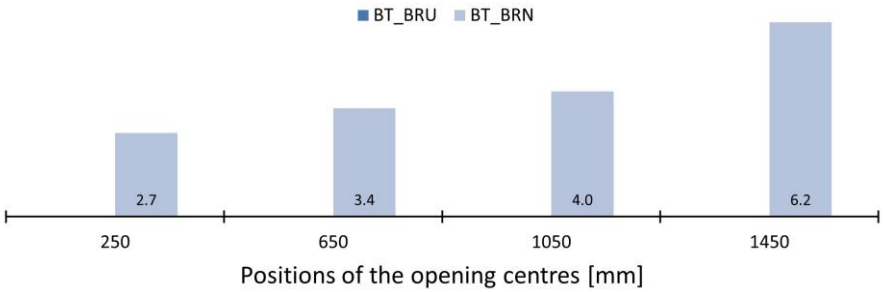

Fig. 6.10 – Change of the shear force proportion for the bottom Tee in the ratio form.

Completing this debate, outcomes regarding horizontal shearing of the web-posts are addressed. In the following, horizontal shear forces derived at certain positions are figured. This is done by integration of shear stresses along the patterns illustrated in Fig. 6.11.

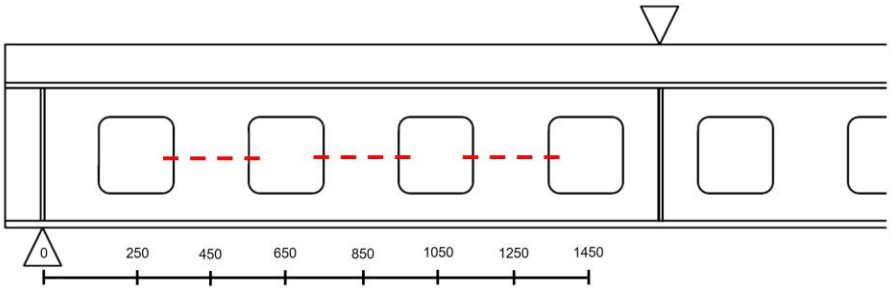

Fig. 6.11 - Horizontal sections at the web-posts needed for evaluation of the horizontal shear forces.

By virtue of this approach, the values of horizontal shear forces could be quantified, see Fig. 6.12.

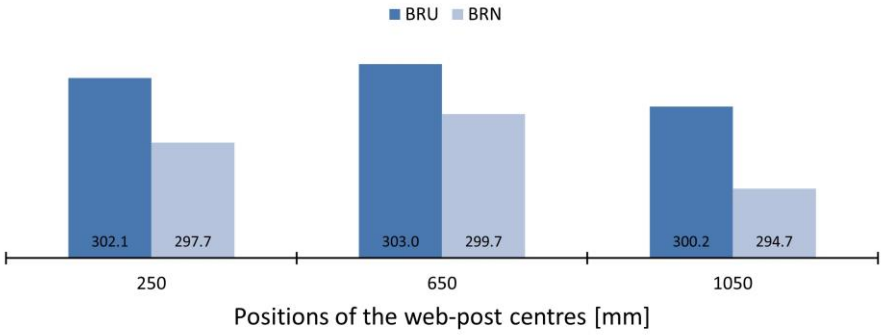

Fig. 6.12 - Horizontal shear forces acting on the web-posts.

Decrease up to 6 kN for BRN sample was encountered, what represents 2% of horizontal shear force acting in BRU sample. Considering this negligible difference, it can be

claimed, the shear connection layout did not display any significant changes. It seems, the global load response was not notably affected. On the other side, distribution of local stressing of individual shear studs could be influenced in a great measure. In fact, this local effect can lead to serious reduction of the global resistance, if the bearing capacity of an individual shear connector is prematurely utilized. Unfortunately, to follow this aspect appropriately, different of both the experimental procedure and FE discretization of the shear connection should be applied.

6.3 Concrete Component

In composite beams, the shear resistance is dominantly prescribed to the steel web. But, as the openings are introduced, considerable amount of shearing is transferred to the top Tee, hence, in the concrete slab as well (Fig. 6.4 b)). This put the fundamentals for alternation of properties of the concrete component and subsequent evaluation of their significance.

6.3.1 Concrete Strength

As the shear resistance of a concrete slab depends strongly on concrete compression strength, its magnitude is of concern at first. Impact of this factor was observed for samples having compression strength of concrete adjusted to level of 40 MPa (BT_40) and 50 MPa (BT_50). These magnitudes were considered due their values convey the nearest lower and higher strength class, respectively, to the experimental one (46 MPa). From Fig. 6.13, negligible effect can be seen. In numbers, the maximal difference was at level of 0.5%.

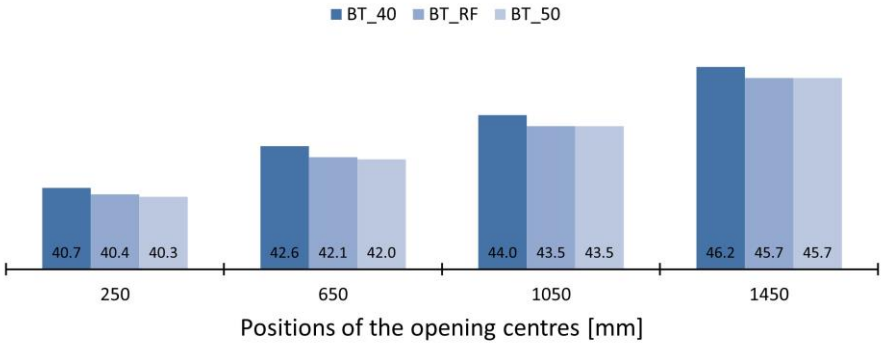

Fig. 6.13 - Shear force proportion for the bottom Tee.

6.3.2 Concrete Slab Depth

As the next important parameter, the concrete slab depth was identified. In this case, the depth of a concrete slab was modified to 80 mm (BT_80) and 120 mm (BT_120), respectively. Unfortunately, the similar outcome to the previous one can be concluded,

see Fig. 6.14. Almost no change was experienced for sample BT_80. On the other side, change of 4.9% for BT_120 was obtained.

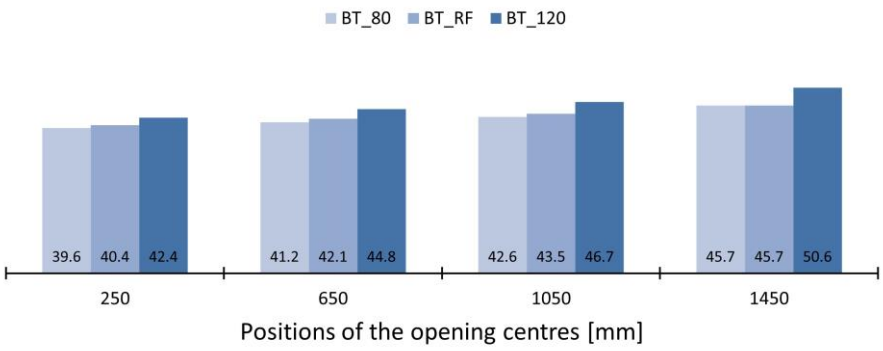

Fig. 6.14 - Shear force proportion for the bottom Tee.

Logically, the aspect of a slab width should have been investigated as well. But inspection of this parameter was omitted due to the configuration of the experimental samples.

6.4 Steel Component

Similarly, to the concrete component, the steel one plays even more crucial role. Based on the up-to-date research, the factors as steel strength, cross-section asymmetry and size of web is of concern.

6.4.1 Steel strength

As strength of a steel component constitutes one of the most important factors regarding the structural design, an influence of its variation was inspected in the first place. To be specific, the stress-strain relation was adjusted in the following manner:

- Yield strength (f_{ya}) for parametric samples was decreased and increased of 10%, respectively, in relation to the reference yield limit (f_{yr}).
- Ultimate strength (f_{ua}) was changed in a way preserving particular ratio of the yield to ultimate strength of the reference sample (f_{ur}), this yields ($f_{ua} = f_{ya}*(f_{ur}/f_{yr})$).

This strength variation (minus 10%, plus 10%) could be easily recognised from Fig. 6.15, in which an example of stress-strain curve adjustment of the bottom flange to the reference (RS) is presented.

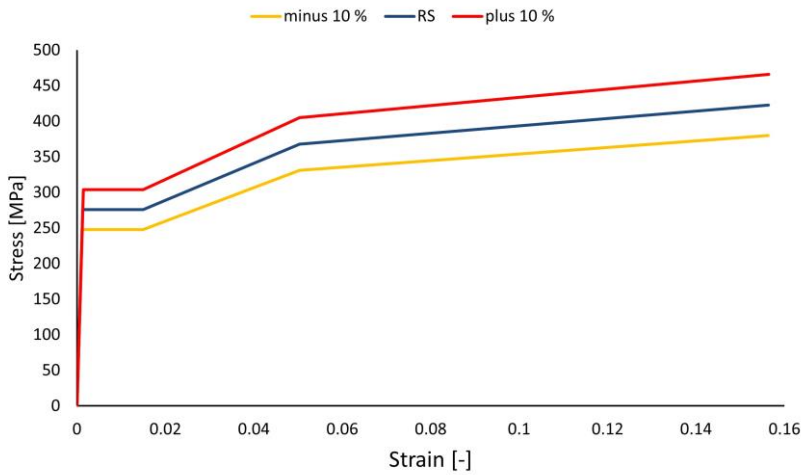

Fig. 6.15 - Example of a steel strength adjustment for the steel web.

Assessing obtained results for the shear forces redistribution (Fig. 6.16), the change was kept in the range from 0.7% to 1.7%. Of course, using greater variation of the strength values could be observed greater change, but its possible influence is considered to be negligible with respect to the presented.

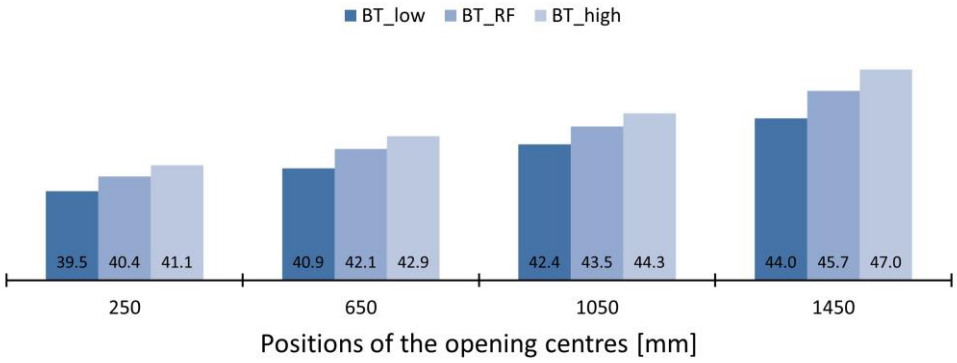

Fig. 6.16 - Shear force proportion for the bottom Tee.

6.4.2 Steel Bottom Flange

Recalling the statement from the beginning of this chapter, which declared the proportion of shear resisted by the bottom Tee depends strongly on the cross-sectional asymmetry, an impact of the bottom flange width change was examined. In this way, the bottom flange was narrowed (BT_nar) and widened (BT_wid) by 20 mm, respectively, in relation to the reference sample. Figuring this adjustment of the overall asymmetry of cross-section, ratios between areas of the top and bottom steel flanges for individual cases are summarized in Tab. 6.1.

- *Tab. 6.1 - Parameters with respect to the asymmetry of cross-sections.*

parameter	BT_nar	BT_RF	BT_wid
bottom flange width [mm]	250	270	290
bottom flange area [mm^2]	4000	4320	4640
top flange area [mm^2]	1680		
ratio	2.38	2.57	2.76

So far, the shear stress is defined as a change of axial force along the element length, the same principle is applied for a beam section but along its depth. In other words, by a rearrangement of a cross-sectional mass, the redistribution of shear stresses, then shear forces as well, are affected. Exploring this in detail, results for samples accounting for this aspect are illustrated in Fig. 6.17.

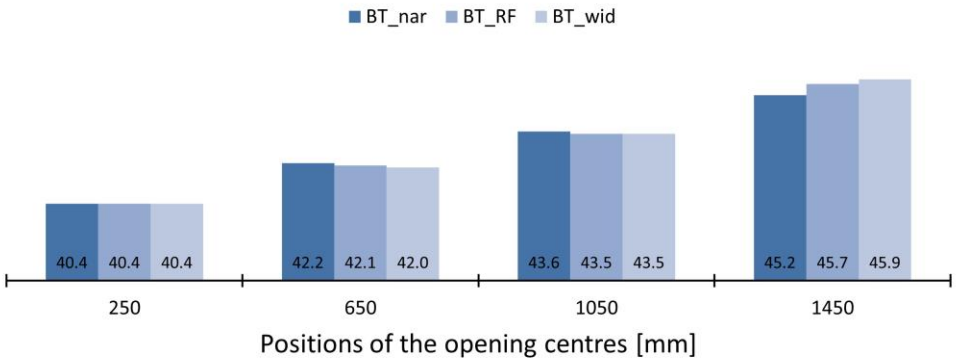

Fig. 6.17 - Shear force proportion for the bottom Tee.

As can be seen, although the moment of inertia was significantly modified, the shear force redistribution did not encounter similar tendency. In fact, the obtained data yielded minuscule differences, only up to 0.5%. On these grounds, it is possible to challenge the previous statements. Moreover, it can be stated, the proportion of shear force for the Tees seems to be not so dependent on the cross-sectional asymmetry as was believed. Despite said, for confirmation of this outcome, an investigation specifically focusing on this issue would constitute an appropriate step for acquiring an unarguable credibility.

6.4.3 Web Thickness

Considering the most significant factor with respect to the shear resistance of composite I-beam sections, the web thickness is placed under the spotlight. In this way, the steel web was narrowed (BT_nar) and widened (BT_wid) by 2 mm, respectively, to the reference sample. As illustrates Fig. 6.18, the change of web thickness caused redistribution of shear forces between the individual samples maximally by 4%.

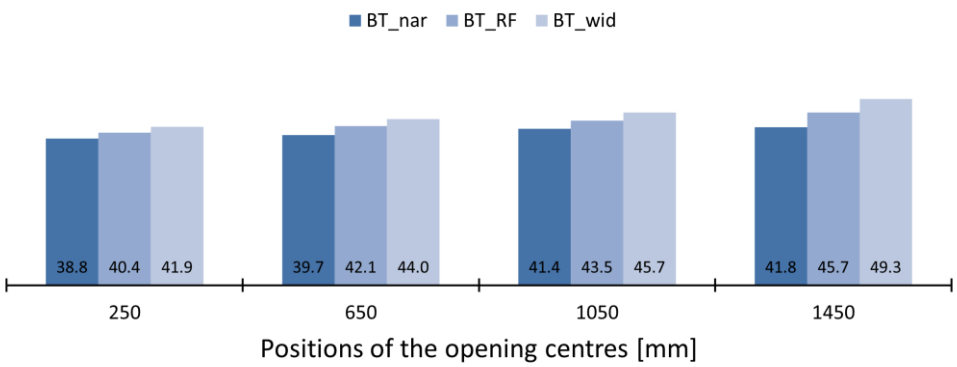

Fig. 6.18 - Shear force proportion for the bottom Tee.

Based on this could be claimed, despite great importance of web thickness for the shear and Vierendeel bending resistance, it does not constitute the key factor for the shear force redistribution between the Tees.

6.4.4 Web Depth

Bringing this section to its final part, an influence of the web depth is subjected to detailed inspection. In this case variation of the web depth was accompanied by appropriate change of the opening depth. Thus, restriction in the form of opening to web depth ratio equal to 0.57 was implemented. The main reason for this treatment laid in ensuring of direct linkage to the configuration of experimental beam samples. Practically that meant, the opening depth varied in accordance with the web depth. To be specific, two alternatives (BR_315 and BT_ 385) for the web depth were considered.

A brief overview of applied dimensions for openings and steel webs can be found in Tab. 6.2. It has to be added, by application of this treatment, not only the cross-sectional area of steel web but also the moment of inertia was modified.

- *Tab. 6.2 - Dimensions of openings and steel webs.*

parameter	BT_315	BT_RF	BT_385
opening depth (mm)	180	200	220
web depth (mm)	315	350	385

As can be seen from Fig. 6.19, the results did not experience any greater change. Expressed in numbers, the maximal discrepancy did not pass the value of 1.1%.

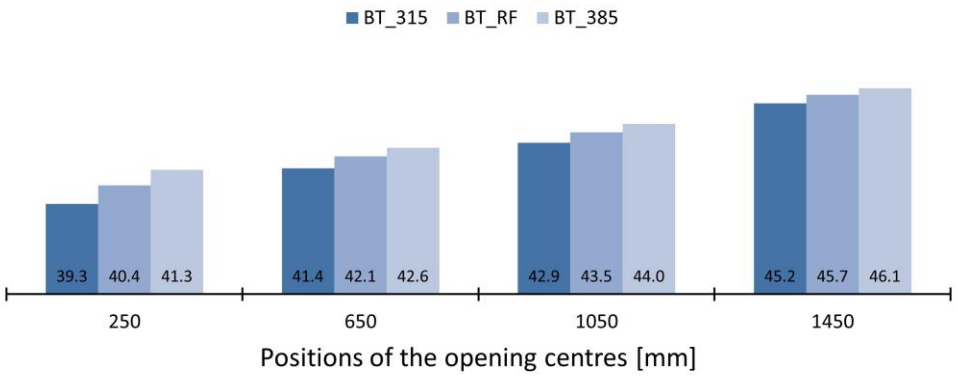

Fig. 6.19 - Shear force proportion for the bottom Tee.

6.5 Opening Size

As the last aspect, an impact of opening size is addressed. By evaluation of this impact, particular limits in relation to the opening size and:

- max. web depth,
- min. Tee depth,
- min. web-post length,

were applied. These are summarized in Table 6.3 and reflect criterions for the general cases using circular and rectangular openings. In addition, dimensions of openings applied for our experimental samples can be found in this table as well. It has to be added, these criterions clearly relate to composite beams having unstiffened openings and experiencing only high magnitudes of shear forces.

In fact, this corresponds exactly to our experimental conditions.

- *Tab. 6.3 - Geometrical limits.*

opening shape	circular	rectangular	our case
max. depth of opening	$0.8*h_w$	$0.7*h_w$	$0.57*h_w$
min. depth of Tee	t_f+30mm	$0.1*h_w$	$0.26*h_w$
max. opening length	-	$1.5*h_o$	$1*h_o$
min. width of web-post	$0.4* h_o$	$1*l_o$	$1*l_o$

The main purpose of these criterions origin in avoidance of transition of the Vierendeel effect, resulting in severe yielding, from web to flange region (Fig. 6.20).

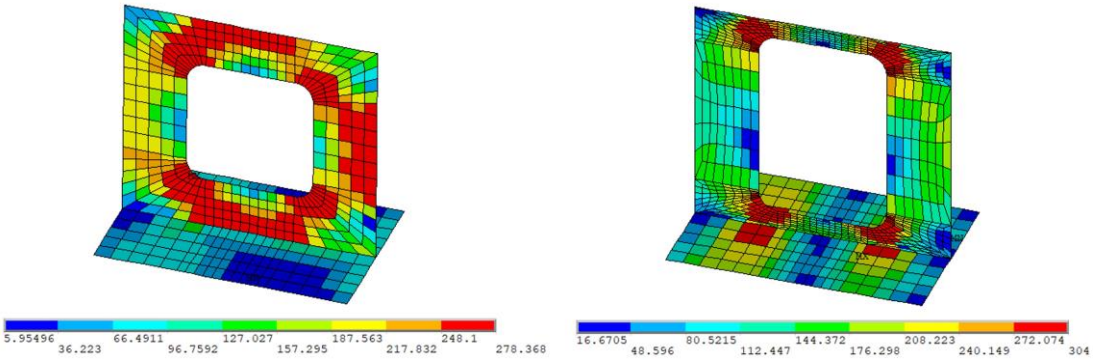

Fig. 6.20 - Vierendeel effects transmitted to the flange region.

In addition, the limitation related to the minimal web-post length constitutes condition for its sufficient local stability.

Noteworthy, demonstration of any results within the following sections is always accompanied by related geometry characteristics of analysed samples in the tabular form.

6.5.1 Opening Length

Firstly, an adjustment of an opening length will be studied. By doing so, opening lengths of 100 mm (BT_100) and 300 mm (BT_300) were taken into account (Tab. 6.4).

- *Tab. 6.4 - Geometrical characteristics.*

parameter	BT_100	BT_RF	BT_300
opening length l_o	100	200	300
opening depth h_o	200	200	200
ratio l_o/h_o	0.50	1.00	1.50
web-post length l_{wp}	300	200	100
ratio l_{wp}/l_o	3.00	1.00	0.33

Under these conditions, the following outcomes were obtained Tee (Fig. 6.21).

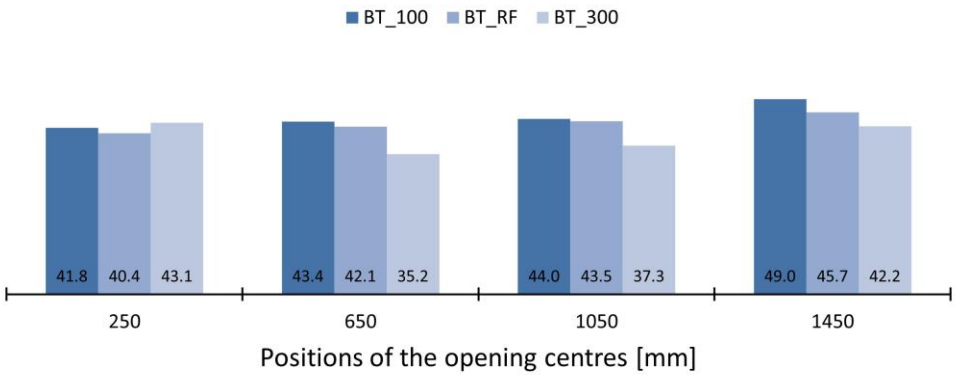

Fig. 6.21 - Shear force proportion for the bottom Tee.

Omitting the opening at distance of 250 mm from the support, a gradual decrease of shear proportion for the bottom Tee could be observed. The maximal change with respect to the reference samples was documented at the level of 6.2%.

Aiming to demonstrate the shear force redistribution in more compact manner, the span of opening lengths was enlarged by values of 150 mm and 250 mm. That meant, the ratio of opening length to depth was completed by values of 0.75, 1.25.

Further, the following results are displayed with respect to both Tees considering variation of the ratio of opening depth to length (Fig. 6.22).

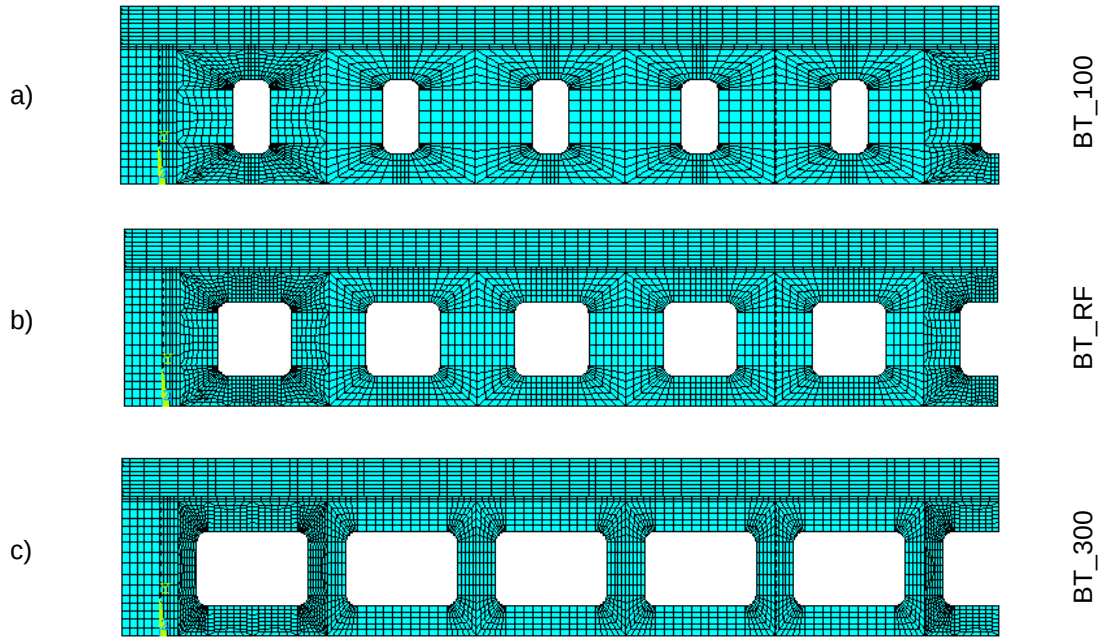

Fig. 6.22 – Illustration of opening width alternation a) BT_100, b) BT_RF and c) BT_300.

But, in this case, only the maximum values of the shear force proportions are taken from individual samples, irrespective of the opening position (Fig. 6.23).

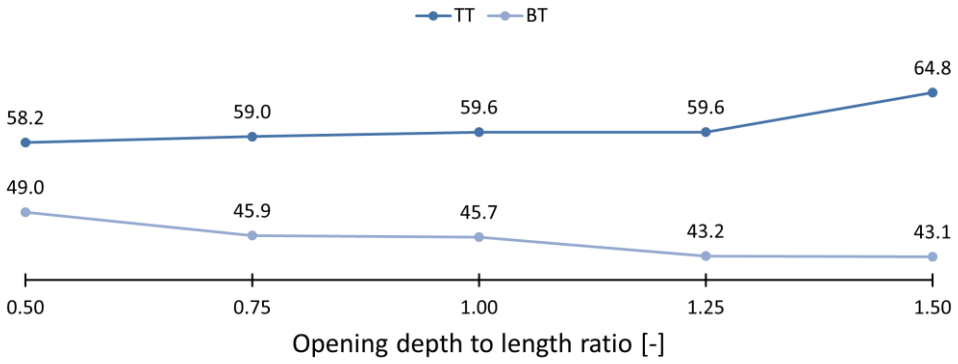

Fig. 6.23 - Shear force proportion for the bottom Tee.

As it can be seen, by variation of the opening depth to length ratio in a scale from 0.5 to 1.5, the following differences were obtained between the minimal and the maximal value:

- for the top Tee, it was 6.6%,
- for the bottom Tee, it was 5.9%.

In conclusion, the shear force redistribution did not encounter any significant change, the variation of values did not pass the range obtained from the already analysed parameters.

6.5.2 Opening Depth

Secondly, outcomes expressing a change of the opening depth are presented. The size variation of openings is condensed in Tab. 6.5.

- *Tab. 6.5 - Geometrical characteristics.*

parameter	BT_100	BT_RF	BT_300
opening length l_o	200	200	200
opening depth h_o	100	200	300
ratio l_o/h_o	2.00	1.00	0.67
web-post length l_{wp}	200	200	200
ratio l_{wp}/l_o	1.00	1.00	1.00

Graphical representation of the opening depth variation can be seen in Fig. 6.24

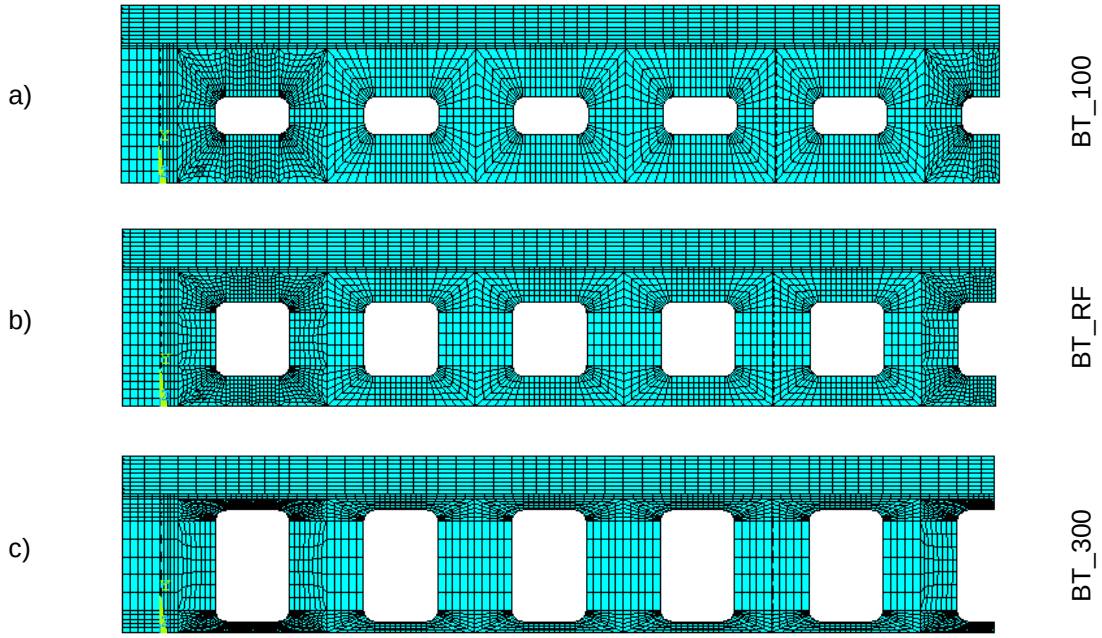

Fig. 6.24 – Illustration of opening depth alternation a) BT_100, b) BT_RF and c) BT_300.

Results capturing an influence of the adopted adjustments are illustrated below (Fig. 6.25).

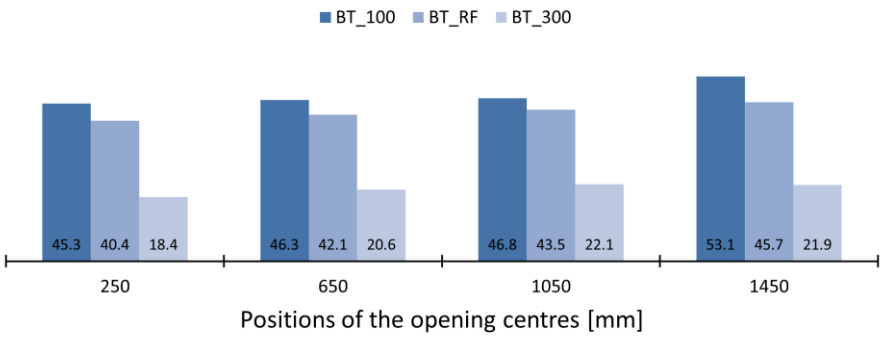

Fig. 6.25 - Shear force proportion for the bottom Tee.

Significance of this parameter is quite easy to recognize. It is documented by enormous difference of shear force proportions by individual samples. Especially, the values for sample BT_100 ranges from 45.3% to 53.1% while for sample BT_300 it is from 18.4% to 21.9%. This change is more visible from Fig. 6.26, wherein it is expressed in a ratio form to the reference sample BT_RF.

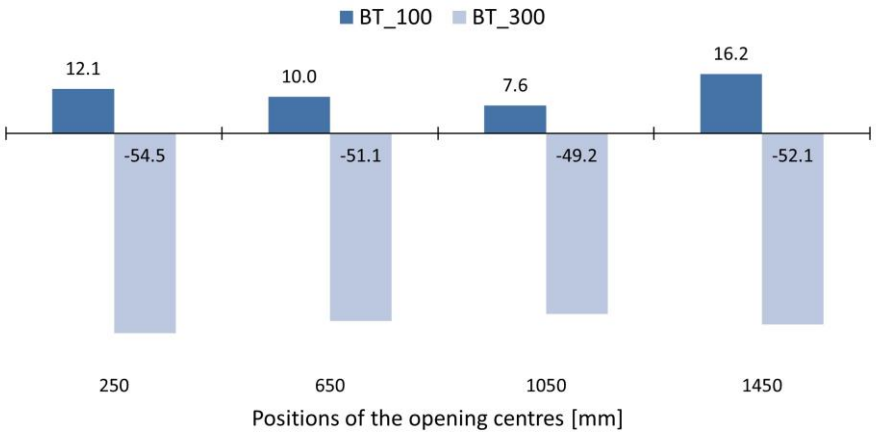

Fig. 6.26 - Change of the shear force proportion for the bottom Tee in the ratio form.

Concretely, sample BT_100 experienced increase hovering 16.2% while sample BT_300 underwent a noteworthy decrease at the level of 54.5%. Hence, we can define the opening depth as the key factor influencing the shear force redistribution between the Tees at most.

Based on these findings, additional FE calculations were conducted. In these, change of the absolute depth of web and opening was applied. In addition, their mutual relative depth ratio was retained. In this way, the findings applicability has been extended also

for beams having the ratio of steel web depth to beam span length in the range from 1/11 to 1/15. The geometrical details are given in Tab. 6.6.

- *Tab. 6.6 - Geometrical characteristics covering additional FE calculations.*

opening to web depth ratio									
0.29		0.43		0.57		0.71		0.85	
depth [mm]									
opening	web	opening	web	opening	web	opening	web	opening	web
87	300	94	300	100	300	109	300	116	300
94	325	140	325	150	325	161	325	172	325
100	350	185	350	200	350	214	350	228	350
109	375	231	375	250	375	266	375	284	375
116	400	276	400	300	400	319	400	340	400

From the derived outcomes, only the maximum values of shear force proportions from each specimen for either the top or bottom Tee were taken - irrespective of the opening position.

Adopting the mentioned approach, two curves conveying the maximal values of shear force proportions for both the top (TT_max) and the bottom (BT_max) Tee under particular opening to web depth ratio were established (Fig. 6.27). As can be seen, the values for TT_max range from 55% to 84%, while the values for BT_max range from 25% to 58%.

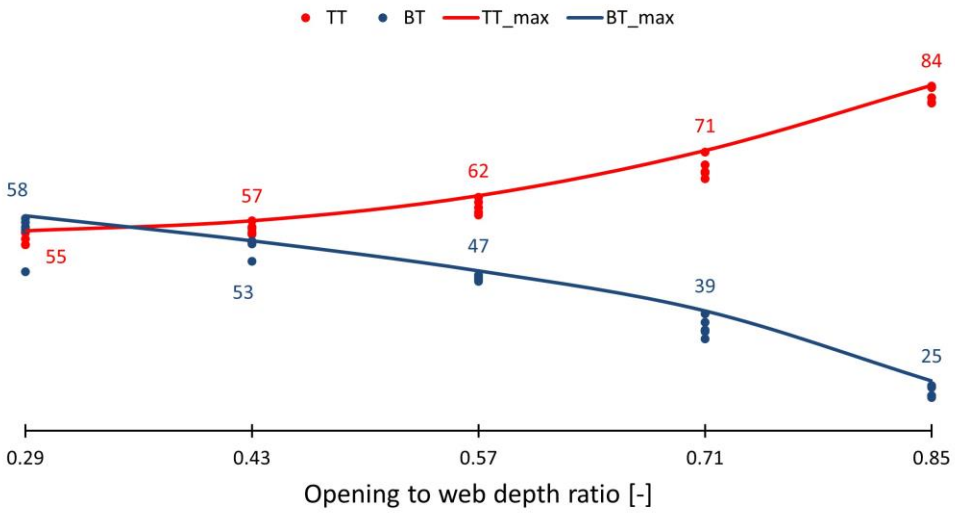

Fig. 6.27 - Maximum shear force proportions for the top and bottom Tee.

On this basis, strong fundamentals have been laid for proposal of a novel concept expressing the shear force redistribution between the Tees by equations of higher order.

6.6 Novel Concept for Redistribution of Shear Forces between the Tees in Composite Beams with Web Openings

Aiming to provide more general form of the already presented findings, relation defining dependence of the shear force proportion for the Tees based on the ratio between opening and web depth yielded the following equations:

top Tee $$y = 0.55 + \frac{x^3}{2};$$ (26)

bottom Tee $$y = 0.65 - \frac{x^2}{2};$$ (27)

function domain $$0.29 \leq x \leq 0.85;$$

where
y = *the shear force proportion*
x = *opening to web depth ratio*

It must be noted, the domain of function (25) and (26) is related to the configuration of the experimental samples and to geometrical limits from [8].

Compared to the results obtained from the parametric FE analysis (TT_FEM, BT_FEM), the derived relations (TT_NC, BT_NC) are graphically represented in Fig. 6.28.

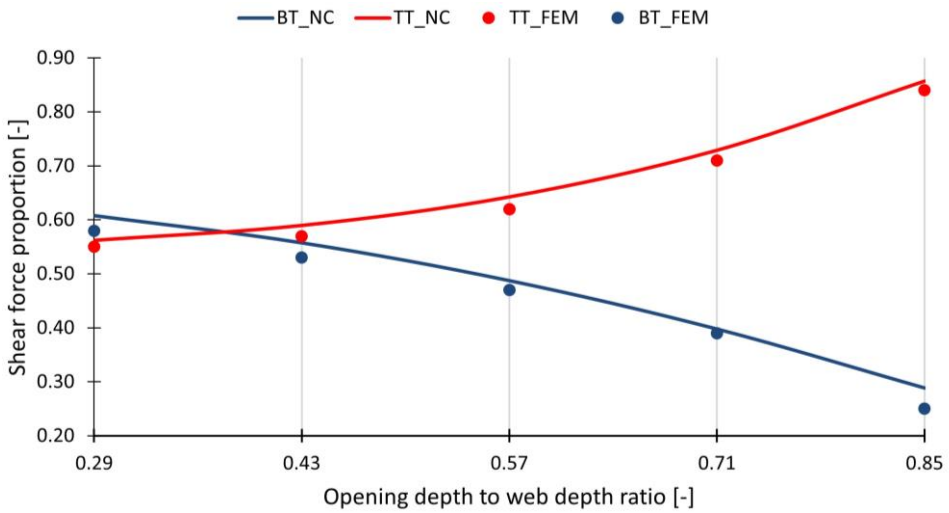

Fig. 6.28 - Proposed concept for definition of the shear force proportion for the Tees.

Explaining the novel concept in detail, by design of composite beams with web openings, as the ratio between opening and web depth is known (x-axis), shear force assigned to the top Tee $V_{t,Ed}$ is defined by multiplication of the design shear force V_{Ed} with appropriate shear force proportion (y-axis). The same principle applies for the bottom Tee ($V_{b,Ed}$). The summation of $V_{t,Ed}$ and $V_{b,Ed}$ may produce values higher than the design shear force V_{Ed} due safety margin.

6.7 Summary

In the first part of the presented parametric FE investigation, it was analysed an effect of layout of shear connectors on behaviour of composite beams with web openings. Reflecting obtained results, an impact of change of layout of shear connectors on both:

- the shear force redistribution between the Tees,
- the horizontal shear force acting within the web-posts,

was not so significant as expected. It seems, this factor primarily influences only stressing of individual shear connectors, not the overall load response of bearing members.

In the second part, attention was paid to deep analysis of the shear force redistribution between the Tees. Summing up the results, an overview of assumed parameters, their values and change of the shear force proportion for the bottom Tee expressed as the ratio to the reference sample is in Tab. 6.7.

- *Table 6.7 – Overview of parameters and results from the parametric FE analysis.*

parameter	parameter value			change	
	sample 1	reference	sample 2	sample 1	sample 2
concrete strength	40 MPa	46.18 MPa	50 MPa	+1.1%	-0.1%
concrete slab depth	80 mm	100 mm	120 mm	+10.7%	-1.8%
steel strength	-10%	Table 3	+10%	-3.8%	+2.8%
bottom flange width	250 mm	270 mm	290 mm	-1.1%	+0.5%
web thickness	10 mm	12 mm	14 mm	-8.6%	+7.9%
web depth	315 mm	350 mm	385 mm	-1.1%	+0.9%
opening length	100 mm	200 mm	300 mm	+7.3%	-7.7%
opening depth	**100 mm**	**200 mm**	**300 mm**	**+16.2%**	**-54.5%**

Based on the presented, the opening depth was identified as the key factor influencing the redistribution of shear forces between the Tees at most. By additional computations, curves defining the shear force proportion under ratio between opening and web depth were derived. On these grounds a novel concept for more accurate and convenient evaluation of shear force proportions for the Tees was proposed.

Besides, a series of valuable facts has been revealed:

- Shear force diagram is significantly affected by presence of web openings. Highly irregular behaviour is present depending on size of openings.
- Concrete slab contributes to the shear loading capacity at the openings by much greater extent. For example, for the reference FE sample, it was about 29.9% from the total shear force.
- Shear forces vary in a periodical manner trying to attain equilibrium with respect to the shear force redistribution between the Tees at the mid-lengths of the web-posts.
- The shear force proportion for the Tees seems to be not so dependent on the cross-sectional asymmetry as was believed.
- The shear force proportion for the bottom Tee was documented in the range of 25% to 58%. Compared to the previously defined values spanning from 10% to 40%, it could be claimed, shear force resisted by the bottom Tee could be higher than thought.

Turning to the assessment of the completion of the thesis aims, it could be concluded, the fourth one:

4. Recommendations refining the current design procedure of non-symmetrical composite beams with web openings,

was partially accomplished. This is documented by the presented findings resulting in formation of a basis for novel concept defining the shear force redistribution between the Tees and several practical recommendations. These are presented in chapter 7 and 8.

7 CONCLUSION

Generally, composite beams are considered to be very efficient by virtue of their ability to fully develop their bearing potential coming from beneficial combination of concrete and steel. However, by implementation of openings into the web region, the occurrence of a complex stress state is inevitable. Despite a significant improvement which has been achieved in the last decade, paucity on particular issues still remains. Hence, the main attention within this research work was devoted to investigation of:

- Influence of layout of shear connectors on behaviour of composite beams with web openings.
- Shear force redistribution between the Tees of composite beams with web openings.

Aiming to broaden comprehension in respect to the main objectives, this research content has followed this framework:

In chapter 1, the methodology for the entire course of this research survey was rigorously defined.

In chapter 2, the state-of-the-art analysis was conducted. As a result, overview of literature, design approaches and up-to-date research related to the main objectives were presented. In detail, description of mechanical behaviour of individual components of the composite beams with web openings was analysed. In the sequel, fundamental design principles were addressed. These were divided into two major groups:

- Global analysis.
- Local analysis.

By deeper analysis of the current design procedure for composite beams with web openings, a lack of evidence and conciseness was witnessed for:

- Influence of layout of shear connectors on the load response.
- Shear force redistribution between the T-sections having great importance for the Vierendeel bending justification by presence of high shear forces.

On the base of this analysis, the subsequent course of this research content was defined.

In chapter 3, a set of analytical-numerical analysis was performed. These were investigating weight of various parameters trying to reveal their significance. These studies focused on:

- behaviour of composite beams with web openings during the erection stage (section 3.2),
- effects of configuration of shear connectors and web openings (section 3.3, 3.4, 3.5),
- possibilities of concrete modelling in ANSYS (section 3.6).

By conduction of these studies, the most complex design approach was selected a used for the experimental samples. In addition, the study focusing on concrete modelling in ANSYS has revealed a set of numerical challenges needing to surmount to provide high credible FE model. Hence, this subject was addressed in chapter 5.

In chapter 4, the experimental programme was conducted. The structure of composite beams was as follows:

- solid concrete slab,
- asymmetric steel I-section,
- squared openings with rounded corners,
- shear connection ensured by headed shear studs.

As the testing configuration, the 4-point bending test was determined. On the fundamentals from the previous chapters, the change of layout of shear connectors was defined as the main dynamic parameter. Therefore, two alternatives of shear studs' arrangement were considered:

- uniform – using the same spacing along the entire beam,
- non-uniform – shear studs grouped above the web-posts.

The configuration of strain gauges was determined using the record & control principle. The samples were loaded gradually using 50 kN increments up to the first occurrence of yielding. The linear capacity was drained at the level of 600 kN. At this phase, the web experienced the very first yielding. The process of loading was determined as accomplished at deflection of 32 mm and load of 637 kN.

Ensuring input parameters with respect to the material properties of concrete and steel part of experimental samples, additional tests (coupon test of steel, compression test of concrete) were performed.

Despite the applied change of shear connectors' layout, it was demonstrated quite excellent agreement between evidence recorded from individual samples. This led to the conclusion, the layout of shear connectors is not so significant for the global load response as was thought. Instead, the local effects at the level of shear connections,

especially stressing of individual connectors important for fatigue assessment, were identified as the main ones influenced by this factor.

In chapter 5, the reference FE model was presented. However, by conduction of one of the studies in chapter 3, several numerical challenges related to concrete modelling in ANSYS have arisen. Hence, quite broad discussion on this subject was delivered. As a side effect, calibration procedure of input parameters for the Microplane model was developed. Also, partial attention was devoted to steel and FE contact modelling.

Completing picture of the entire process of the reference FE model building, solution process configuration, structure of the finite element model and mesh sensitivity study were delivered. As the last step, validation of the finite element model is provided. By doing so, minimal discrepancies were documented. Following this course, a corner stone for the credible parametric FE investigation has been laid.

In chapter 6, the parametric FE study was conducted. Their main challenges, with respect to the composite beam with web openings, laid in:

- evaluation of impact of layout of shear connectors on the load response,
- identification of the key factor influencing the shear force proportions for the T-section at most.

On the basis of documented also in chapter 4, it was demonstrated, impact of the layout of shear connectors has predominantly local meaning - stressing of individual connectors, no significant global effects were distinguished. But these findings shall be verified using appropriate experimental procedure.

Focusing on the latter of the challenges, several parameters have been inspected, namely:

- layout of shear connectors,
- concrete strength,
- concrete slab depth,
- steel strength,
- bottom flange width,
- web thickness,
- web depth,
- opening size.

In the end, the opening depth was identified as the main factor. Using additional calculation, curves conveying percentual proportion for the Tees from the total shear force acting on a beam were established.

In chapter 7, by subsequent analysis of derived data in chapter 6, a novel concept for the shear force redistribution between the Tees in composite beams with web openings was proposed. This uses ratio between depth of opening and web as the main factor defining particular shear force proportion for the top or bottom Tee. By dint of this concept, the current approach was significantly simplified and concise manner for definition of the mentioned quantity was established.

In conclusion, several **practical recommendations** are formed for composite beam with web openings in relation to:

- By justification of stability in bending in composite beams with web openings during the erection stage of construction, the most exact procedure for definition of critical load multiplier α_{cr} constitutes a general FE analysis using shell elements. The current design approach is not able to incorporate contribution of the web-posts.
- Employment of web openings curved in shape is advised. The main reason is they produce strains having not so sharp behaviour of strain gradient.
- It was documented, almost 30% of the total shear force can be transferred to the concrete slab. Hence, it is suitable to apply particular attention to design of shear resistance of a concrete slab and reduce the shear force proportion by appropriate size and positioning of the web openings.
- Trying to provide high quality FE computations expressing accurate load response of concrete elements, usage of the Microplane model implemented in ANSYS and other software is highly recommended.
- Discretization of a headed shear stud by FE contact seems to be applicable for cases which analyses the global load response of a bearing member.
- Layout of shear studs does not significantly influence the global load response of the composite beams with web openings as was expected, but a great caution has to be paid by its non-uniform spacing due possible localisation of stressing at the level of individual connectors, especially in the case of fatigues loads.
- By justification of the Vierendeel bending considering presence of high shear forces, it is highly recommended to use the proposed concept. By doing so, accurate proportion of the shear force can be assigned to the top and bottom Tee with certain safety margin.

Moving to assessment of completion of the thesis aims:

1. Proposal and realisation of the experiment focused on the resistance and behaviour of composite beams with web openings.

2. Creation and calibration of a numerical model based on the FE method.
3. Conduction of the following parametric studies focusing on:
    a. shear flow at beams with web openings with uneven distribution of shear studs,
    b. effect of the presence of openings on the resistance in lateral-torsional stability of composite beams with web openings in the assembly and operational stages.
4. Recommendations refining the current design procedure of non-symmetrical composite beams with web openings.

It could be claimed, their content was successfully accomplished by the presented findings and conclusions within this research work.

To the end, the author takes the liberty to suggest course of the future research.

8 FUTURE WORK

On the basis of collected evidence, the following topics were identified as worth investigating in the future:

1. Actual bending resistance of composite beams with web openings

The plastic bending resistance of a composite beam is generally defined by axial force acting within the concrete or the steel component multiplied by related lever arm. Concentrating on the former, the compression resistance of a concrete slab $N_{c,Rd}$ depends predominantly on a count of shear connectors. These connectors have certain shear resistance. This resistance is in composite beams with web openings affected into some measure by local effects (push and pull-out forces) arising due the Vierendeel action. In the case of pull-out forces, the mutual loading of shear connector in shear and tension results in reduction of its bearing capacity. If this applies, evaluation of the compression resistance of a concrete slab $N_{c,Rd}$ is affected and the plastic bending resistance as well. Hitherto, no concept with respect to this topic is present.

2. Actual stressing of shear connectors

As was documented, alternation of layout of shear connectors displayed minimal effects on the global load response of the investigated samples. Aiming to provide deeper understanding of the stress state at the level of shear connection, more advanced experimental measurements directly at the shear connectors could be vital. In addition, the third alternative (Alt. 3) of shear connectors layout might join to the two formers (Fig. 8.1). In particular, the connectors could be grouped over the openings.

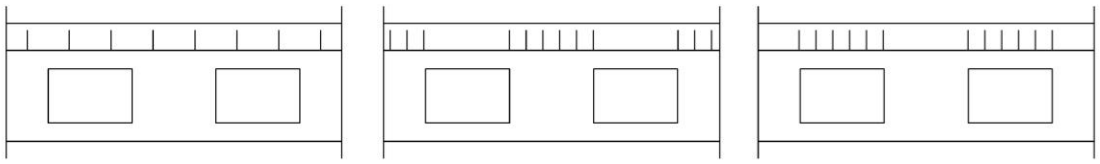

(a) (b) (c)

Fig. 9.1 - Alternatives of layout of shear studs a) uniform, b) grouped above the web-posts and c) grouped above the openings.

3. Advanced experimental measurements at the level of shear connection

Attempting for more explicit measurements of shear connector stressing, the application of strain gauges exact at the shank of connector should be applied. Despite a threat of damage of measuring equipment, this treatment was already used in [17] yielding both minor issues and fruitful results.

In the case of recording of a slip at the material interface, the concept using strain gauges instead of linear transducers is advised (Fig. 8.2). This recommendation originates in a method determining the interface slip based on the concept of the slip strain. Said straightforwardly, the slip strain is derived as a difference of concrete and steel strains at the material interface. So, by subsequent integration of the slip strain, the result yields the slip. This concept proposes creation of a canal of suitable size in a concrete slab during casting process. Even though this treatment might represent a partial complication compared to the usage of LVTDs, it offers more accurate outcome and clear evidence for the FE model validation.

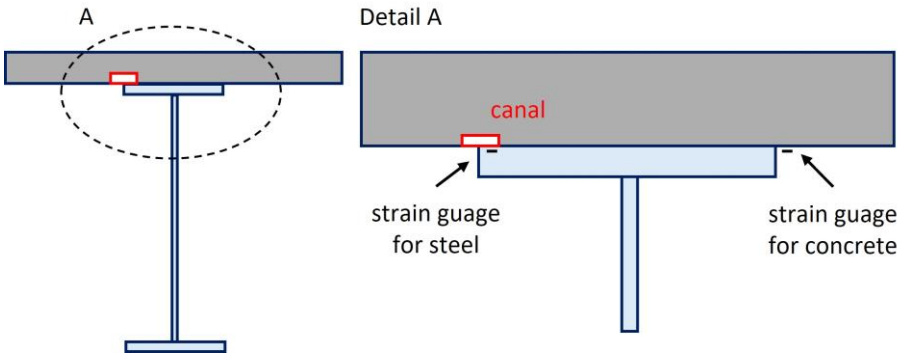

Fig. 9.2 - Novel concept of a slip measurement at the material interface.

4. Pathological effects of the Microplane model in ANSYS under biaxial loading

By development of the calibration code for the input parameters of the Microplane model, a notable inconsistency was witnessed worth critical discussion. Hence, a concise manner identifying and resolving the pathological phenomenon likely-to-occur under the biaxial loading should be delivered. Yet, the author ventures to suggest broader numerical focusing on inspection of individual input parameters for the Microplane model in ANSYS and their influence on the concrete load response under various loading conditions.

5. Headed shear connector discretized by 3-D model in ANSYS

Aiming to provide more suitable discretisation of shear connection compared to currently used 2-D contact approach, a 3-D model of shear connection employing admissible contact properties seems to represent suitable alternative (Fig. 8.3).

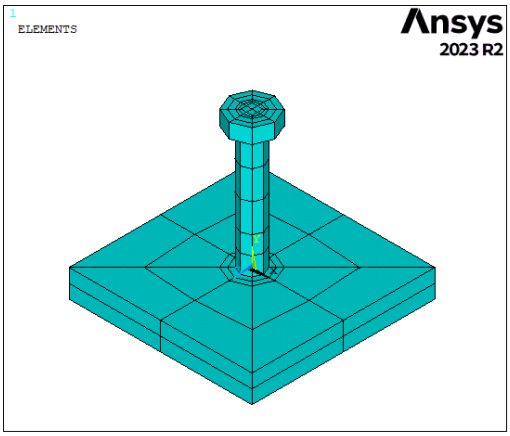

Fig. 9.3 – 3-D FE model a shear headed stud.

Of course, this model demands yet a quite comprehensive numerical work to remedy some issues, but in the author eyes, it emerges the most precise and rigorous method for shear connection description using finite elements. After validation of this 3-D FE model of headed shear stud against analytical models and experimental evidence, its possible accurateness can be exploited as in the case of rib shear connectors [17].

References

1. Granade, Charles J. An investigation of composite beams having large rectangular openings in their webs. Master's Thesis, University of Alabama at Tuscaloosa, 1968.
2. Todd, D. M., Cooper, P. B. Strength of Composite Beams with Web Openings. Journal of the Structural Division, 1980, 106(2), 431–444.
3. Clawson, W. C., Darwin, D. Strength of Composite Beams at Web Openings. Journal of the Structural Division, 1982, 108(ST3), 623–641.
4. Redwood, R., Cho, S. H. Design of steel and composite beams with web openings. Journal of Constructional Steel Research, 1993, 25(1–2), 23–41.
5. Donoghue, C. M., Mang, H. A. Composite Beams with Web Openings: Design. Journal of the Structural Division, 1982, 108(ST12), 2652–2667.
6. Oehlers, D. J., Bradford, M. A. Elementary Behaviour of Composite Steel and Concrete Structural Members, CRC Press, London, 1999.
7. Technical research - Final Report. Large web openings for service integration in composite floors, Contract No. 7210-PR/315, 2003.
8. R.M. Lawson, S.J. Hicks, Design of Beams with Large Web Openings, The Steel Construction Institute, 2011.
9. Sameer, S. et.al. Design Guide 31: Castellated and Cellular Beam Design, AISC, Chicago, 2017.
10. Patrick, M. Design of Simply Supported Composite Beams with Large Web Penetrations, One Steel Manufacturing Pty Limited, Sydney, 2001.
11. Lawson, R. M., Lim, J., Hicks, S. J., Simms, W. I. Design of composite asymmetric cellular beams and beams with large web openings. Journal of Constructional Steel Research, 2006, 62(6), 614–629.
12. Chung, K. F., Liu, C. H., Ko, A. C. H. Steel beams with large web openings of various shapes and sizes: An empirical design method using a generalised moment-shear interaction curve. Journal of Constructional Steel Research, 2003, 59(9), 1177–1200.
13. Benitez M A. et al.. Deflection of composite beams with web openings, Journal of Structural Engineering, 1998, Vol. 124, 1139-1147.
14. Lawson R.M. et al.. Pull-out forces in shear connectors in composite beams with large web openings, Journal of Constructional Steel Research, 2013, Vol. 87, 48-59.
15. Classen, M., Kurz, W., Schäfer, M., Hegger, J. A mechanical design model for steel and concrete composite members with web openings. Engineering Structures, 2019, 197, 109417.
16. Xinggui Zeng et al. Effect of Shear Connector Layout on the Behavior of Steel-Concrete Composite Beams with Interface Slip, Applied Sciences, 2019, Vol. 9, 207.
17. Classen M. On the structural behavior of composite beams with composite dowels and large web openings. PhD thesis, RWTH Aachen University Institute of Structural Concrete (No. RWTH-2017-01834), 2016.
18. Tsavdaridis, K. D. Structural performance of perforated steel beams with novel web openings and with partial concrete encasement. PhD thesis, City University London, 2010.

19. Wang, P., Guo, K., Liu, M., Zhang, L. Shear buckling strengths of web-posts in a castellated steel beam with hexagonal web openings. Journal of Constructional Steel Research, 2016, 121, 173–184.
20. EN 1993-1-1 (2005), Eurocode 3, Design of steel structures, Part 1-1: General rules for buildings, CEN, Brussels, 2005.
21. EN 1994-1-1 (2004), Eurocode 4, Design of composite steel and concrete structures, Part 1-1: General rules and rules for buildings, CEN, Brussels, 2004.
22. Saleh, S. M., Majeed, F. H. Shear Strength of Headed Stud Connectors in Self-Compacting Concrete with Recycled Coarse Aggregate. Buildings, 2022, 12(5), 505.
23. Malm, R., Shear cracks in concrete structures subjected to in-plane. PhD. Thesis, Royal Institute of Technology, Sweden, 2006.
24. Taylor, G. I., “Plastic Strain in Metals,” Journal of Inst. Metals, Vol. 62, 1938, pp. 307–324.
25. Bažant, Z. P., Gambarova, P. G., Crack Shear in Concrete: Crack Band Microplane Model. Journal of Structural Engineering, 1984, 110(9), 2015–2035.
26. Zreid, I., Kaliske, M. A gradient enhanced plasticity–damage microplane model for concrete. Computational Mechanics, 2018, 62(5), 1239–1257.
27. Popovics, S. A numerical approach to the complete stress-strain curve of concrete. Cement and Concrete Research, 1973, 3(5), 583–599.
28. Cintora, T. Softening response of concrete in direct tension, Master thesis, New Jersey Institute of Technology, 1988.
29. Kupfer, H. B., Gerstle, K. H., Behavior of Concrete Under Biaxial Stresses. ASCE J Eng Mech Div, 1973, 99(EM4), 853–866.
30. Caner, F. C., Bažant, Z. P., Microplane Model M7 for Plain Concrete. I: Formulation. Journal of Engineering Mechanics, 2013,139(12), 1714–1723.
31. Caner, F. C., Bažant, Z. P., Microplane Model M7 for Plain Concrete. II: Calibration and Verification. Journal of Engineering Mechanics, 2013, 139(12), 1724–1735.
32. Yun, X., Gardner, L. Stress-strain curves for hot-rolled steels. Journal of Constructional Steel Research, 2017, 133, 36–46.
33. Classen, M. Limitations on the use of partial shear connection in composite beams with steel T-sections and uniformly spaced rib shear connectors. Journal of Constructional Steel Research, 2019, 142, 99–112.
34. Lam, D., El-Lobody, E. Behavior of headed stud shear connectors in composite beam. Journal of Structural Engineering, 2005, 131(1), 96–107.
35. Johnson, K.L. Contact mechanics. Cambridge University Press, London, 1985.
36. Ansys User’s Manual, Swanson Analysis Systems, Inc.1995 -2023.
37. Yang, F., Liu, Y., Liang, C. Analytical study on the tensile stiffness of headed stud connectors. Advances in Structural Engineering, 2019, 22(5), 1149–1160.
38. Mouras, J. M., et. al., The Tensile Capacity of Welded Shear Studs, Technical Report, 9-5498-2, Texas, 2008.

Appendix A - Drawings of the experimental samples

Structural scheme of the investigated samples - BRU alternative.

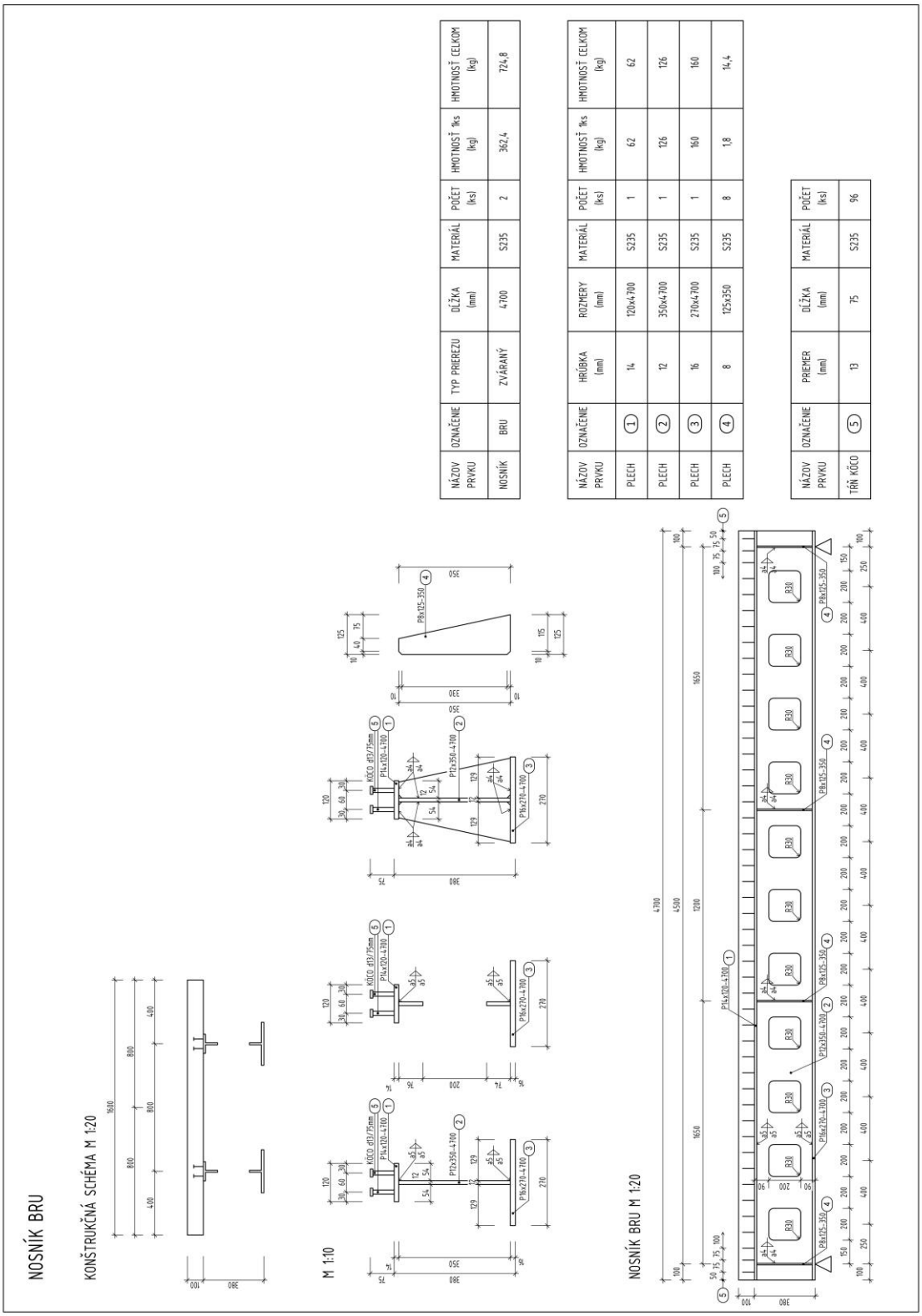

NÁZOV PRVKU	OZNAČENIE	TYP PRIEREZU	DĹŽKA (mm)	MATERIÁL	POČET (ks)	HMOTNOSŤ 1ks (kg)	HMOTNOSŤ CELKOM (kg)
NOSNÍK	BRU	ZVÁRANÝ	4700	S235	2	362,4	724,8

NÁZOV PRVKU	OZNAČENIE	HRÚBKA (mm)	ROZMERY (mm)	MATERIÁL	POČET (ks)	HMOTNOSŤ 1ks (kg)	HMOTNOSŤ CELKOM (kg)
PLECH	①	14	120x4700	S235	1	62	62
PLECH	②	12	350x4700	S235	1	126	126
PLECH	③	16	270x4700	S235	1	160	160
PLECH	④	8	125x350	S235	8	1,8	14,4

NÁZOV PRVKU	OZNAČENIE	PRIEMER (mm)	DĹŽKA (mm)	MATERIÁL	POČET (ks)
TŔŇ KÔČO	⑤	13	75	S235	96

Structural scheme of the investigated samples - BRN alternative.

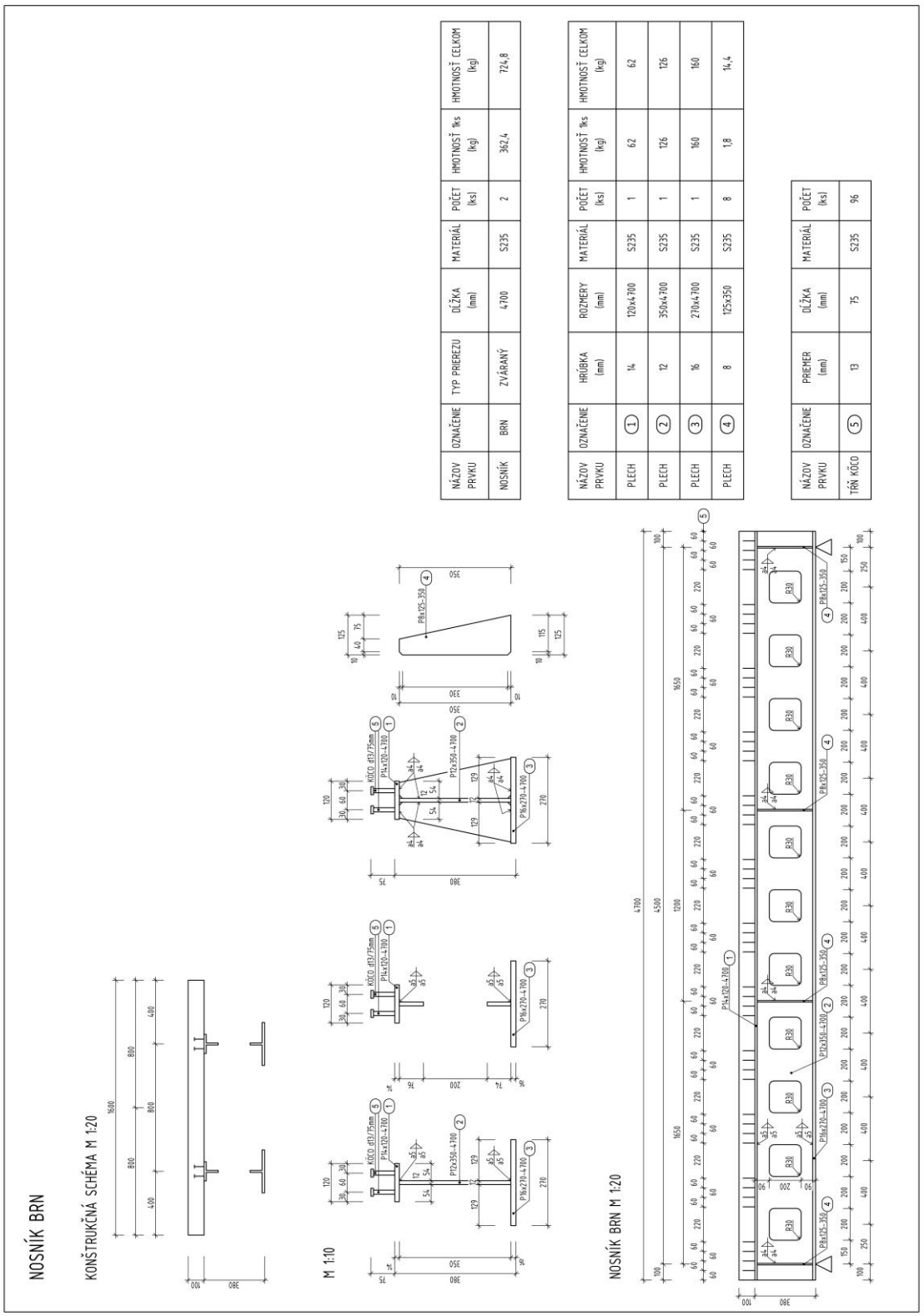

NÁZOV PRVKU	OZNAČENIE	TYP PRIEREZU	DĹŽKA (mm)	MATERIÁL	POČET (ks)	HMOTNOSŤ (kg)	HMOTNOSŤ 1ks (kg)	HMOTNOSŤ CELKOM (kg)
NOSNÍK	BRN	ZVÁRANÝ	4700	S235	2	362,4		724,8

NÁZOV PRVKU	OZNAČENIE	HRÚBKA (mm)	ROZMERY (mm)	MATERIÁL	POČET (ks)	HMOTNOSŤ (kg)	HMOTNOSŤ 1ks (kg)	HMOTNOSŤ CELKOM (kg)
PLECH	①	14	120x4700	S235	1	62	62	62
PLECH	②	12	350x4700	S235	1	126	126	126
PLECH	③	16	270x4700	S235	1	160	160	160
PLECH	④	8	125x350	S235	8	1,8	14,4	14,4

NÁZOV PRVKU	OZNAČENIE	PRIEMER (mm)	DĹŽKA (mm)	MATERIÁL	POČET (ks)
TRŇ KÔŠTO	⑤	13	75	S235	96

Structural scheme of the investigated samples - reinforcement.

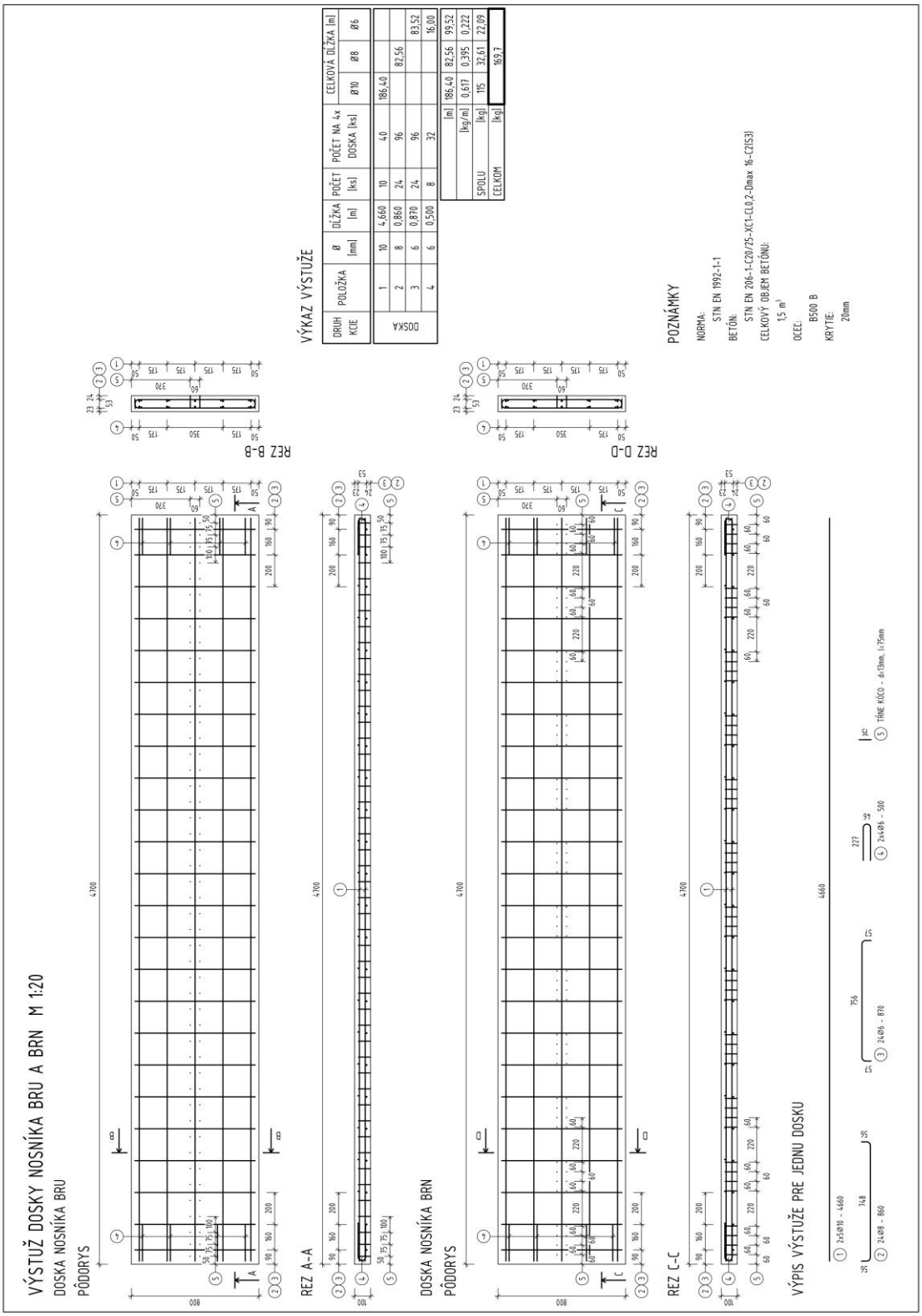

Structural scheme of the investigated samples - configuration of measurement devices - alternative 1.

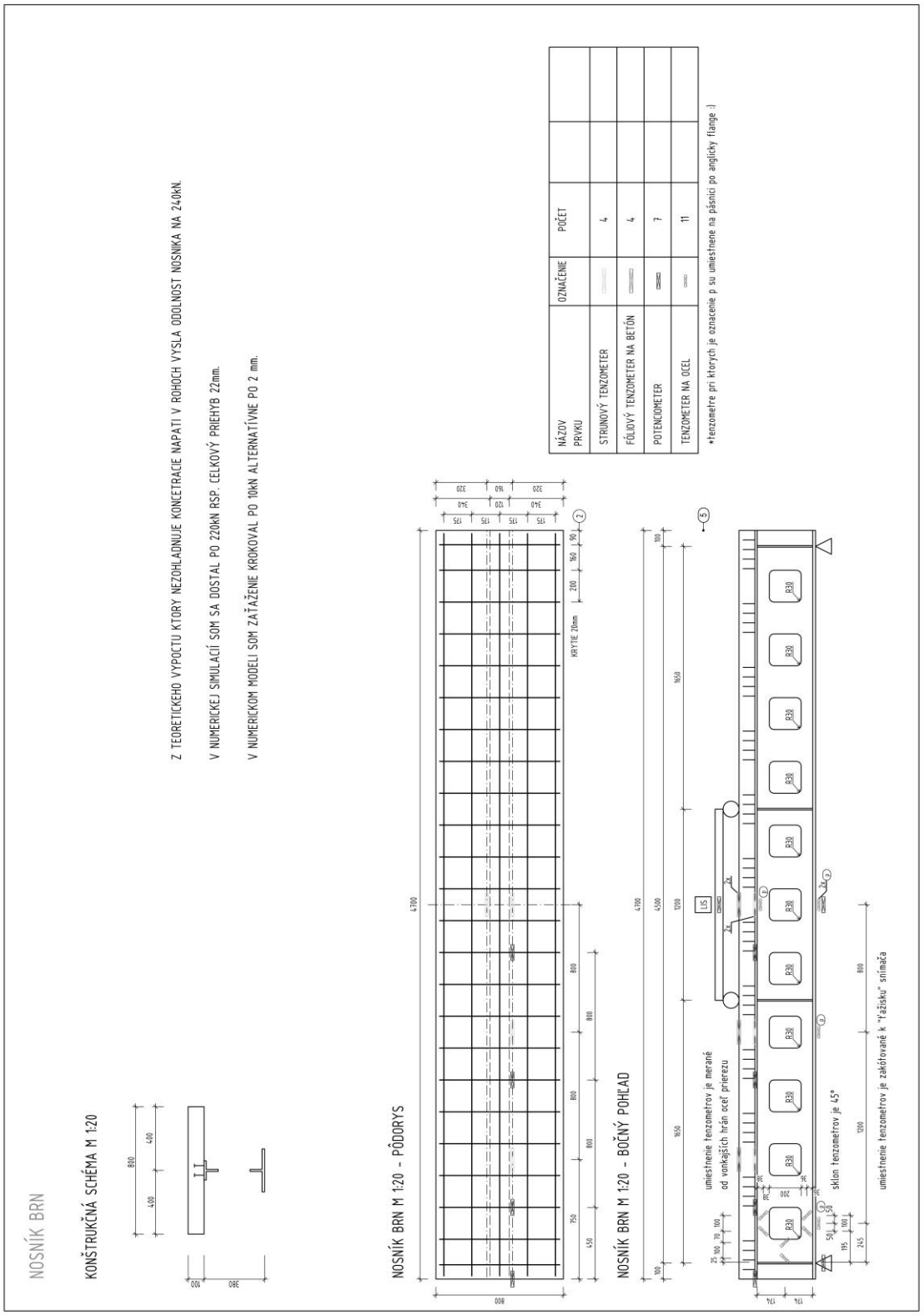

Structural scheme of the investigated samples - configuration of measurement devices - alternative 2.

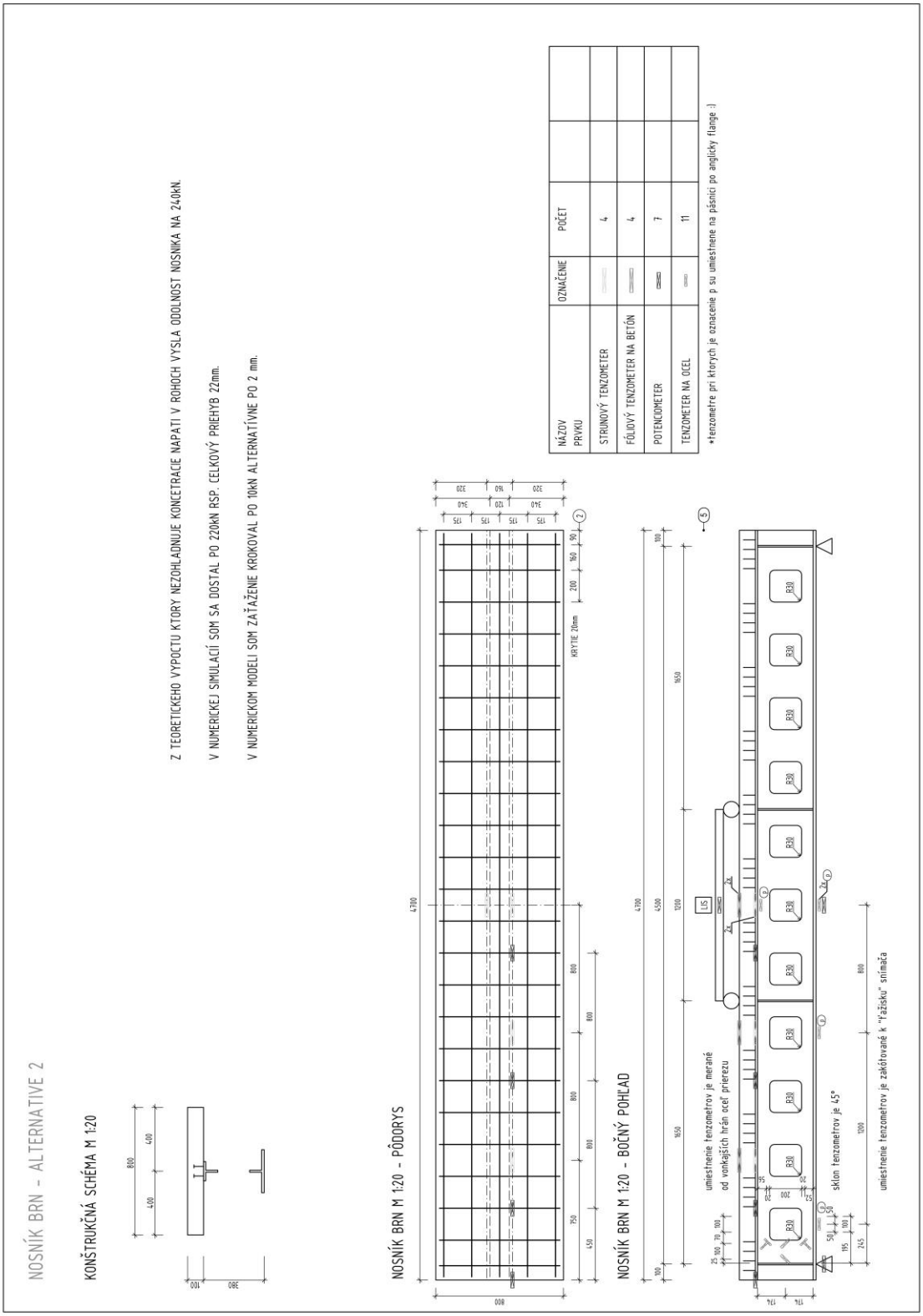

Appendix B - Correlation of the experimental and numerical results

Simplified depiction of configuration of measurements devices.

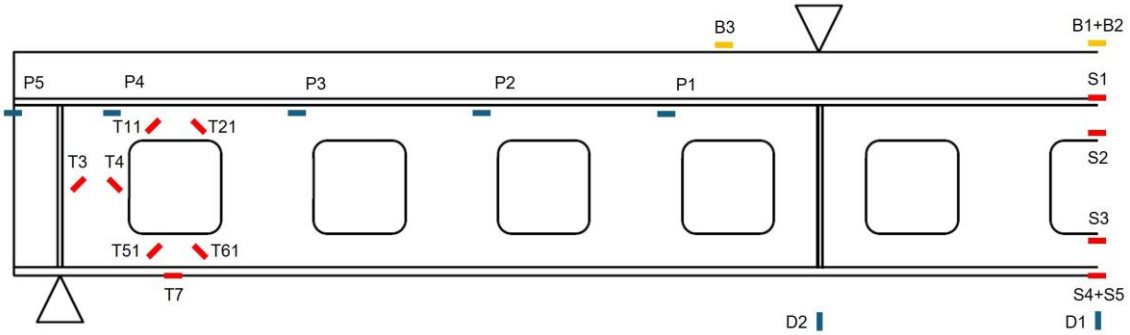

Alternation of configuration of measurements devices.

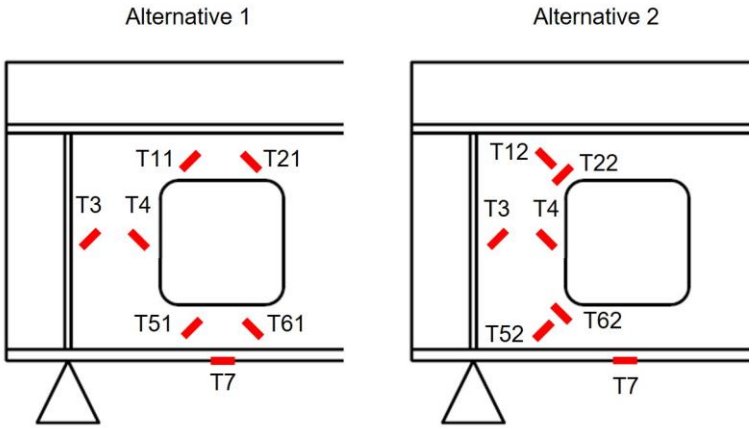

D1	D2
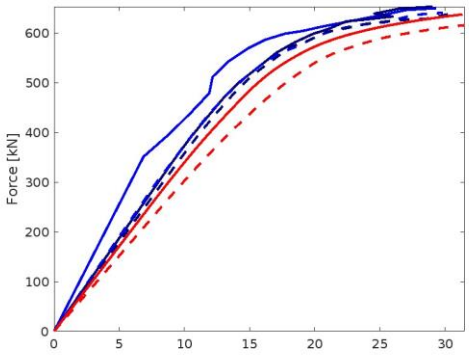	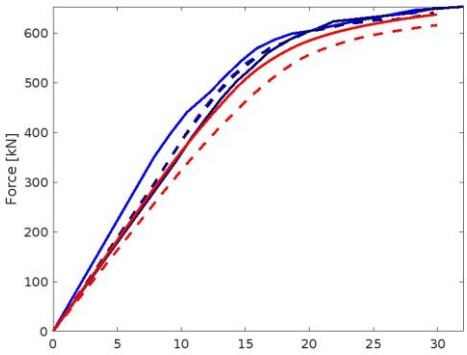
B1	**B2**
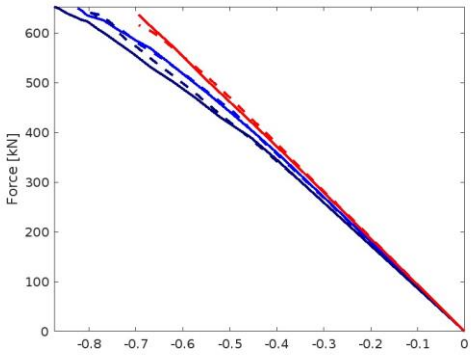	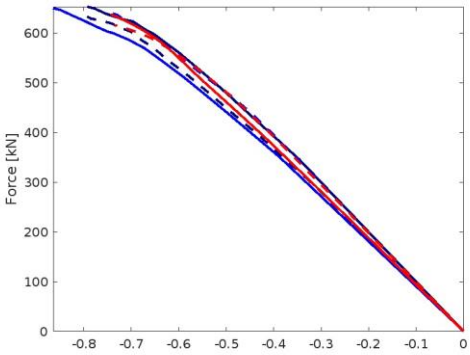
B3	**S1**
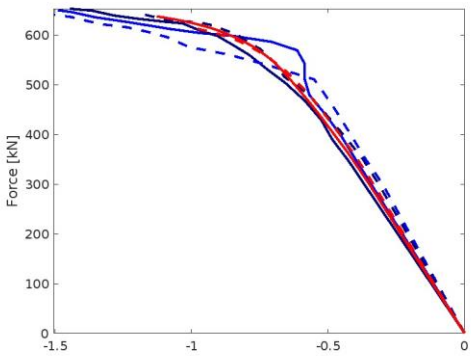	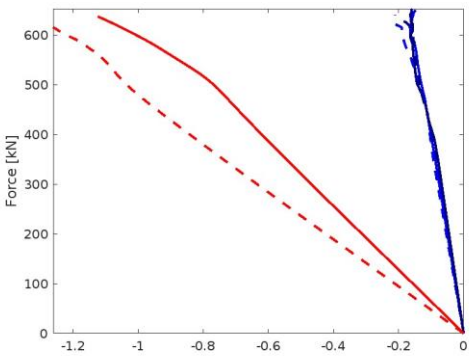

S2	S3
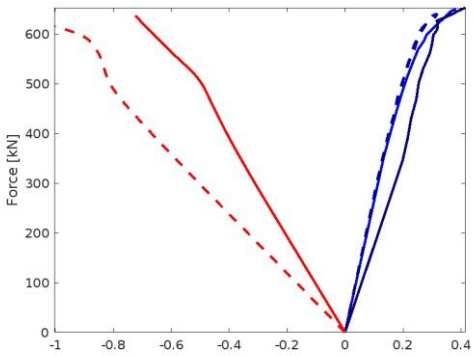	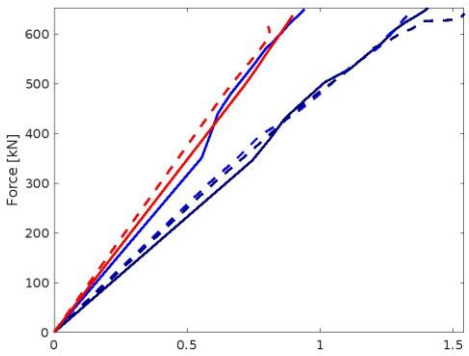
S45	**P1**
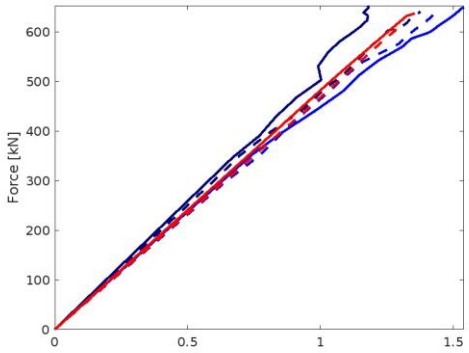	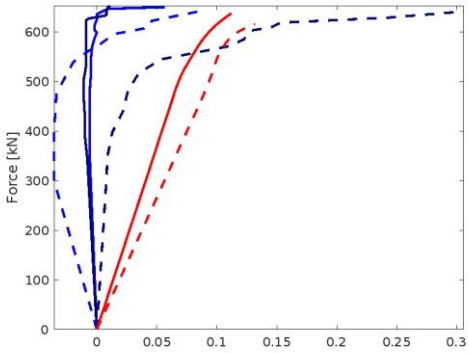
P2	**P3**
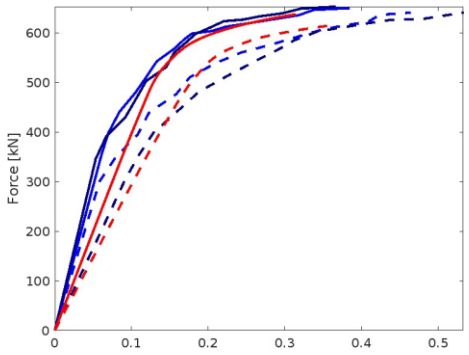	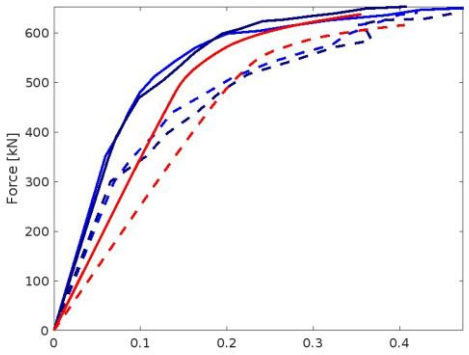

P4	P5
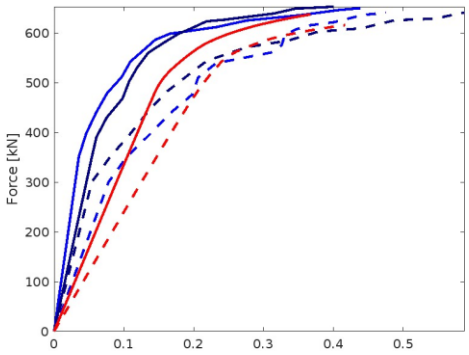	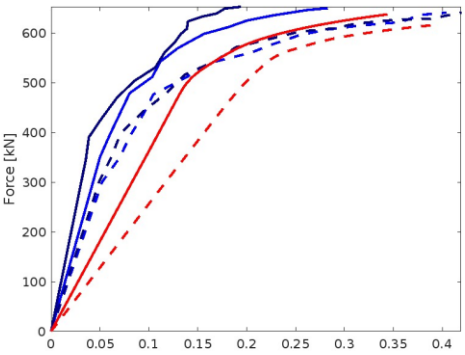
T11	**T21**
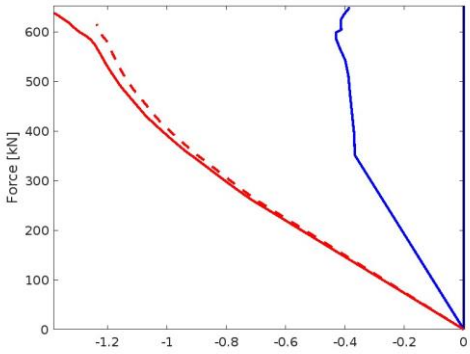	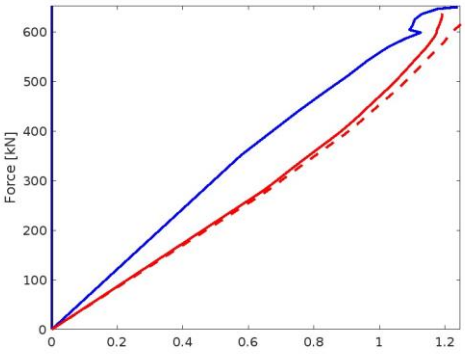
T3	**T4**
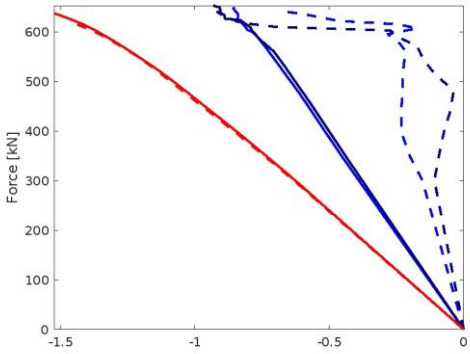	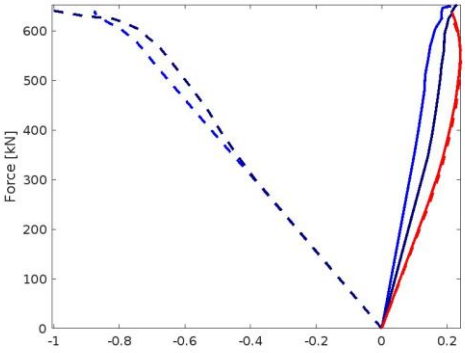

T51	T61
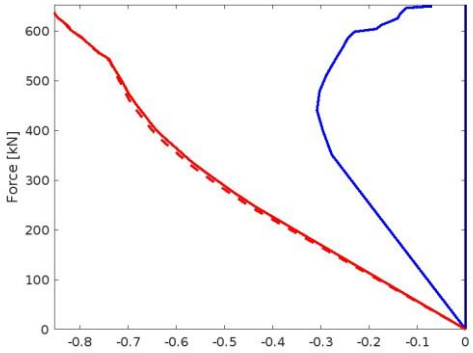	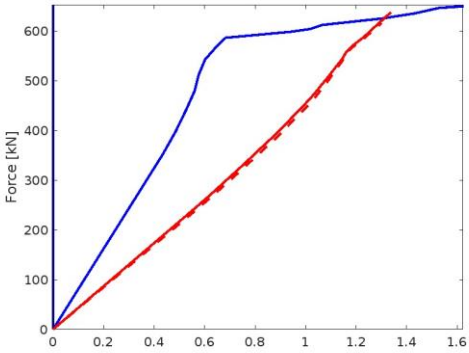
T7	**T12**
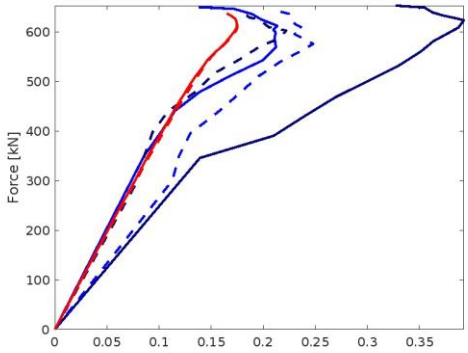	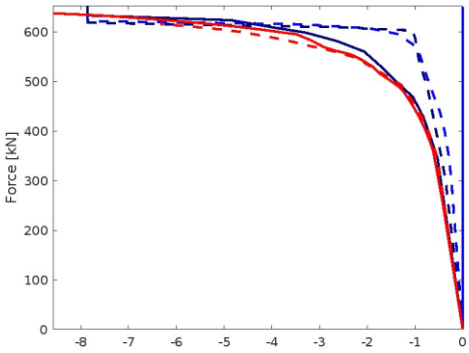
T22	**T52**
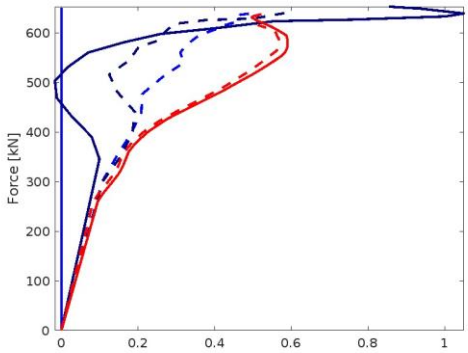	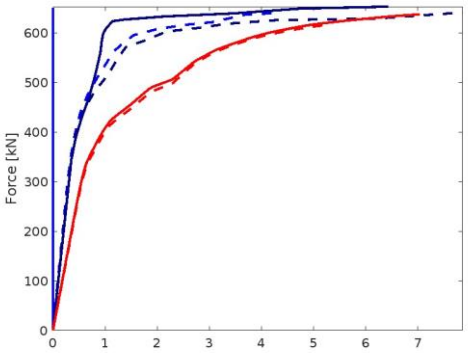


EXP BRU 1
EXP BRU 2
EXP BRN 1
EXP BRN 2
FEM BRU
FEM BRN

T26	
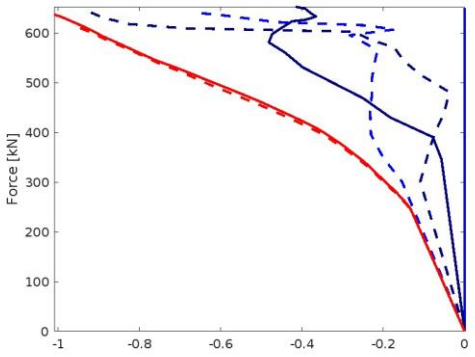	

Force [kN]
600
500
400
300
200
100
0
-1
-0.8
-0.6
-0.4
-0.2
0

Appendix C - Supplementary results of the parametric study.

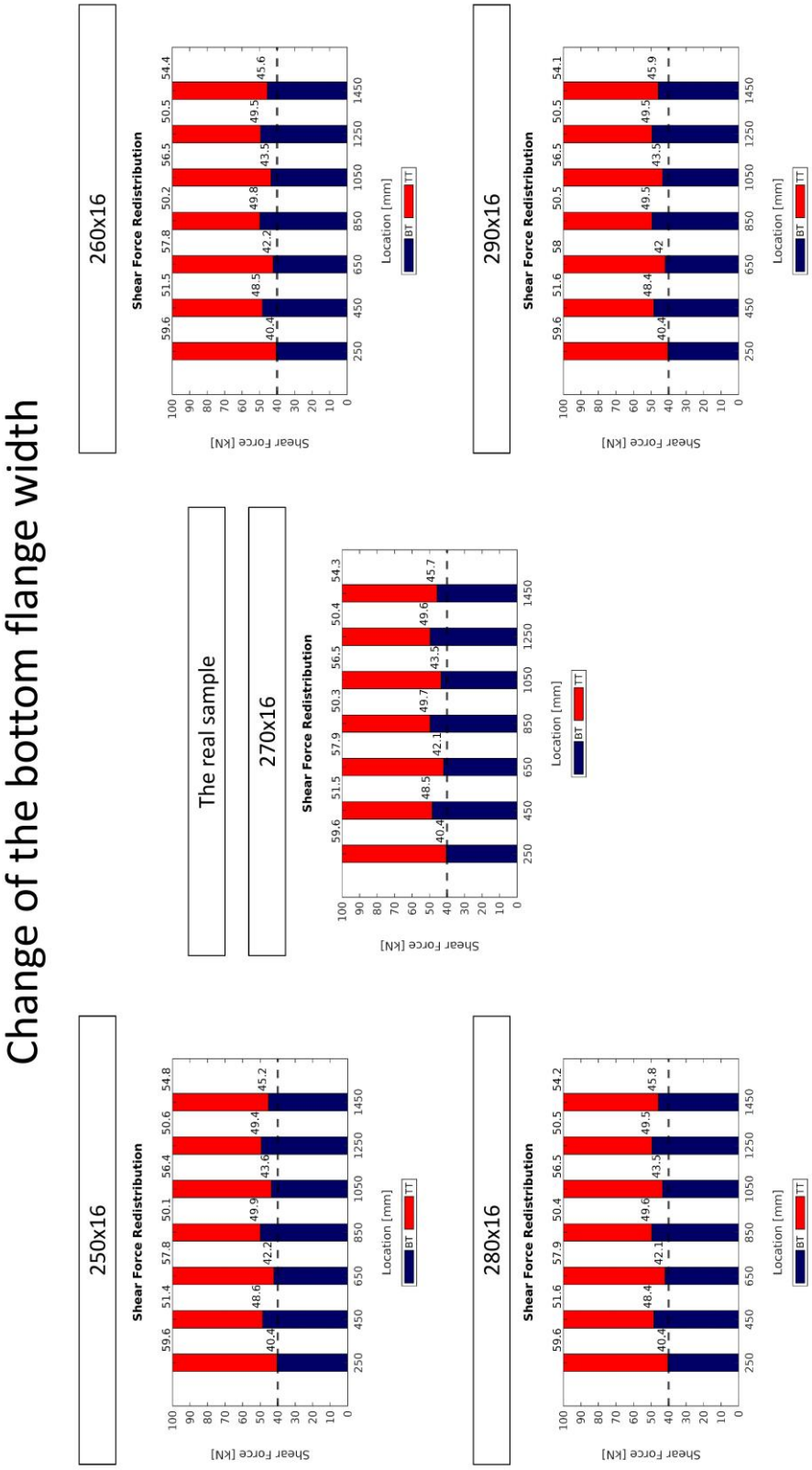

Change of the concrete slab depth

90

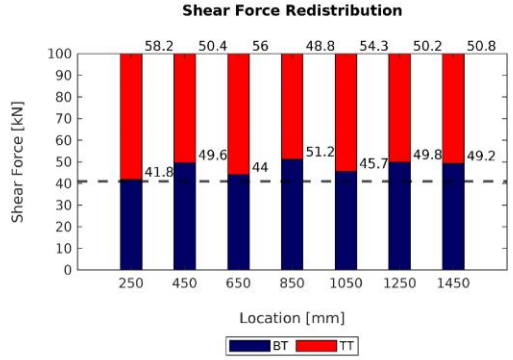

The real sample

100

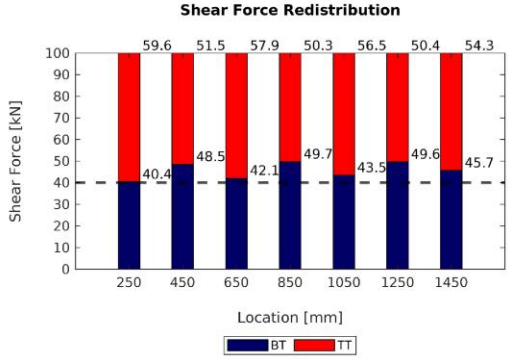

110

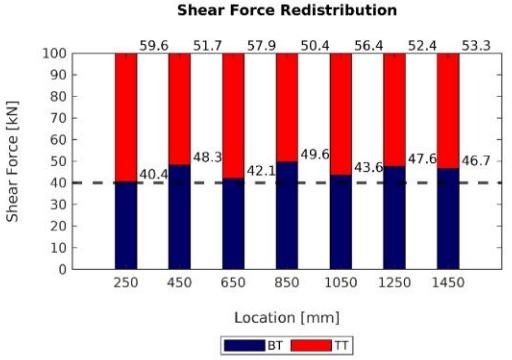

Change of the concrete compression strength

40

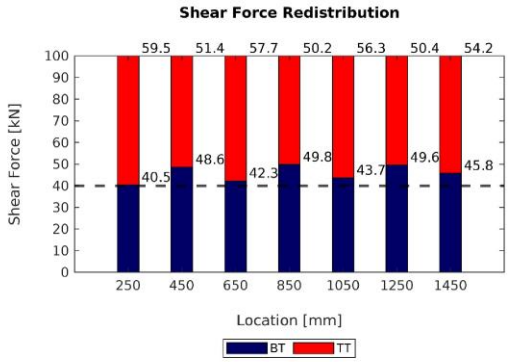

The real sample

46

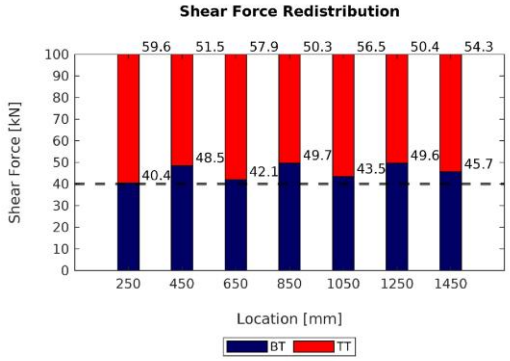

50

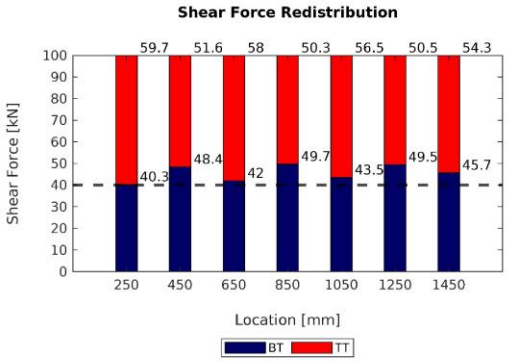

Change of the shear connector layout

BRU

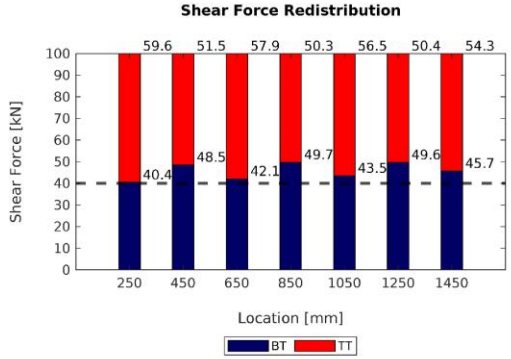

BRN

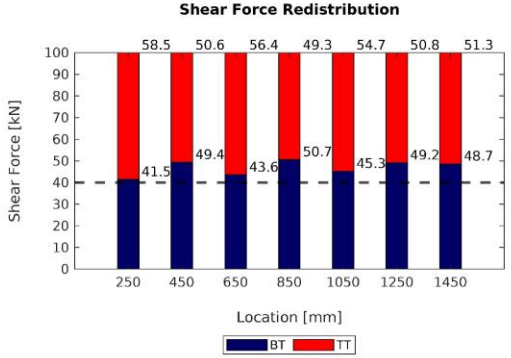

Something in between

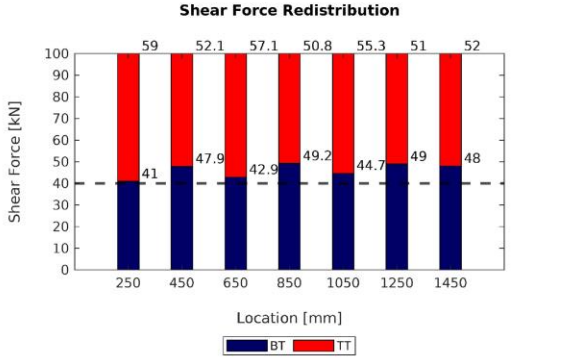

BRU

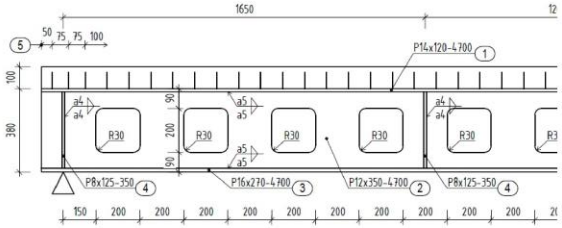

BRN

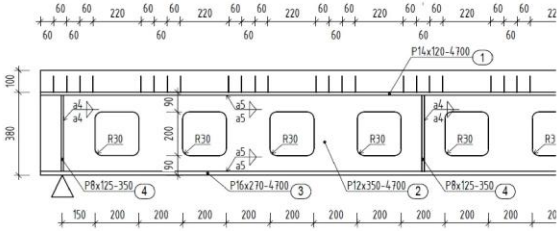

Change of the web depth
respecting opening to web depth ratio

195/348*

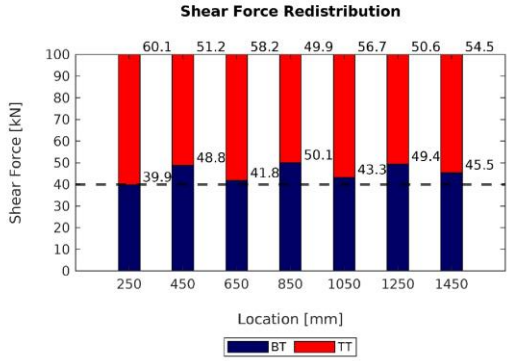

opening to web depth ratio = 0.55

The real sample

200/358*

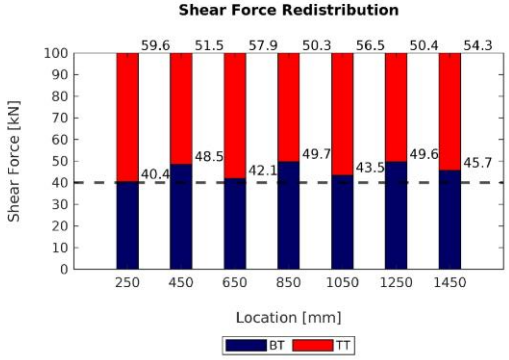

205/368*

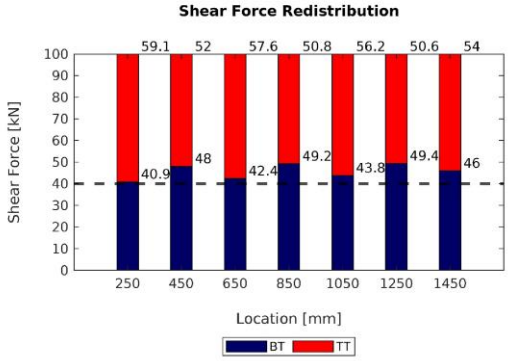

Change of the web thickness

11

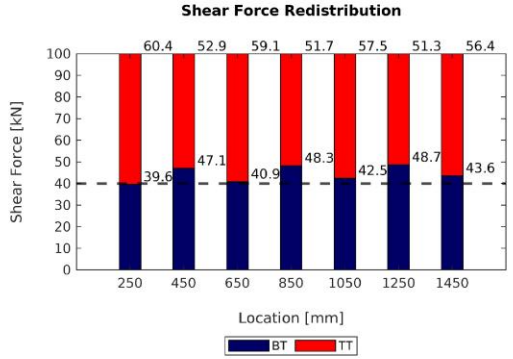

The real sample

12

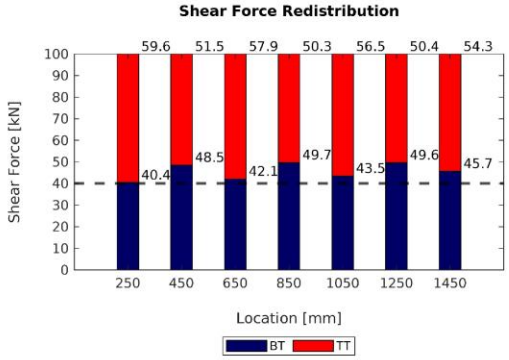

13

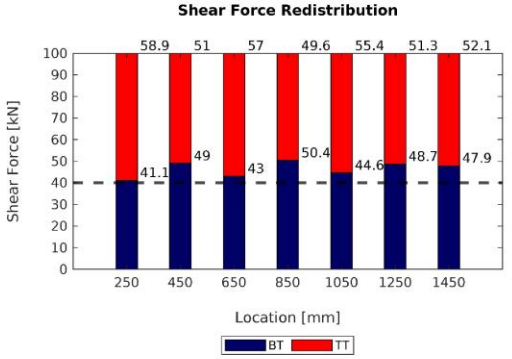

Change of the opening size

100x100	The real sample = 200x200	100x200
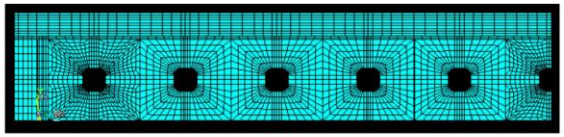	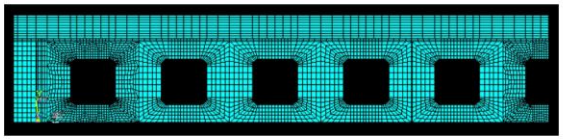	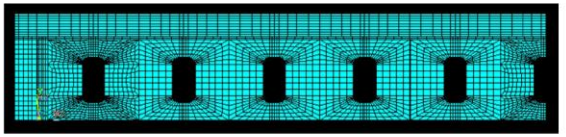
200x100	**No openings**	**200x300**
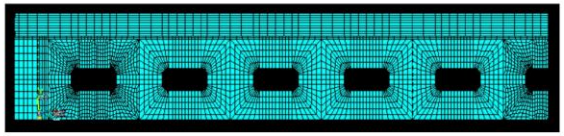	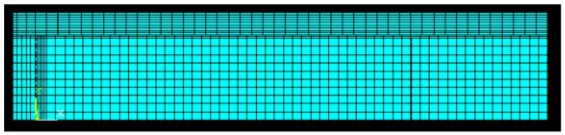	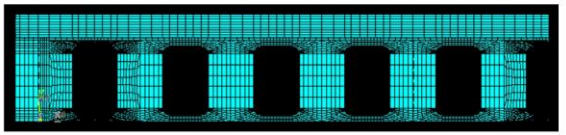

Change of the opening size

100x100

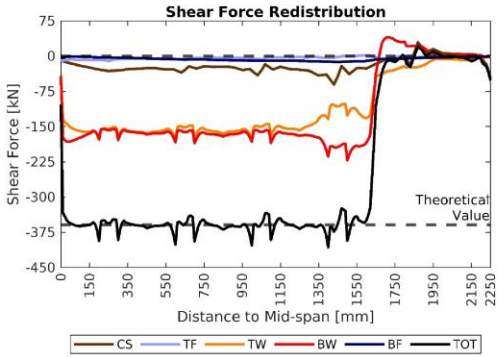

The real sample = 200x200

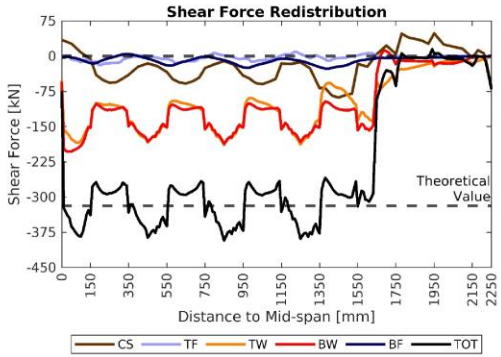

100x200

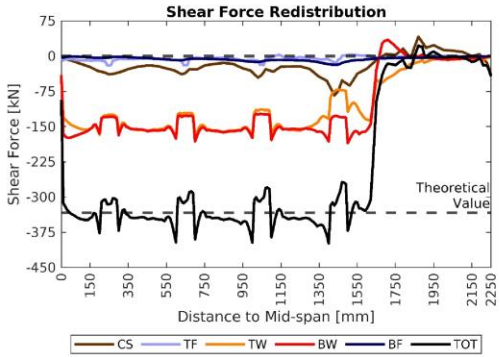

200x100

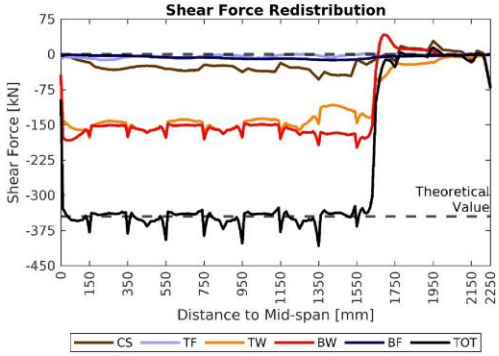

No openings

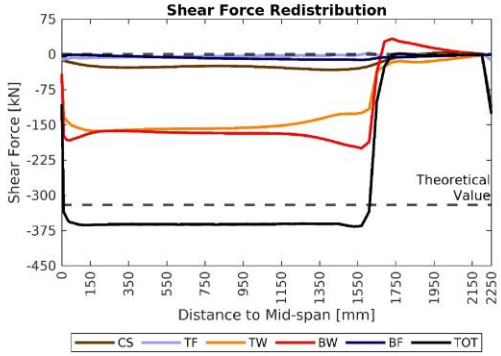

200x300

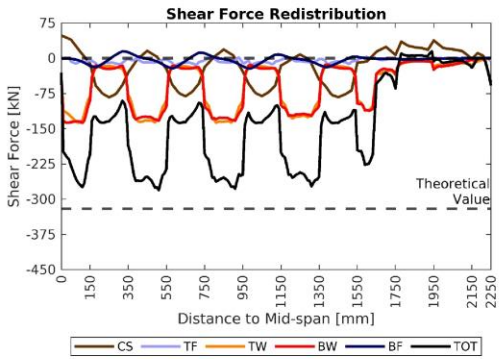

Change of the opening size

100x100

The real sample = 200x200

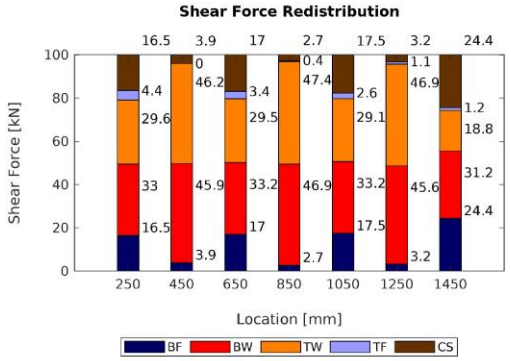

100x200

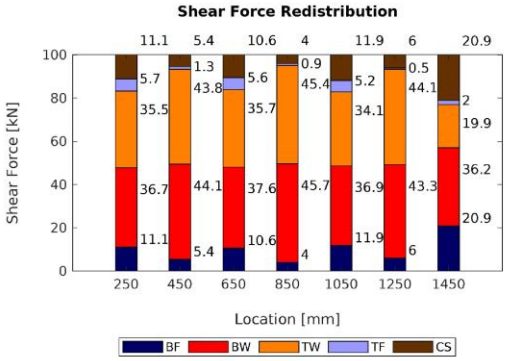

200x100

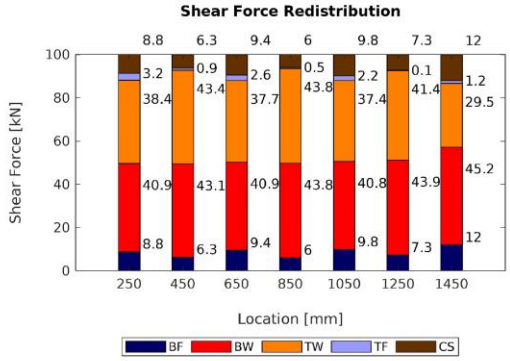

No openings

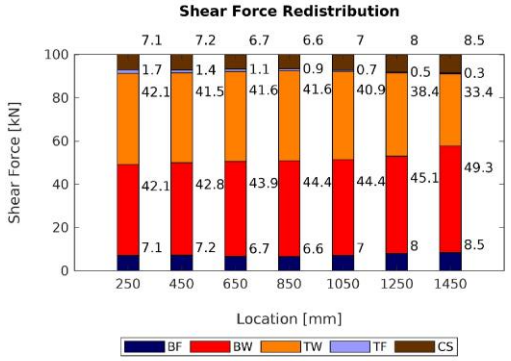

200x300

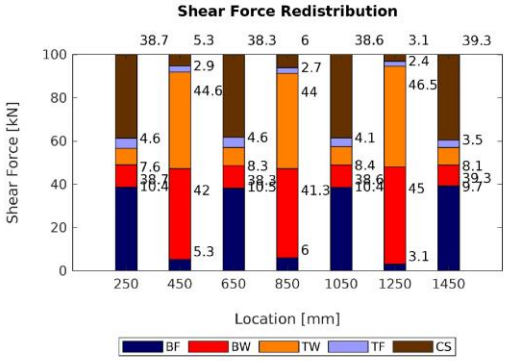

Change of the opening size

100x100

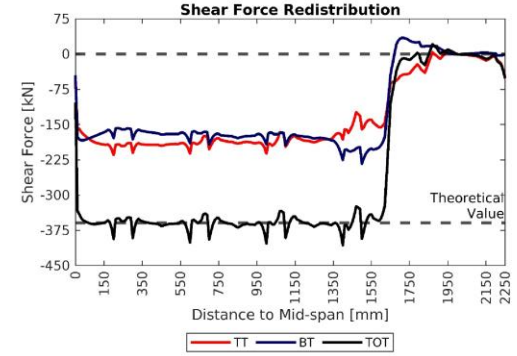

The real sample = 200x200

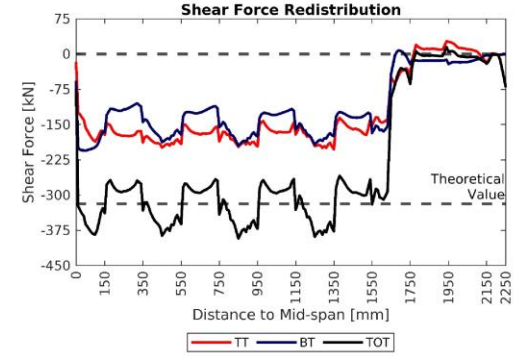

100x200

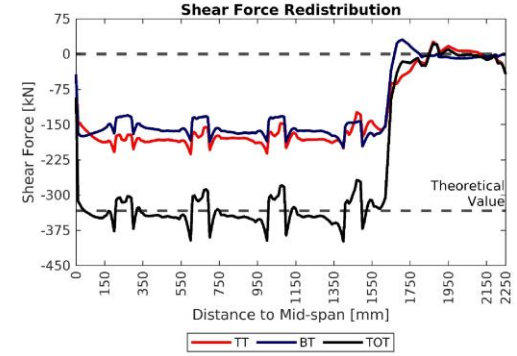

200x100

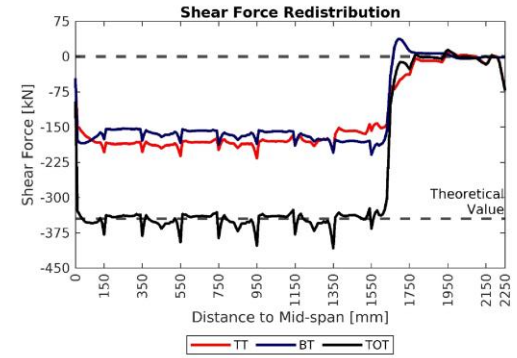

No openings

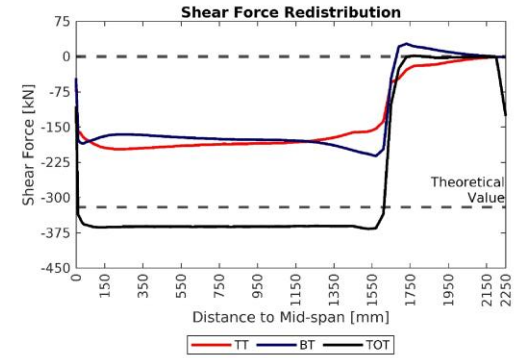

200x300

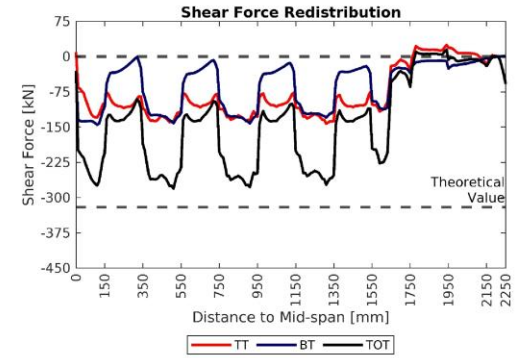

Change of the opening size

100x100

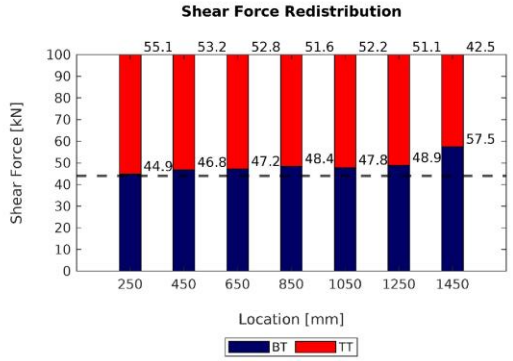

The real sample = 200x200

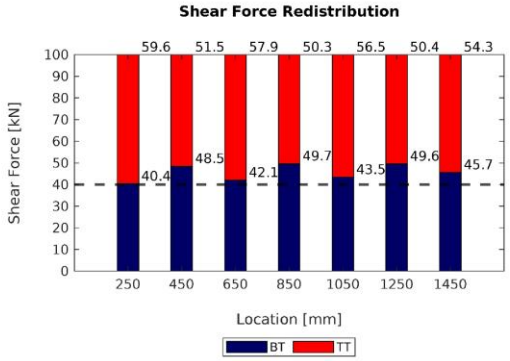

100x200

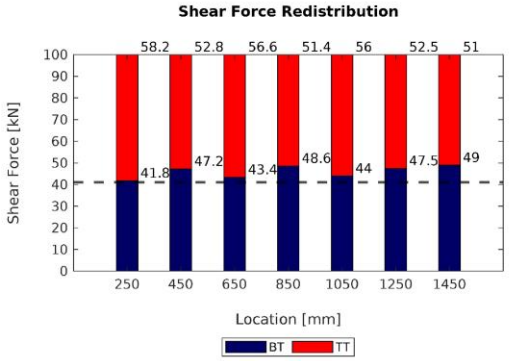

200x100

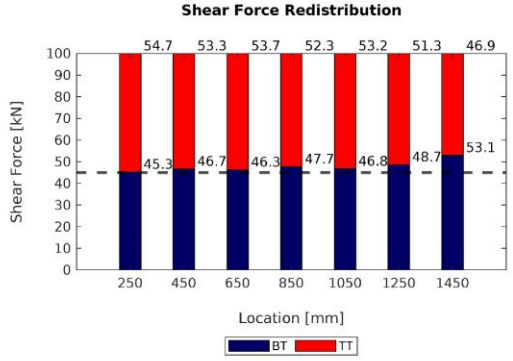

No openings

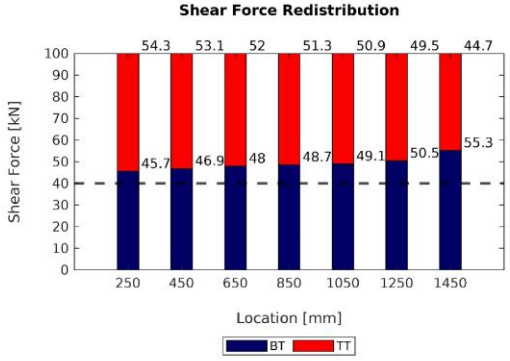

200x300